Stellar Evolution and Explosions: Contributions to the Abundance Evolution in Galaxies

attempt of a survey with many contributions from present and past collaborators

Friedrich-Karl Thielemann
Department of Physics
University of Basel
Switzerland

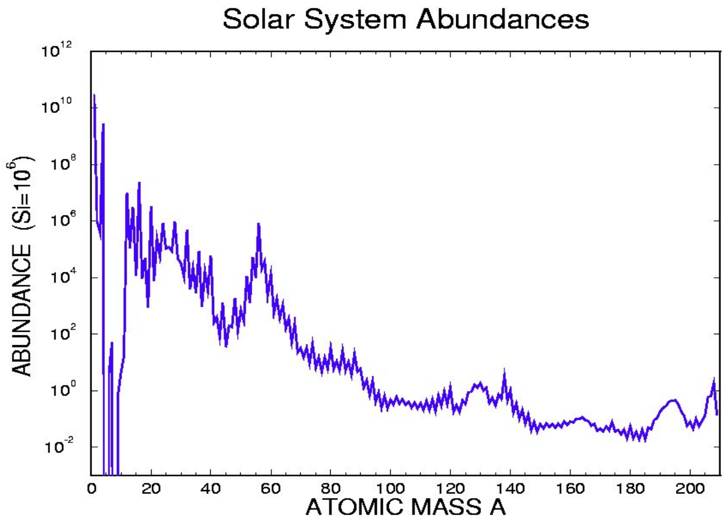

How do we understand: solar system abundances..

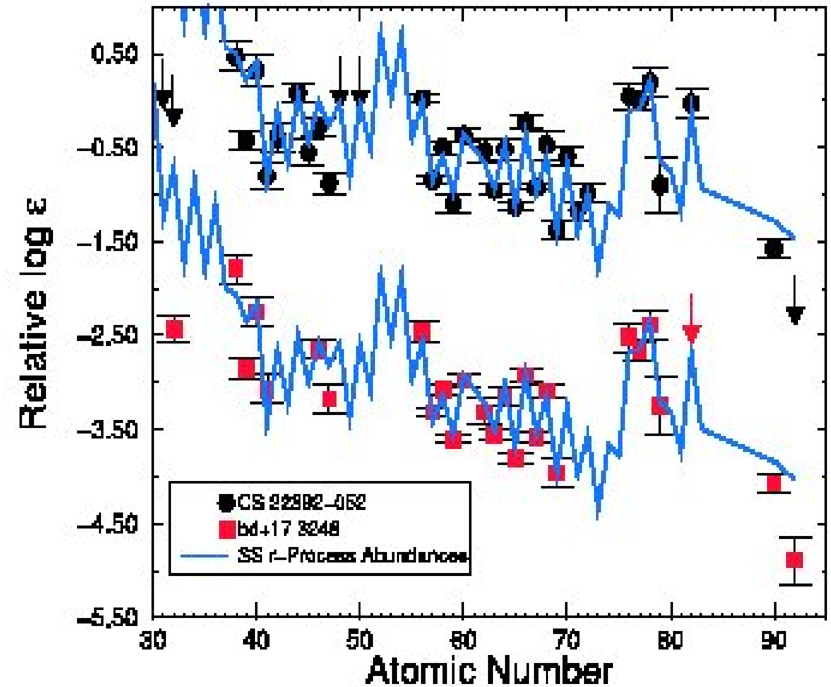

low metallicity stars ...

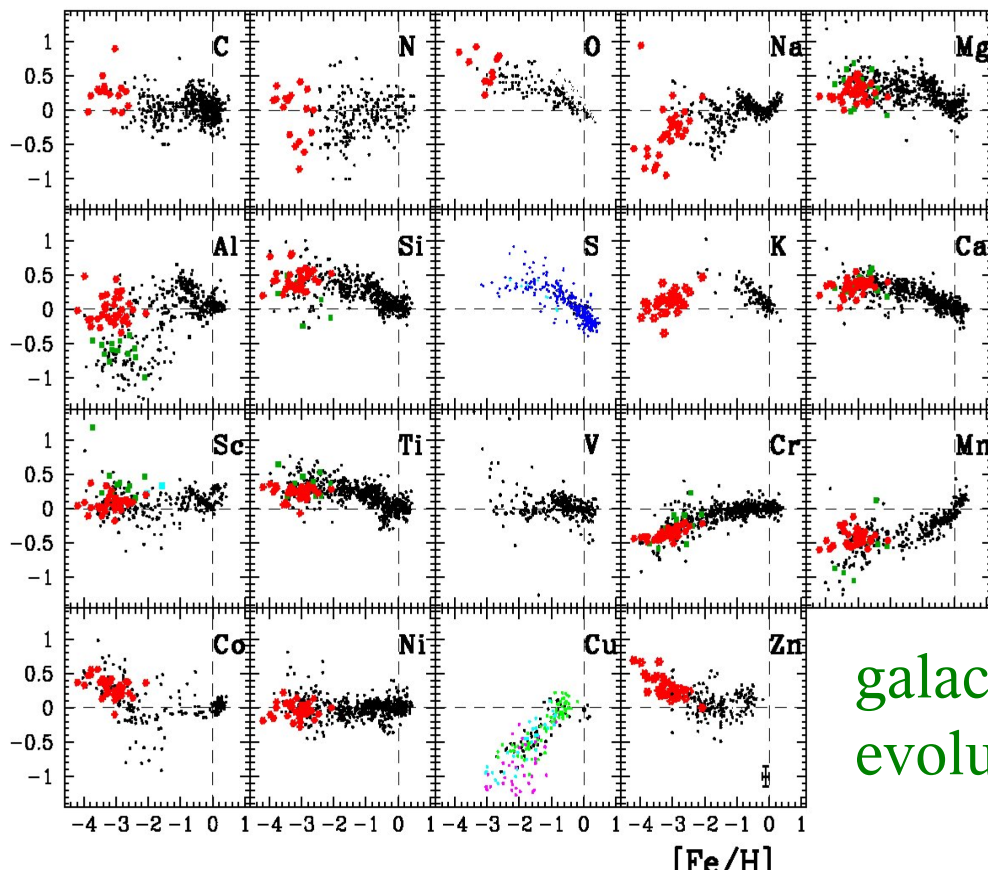

galactic evolution?

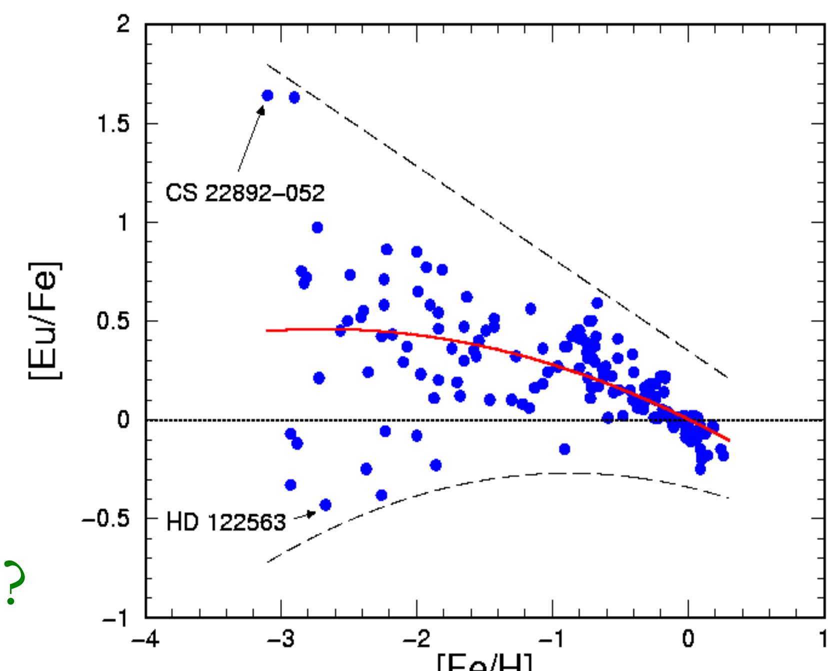

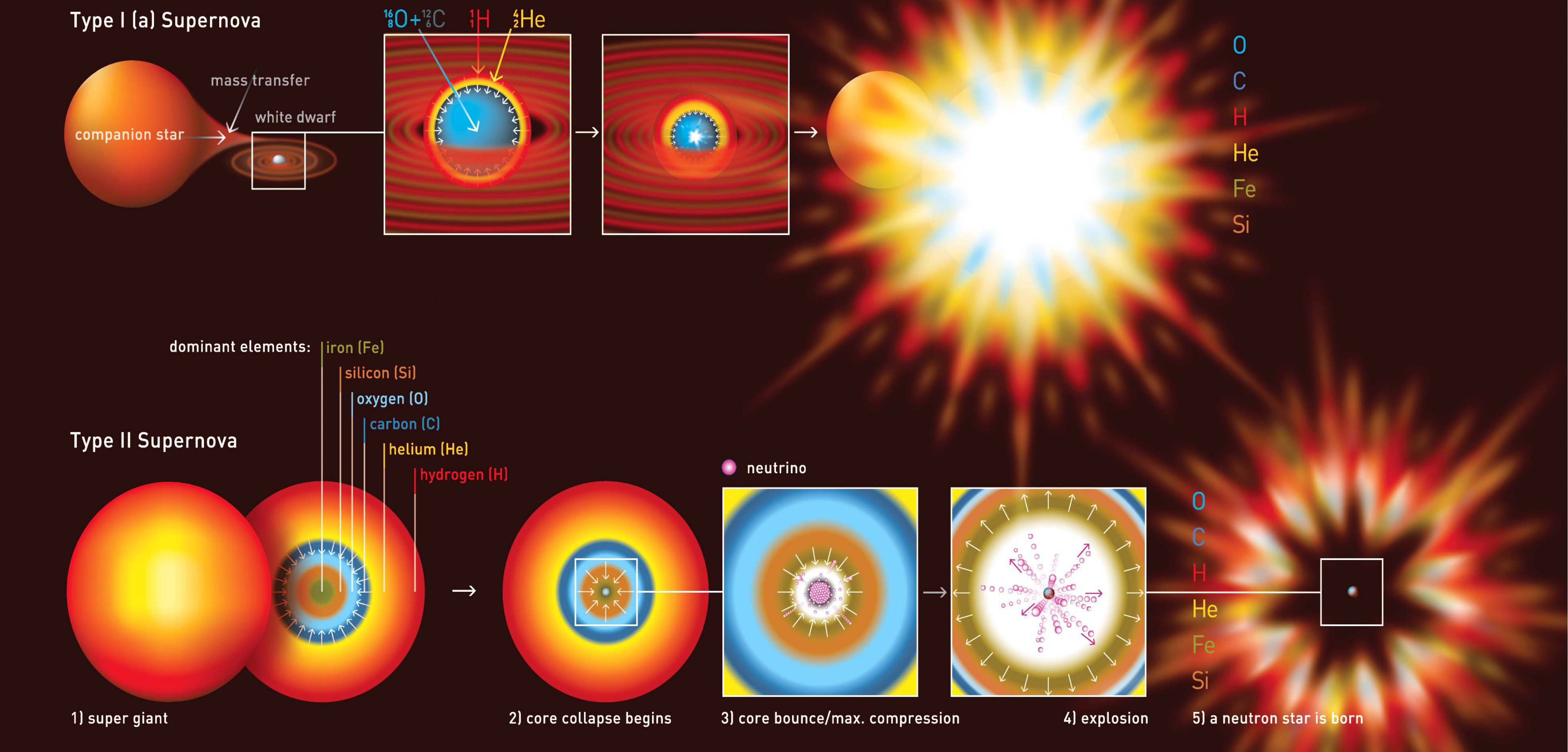
Type I (a) Supernova
$^{16}_{8}O + ^{12}_{6}C$
$^{1}_{1}H$
$^{4}_{2}He$
mass transfer
white dwarf
companion star
O
C
H
He
Fe
Si
dominant elements:
iron (Fe)
silicon (Si)
oxygen (O)
carbon (C)
helium (He)
hydrogen (H)
Type II Supernova
neutrino
O
C
H
He
Fe
Si
1) super giant
2) core collapse begins
3) core bounce/max. compression
4) explosion
5) a neutron star is born

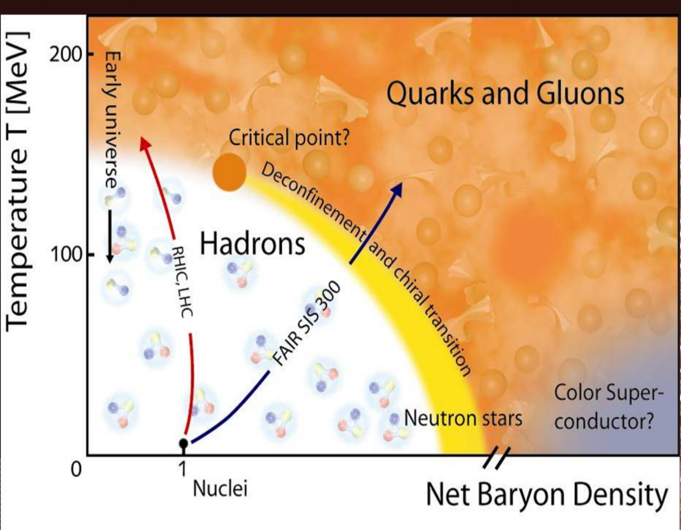
Temperature T [MeV]
200
100
0
Early universe
Quarks and Gluons
Critical point?
Deconfinement and chiral transition
Hadrons
RHIC, LHC
FAIR SIS 300
Neutron stars
Color Super-
conductor?
1
Nuclei
Net Baryon Density

SN 1987A

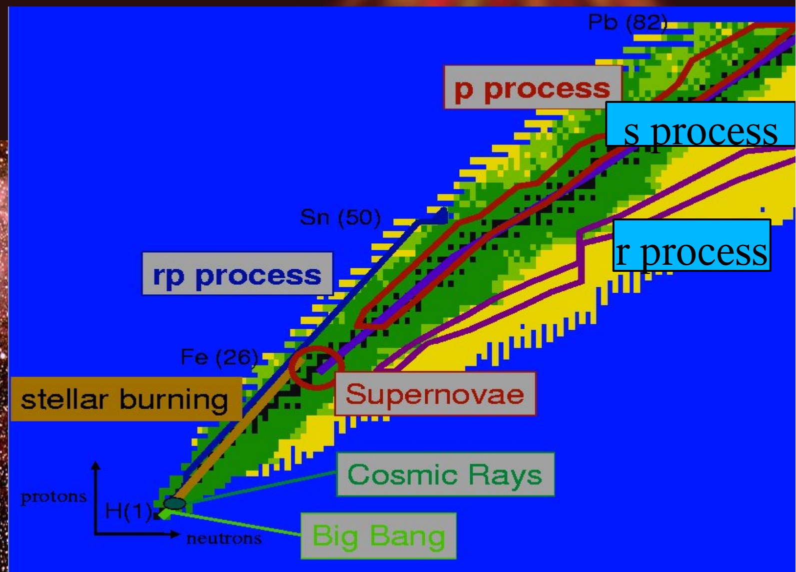
Pb (82)
p process
s process
Sn (50)
r process
rp process
Fe (26)
stellar burning
Supernovae
Cosmic Rays
protons
H(1)
neutrons
Big Bang

Supernova Classification According to Spectra

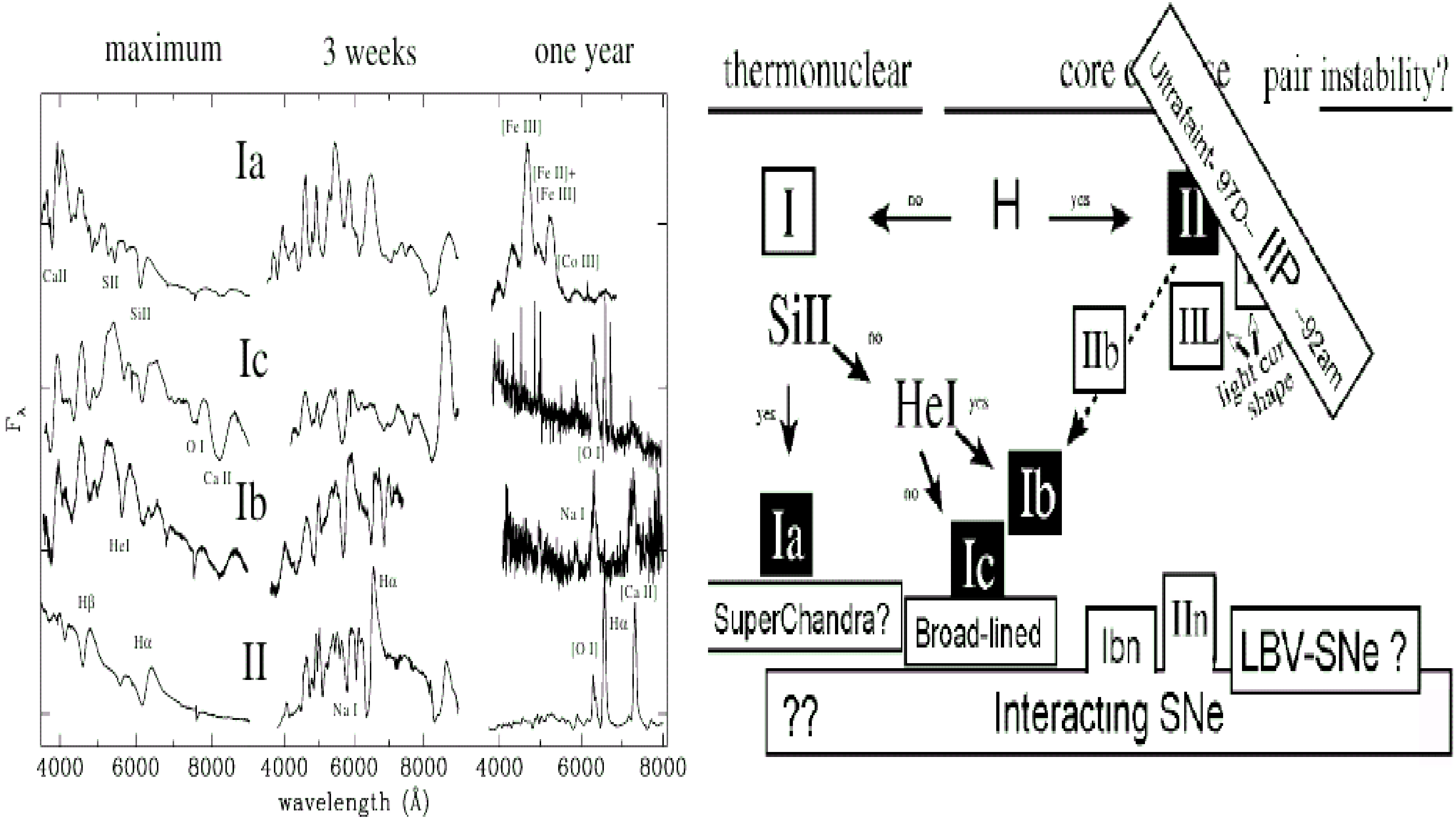

from Turatto (2003) and Turatto et al. (2007)

Brief Summary of Burning Stages (Major Reactions)

1. Hydrogen Burning — $T = (1\text{-}4)\times10^{7}K$
   - pp-cycles -> $^{1}H(p,e^{+}\nu)^{2}H$
   - CNO-cycle -> slowest reaction $^{14}N(p,\gamma)^{15}O$
2. Helium Burning — $T=(1\text{-}2)\times10^{8}K$
   - $^{4}He+^{4}He \Leftrightarrow {}^{8}Be$ $\quad$ $^{8}Be(\alpha,\gamma)^{12}C[(\alpha,\gamma)^{16}O]$
   - $^{14}N(\alpha,\gamma)^{18}F(\beta^{+})^{18}O(\alpha,\gamma)^{22}Ne(\alpha,n)^{25}Mg$ (n-source, alternatively $^{12}C((\alpha,□)^{16}O)$
3. Carbon Burning — $T=(6\text{-}8)\times10^{8}K$
   - $^{12}C(^{12}C,\alpha)^{20}Ne$ $\quad$ $^{23}Na(p,\alpha)^{20}Ne$
   - $^{12}C(^{12}C,p)^{23}Na$ $\quad$ $^{23}Na(p,\gamma)^{24}Mg$
4. Neon Burning — $T=(1.2\text{-}1.4)\times10^{9}K$
   - $^{20}Ne(\gamma,\alpha)^{16}O$
   - $^{20}Ne(\alpha,\gamma)^{24}Mg[(\alpha,\gamma)^{28}Si]$ $\quad$ $30kT = 4MeV$
5. Oxygen Burning — $T=(1.5\text{-}2.2)\times10^{9}K$
   - $^{16}O(^{16}O,\alpha)^{28}Si$ $\quad$ $^{31}P(p,\alpha)^{28}Si$
   - $......,p)^{31}P$ $\quad$ $...,n)^{31}S(\beta^{+})^{31}P$ $\quad$ $^{31}P(p,\gamma)^{23}S$
6. "Silicon" Burning — $T=(3\text{-}4)\times10^{9}K$

(all) photodisintegrations and capture reactions possible

$\Rightarrow$ thermal (chemical) equilibrium

ongoing measurements of key fusion reactions at low energies

Global Chemical (=Nuclear Statistical) Equilibrium (NSE)

$$\bar{\mu}(Z,N) + \bar{\mu}_n = \bar{\mu}(Z,N+1)$$
$$\bar{\mu}(Z,N) + \bar{\mu}_p = \bar{\mu}(Z+1,N)$$

$$\bar{\mu}_i = kT \ln \left(\frac{\rho N_A Y_i}{G_i} \left(\frac{2\pi\hbar^2}{m_i kT} \right)^{3/2} \right) + m_i c^2$$

$$N \text{neutrons} + Z \ \text{ protons} \rightleftharpoons (Z,N)$$

$$N\bar{\mu}_n + Z\bar{\mu}_p = \bar{\mu}_{Z,N}.$$

$$Y(Z,N) = G_{Z,N}(\rho N_A)^{A-1} \frac{A^{3/2}}{2^A} \left(\frac{2\pi\hbar^2}{m_u kT} \right)^{\frac{3}{2}(A-1)} \exp(B_{Z,N}/kT) Y_n^N Y_p^Z$$

$$\sum_i A_i Y_i = 1$$
$$\sum_i Z_i Y_i = Y_e$$

Astrophysical Sites

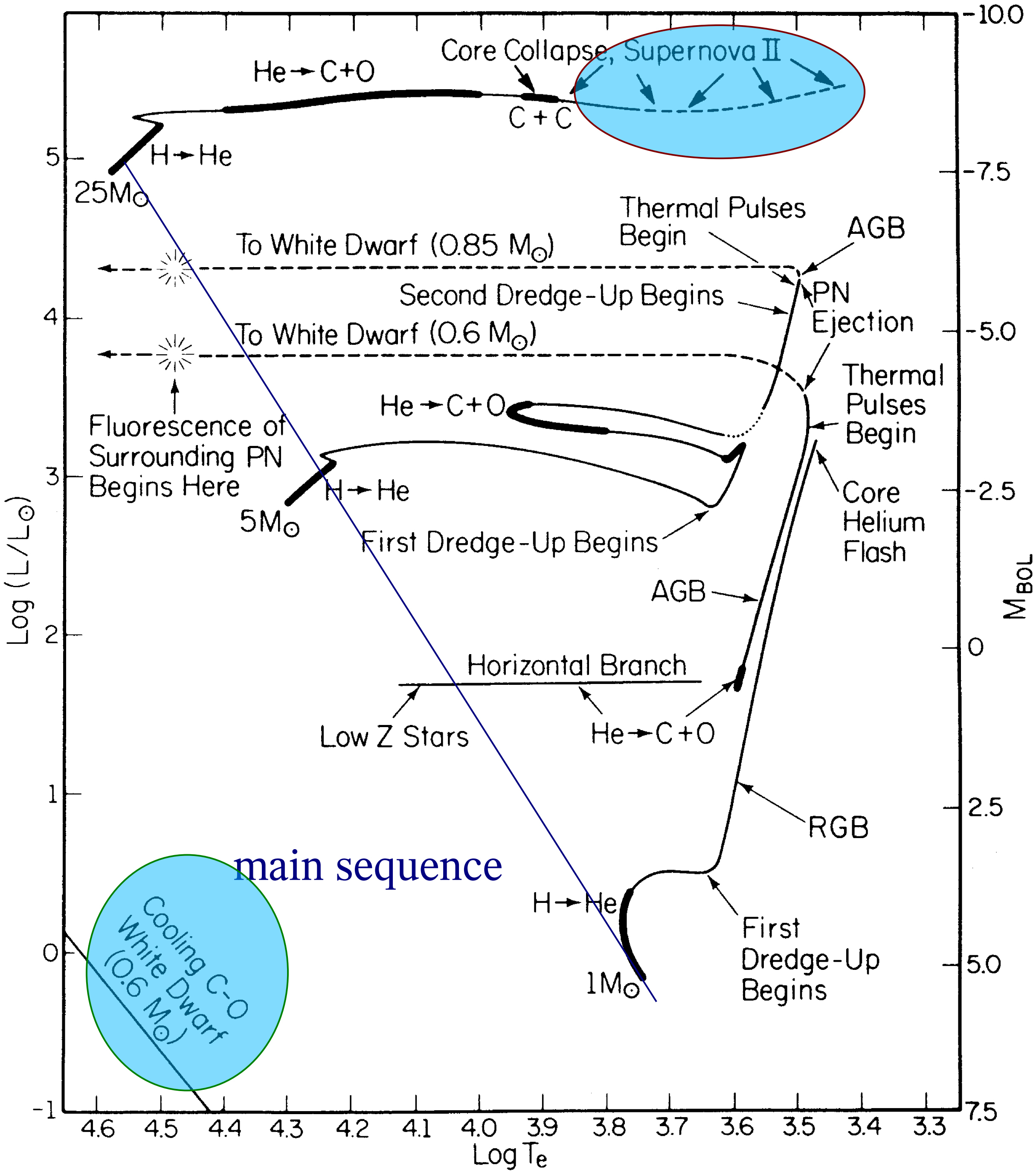

Hertzsprung-Russell Diagram of Stellar Evolution from Iben, showing as end stages

- white dwarfs

and

- core collapse (supernovae/neutron stars, black holes, hypernovae, GRBs?)

influence of reaction cross sections, e-capture in late burning stages, metallicity, rotation, magnetic fields, stellar winds *on final outcome*

Explosive Burning

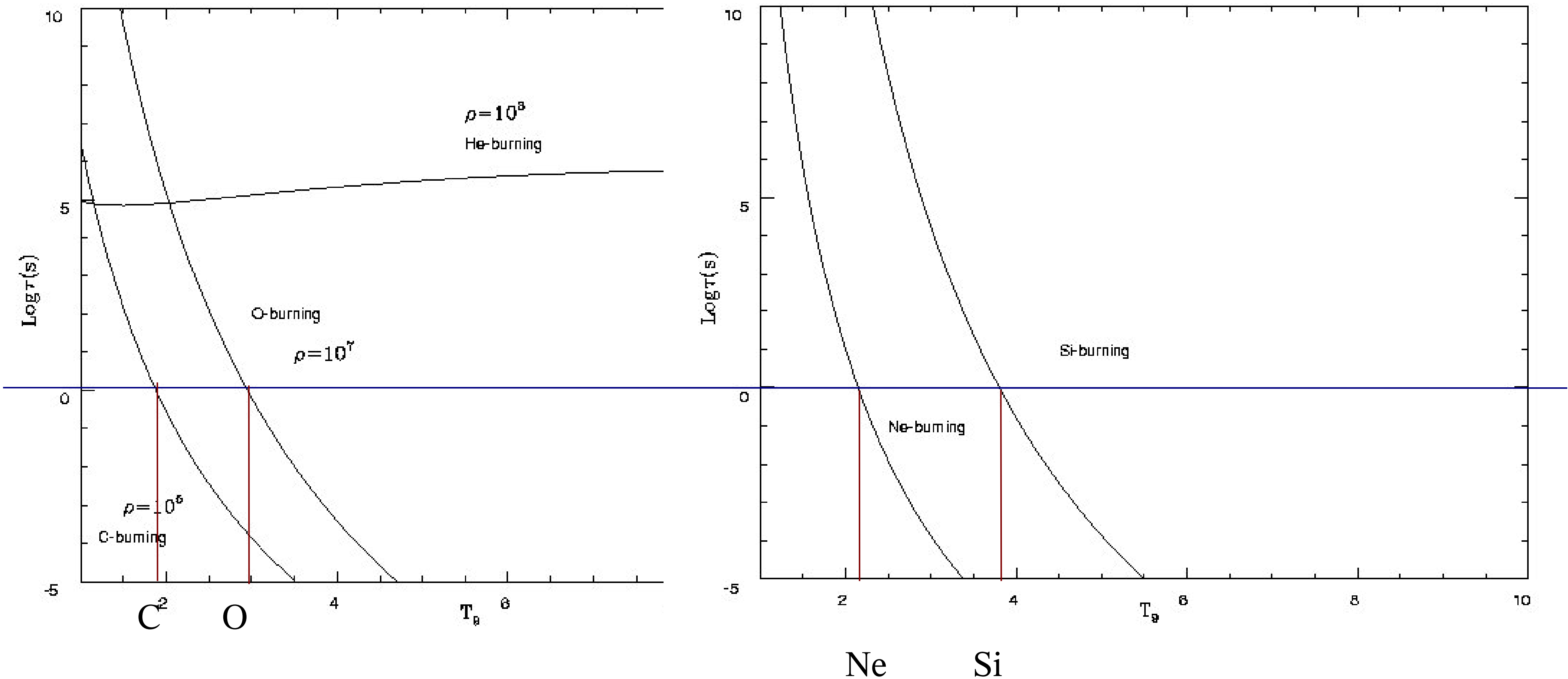

typical explosive burning process timescale order of seconds: fusion reactions (He, C, O) density dependent (He quadratic, C,O linear) photodisintegrations (Ne, Si) not density dependent

Explosive Si-Burning

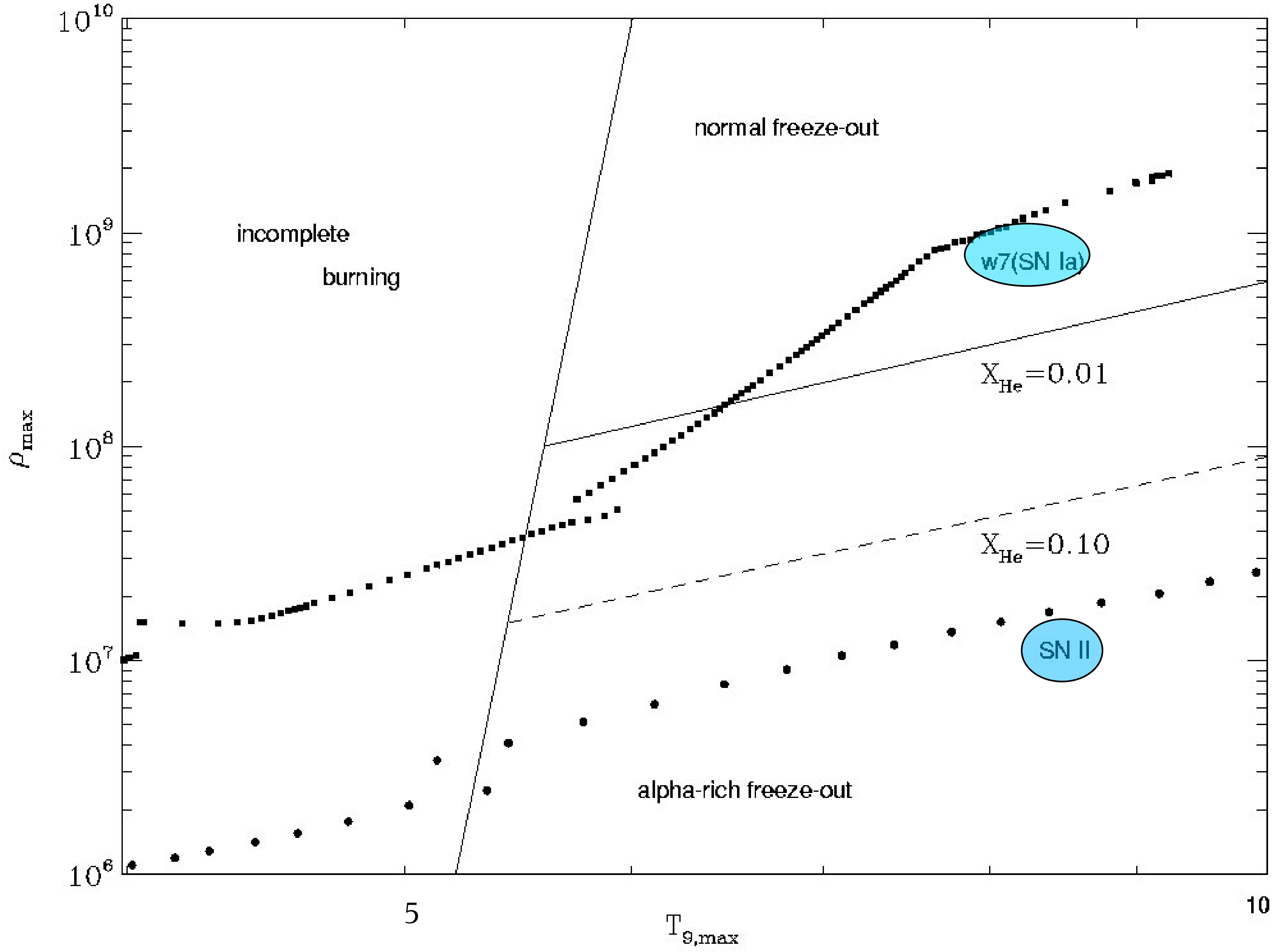

Explosive Burning above a critical temperature destroys (photodisintegrates) all nuclei and (re-)builds them up during the expansion. Dependent on density, the full NSE is maintained and leads to only Fe-group nuclei (normal freeze-out) or the reactions linking ^{4}He to C and beyond freeze out earlier (alpha-rich freeze-out).

Quasi-Equilibrium (QSE)

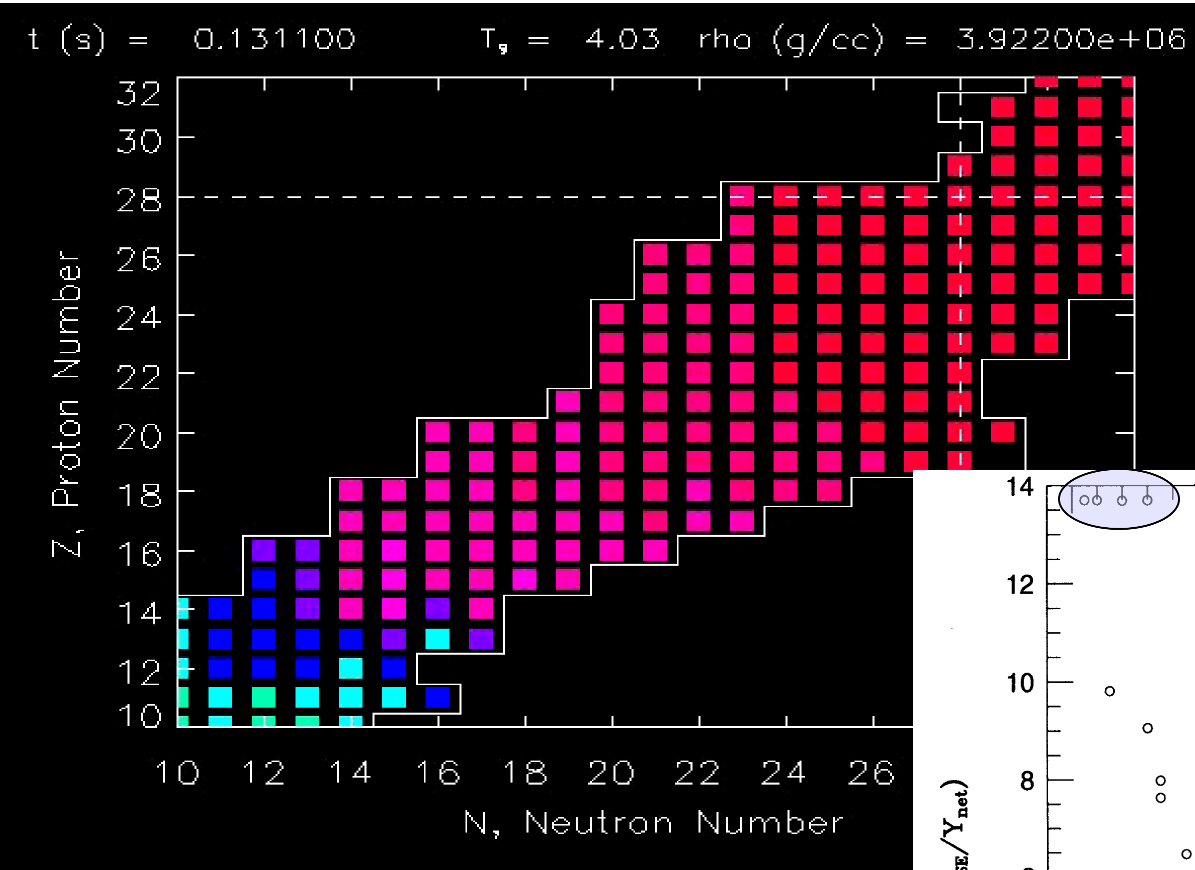

full NSE is not attained, but there exist equilibrium groups around ^{28}Si, ^{56}Ni and n,p,^{4}He, which are separated by slow reactions

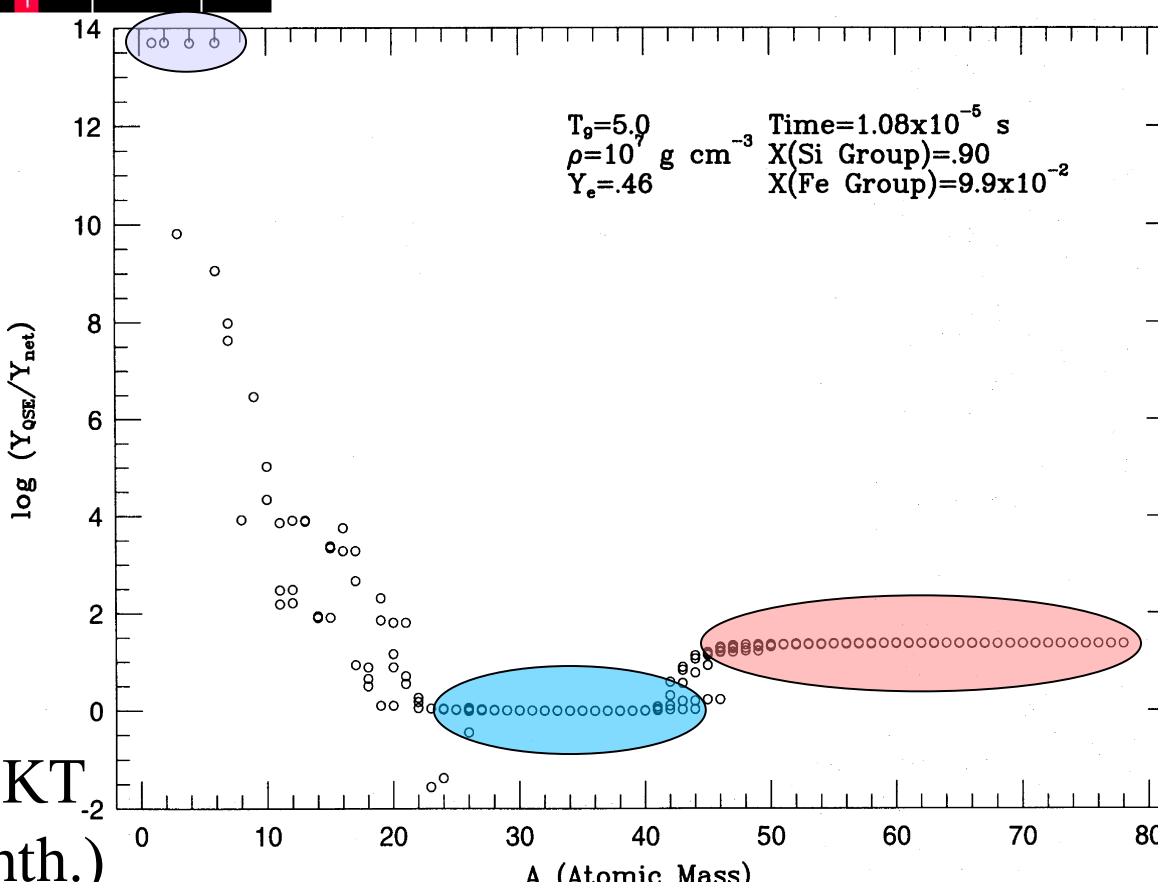

Sample Calculations from

- B.S. Meyer and
- Hix and Thielemann
- Hix, Parete-Koon, Freiburghaus, FKT (2007, advantages in 3D nucleosynth.)

s-, r- and p-Process

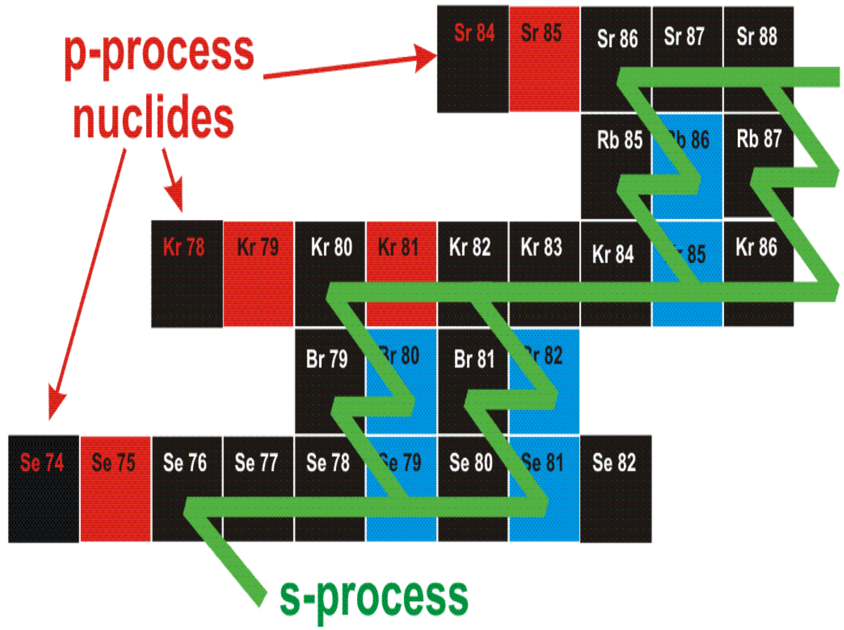

F. Käppeler

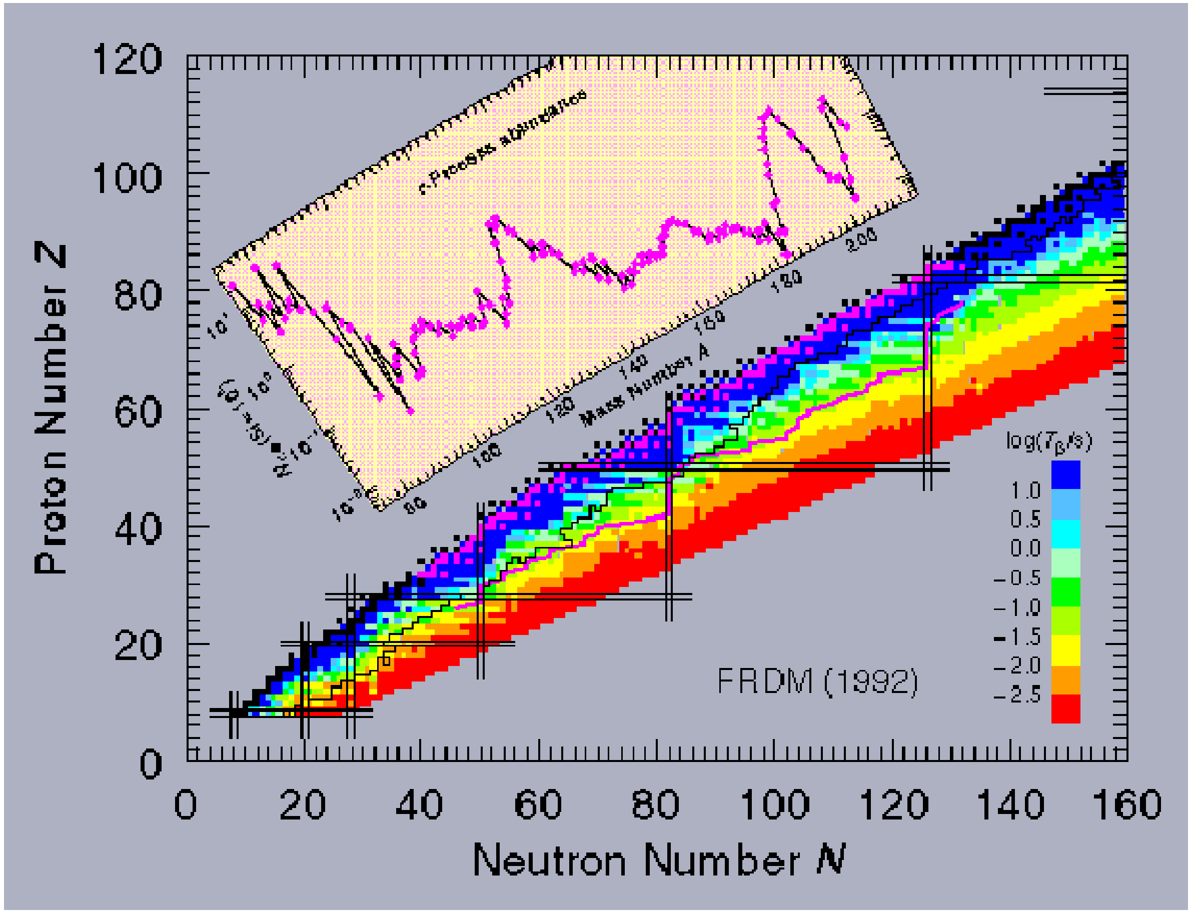

P. Möller

Wind Losses During Stellar Evolution (Effects of Rotation)

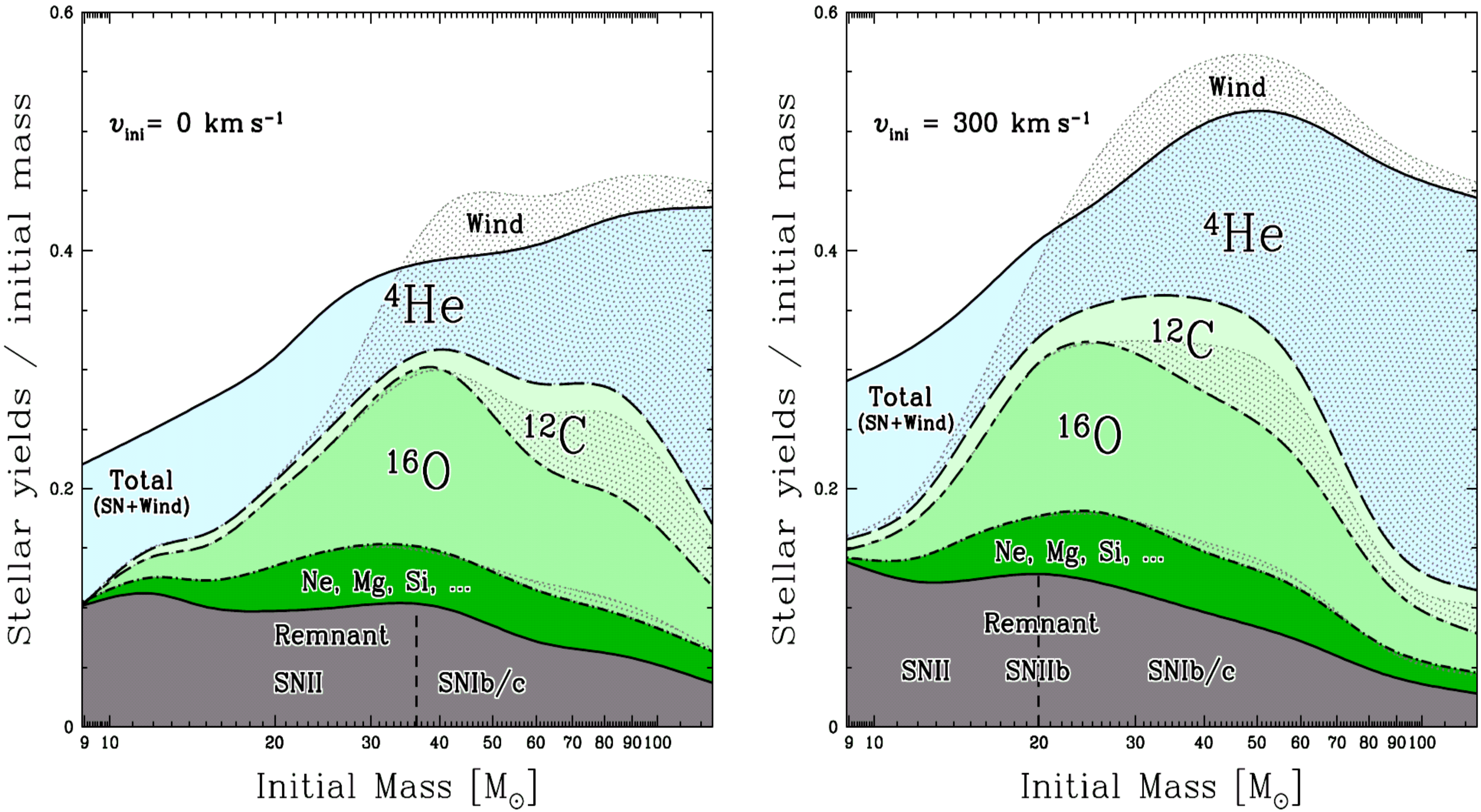

Stellar yields divided by the initial mass as a function of the initial mass for non–rotating (left) and rotating (right) models at solar metallicity (Hirschi et al. 2005)

Effect of fast Rotation on Stellar Evolution and Wind Losses

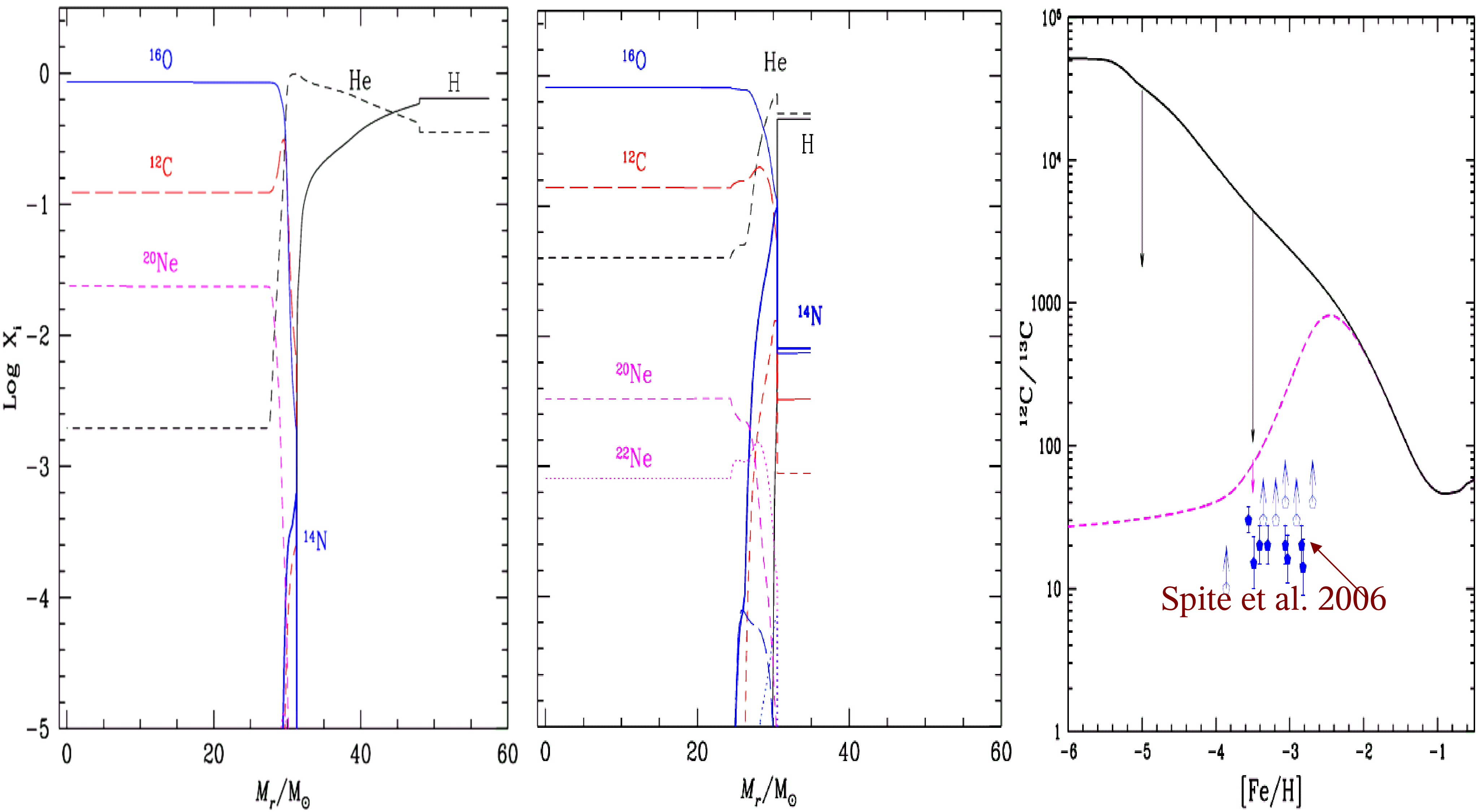

Predicted evolution of 60 M_{sol} PopIII star with 52 or 65% critical rotation (Meynet et al. 2007). Evolution of $^{12}C/^{13}C$ ratio for stellar yields without or with the inclusion of fast rotators for metallicities below $Z = 10^{-5}$ solid line/dashed line (Chiappini et al. 2009), also producing primary N and increasing N/O and C/O (Hirschi et al. 2008)

s-Process (neutron) Sources

Core burning of massive stars (weak s-process)

1. Helium Burning T=(1-2)x10^8K

$^4He + ^4He \Leftrightarrow ^8Be$ $^8Be(\alpha,\gamma)^{12}C[(\alpha,\gamma)^{16}O]$

$^{14}N(\alpha,\gamma)^{18}F(\beta^+)^{18}O(\alpha,\gamma)^{22}Ne(\alpha,n)^{25}Mg$

2. Carbon Burning T=(6-8)x10^8K

$^{12}C(^{12}C,\alpha)^{20}Ne$ $^{12}C(p,\gamma)^{13}N(\beta^+)^{13}C$

$^{12}C(^{12}C,p)^{23}Na$ $^{13}C(\alpha,n)^{16}O$

protons as well as alphas are not existing intrinsically in C-burning, as destroyed in prior H-burning and He-burning. They come from the C-fusion reaction

He-shell flashes in AGB stars (strong s-process)

protons are mixed in from the H-shell and produce ^{13}C (as in 2. above), but the latter can react with the full He-abundance in He-burning and produce a strong neutron source.

in low and intermediate mass stars the H- and He-shells are located at small distances. They do not burn in a constant fashion. If the H-burning zone is on, it creates He fuel. After sufficient He is produced, He is ignited in an unburned He-rich zone (at sufficient densities and temperatures). The burning is not stable, the amount of energy created in a shallow zone is not sufficient to lift the overlaying H-shell which would cause expansion + cooling, i.e. steady burning. Instead He-burning, being dependent on the density squared, burnes almost explosively (flash), causing then a stronger expansion which even stops H-burning in the H-shell. This behavior repeats in recurrent flashes. H is mixed into the unburned He fuel.

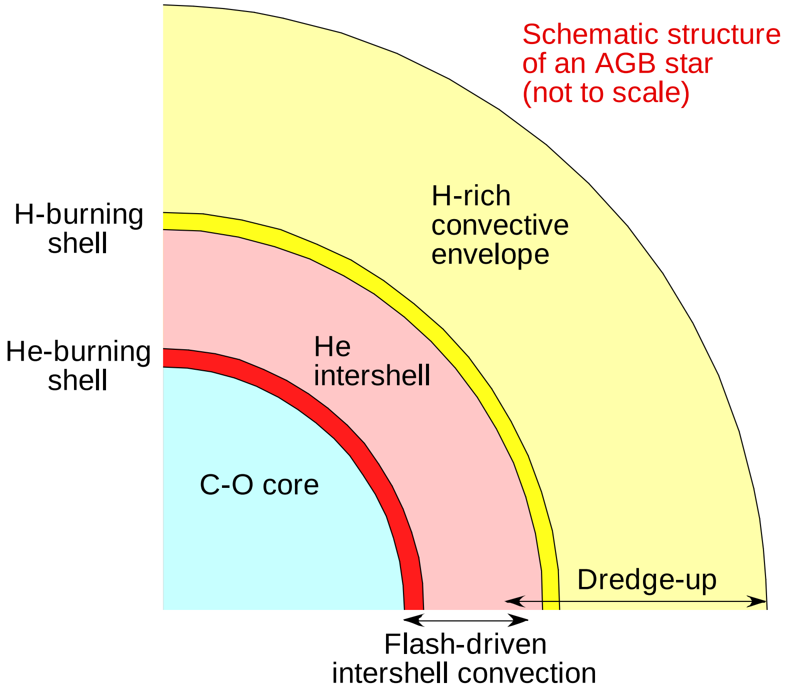

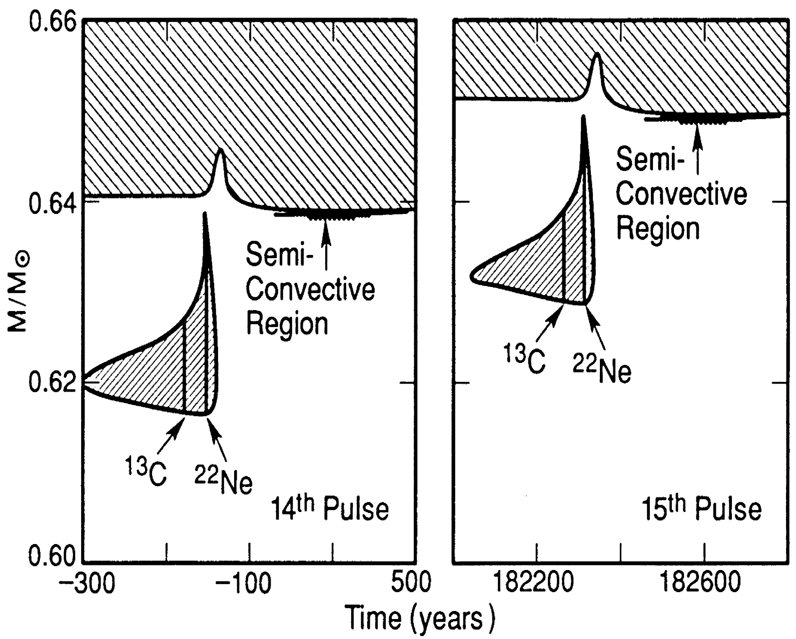

Observations of post-AGB stars, indicating the intrinsic pollution due to strong s-processing

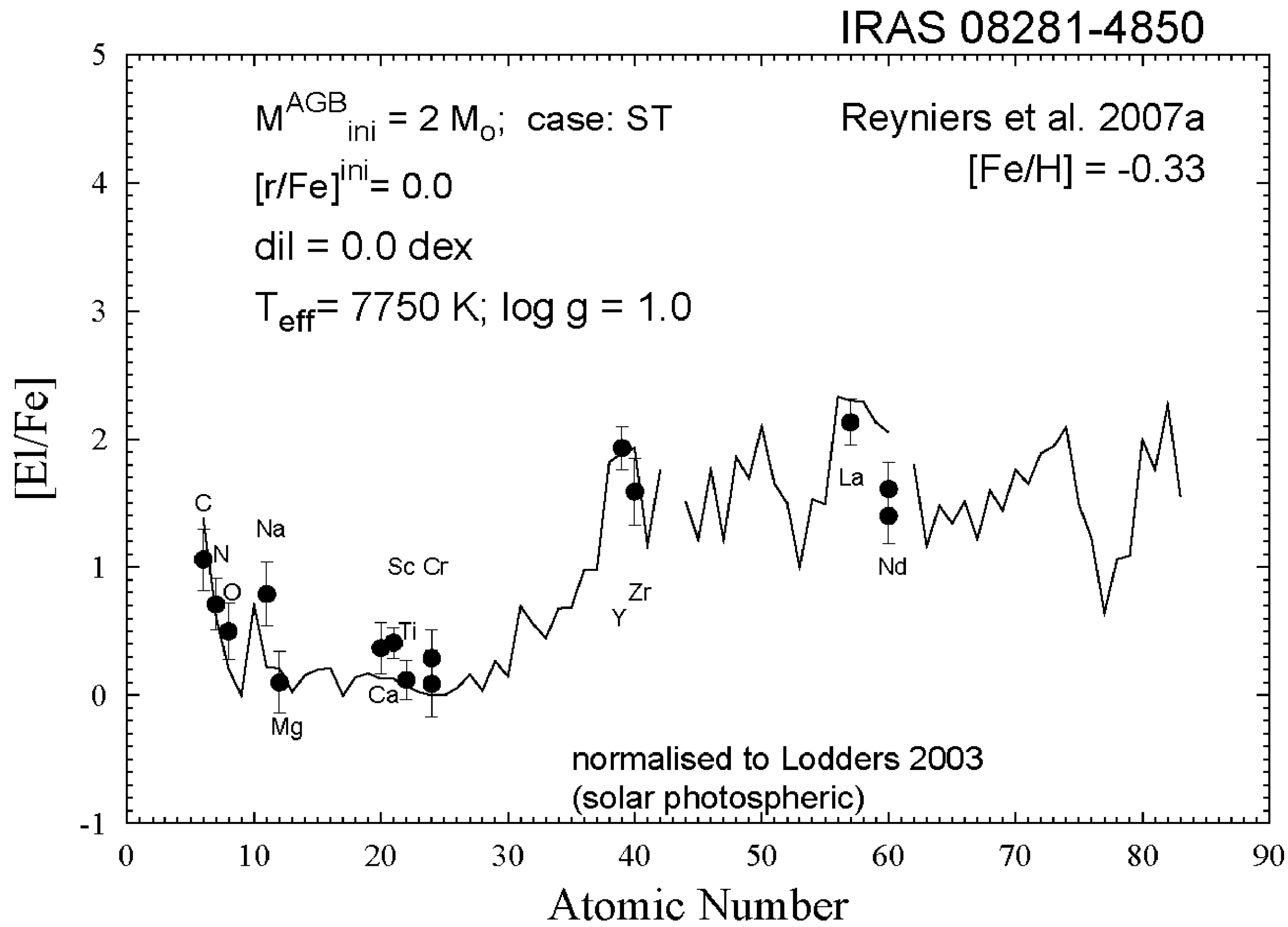

FIGURE 1. Theoretical interpretation of the post-AGB star IRAS 08281-4850 by Reyniers et al. (2007a) [2], with $M_{ini}^{AGB} = 2\ M_{\odot}$, case ST.

Gallino et al. (2008)

The s-process is secondary process (capturing neutrons on pre-existing Fe-group nuclei). A similar neutron exposure on smaller amounts of Fe-seeds leads to stronger production of the heaviest s-nuclei (so-called lead stars).

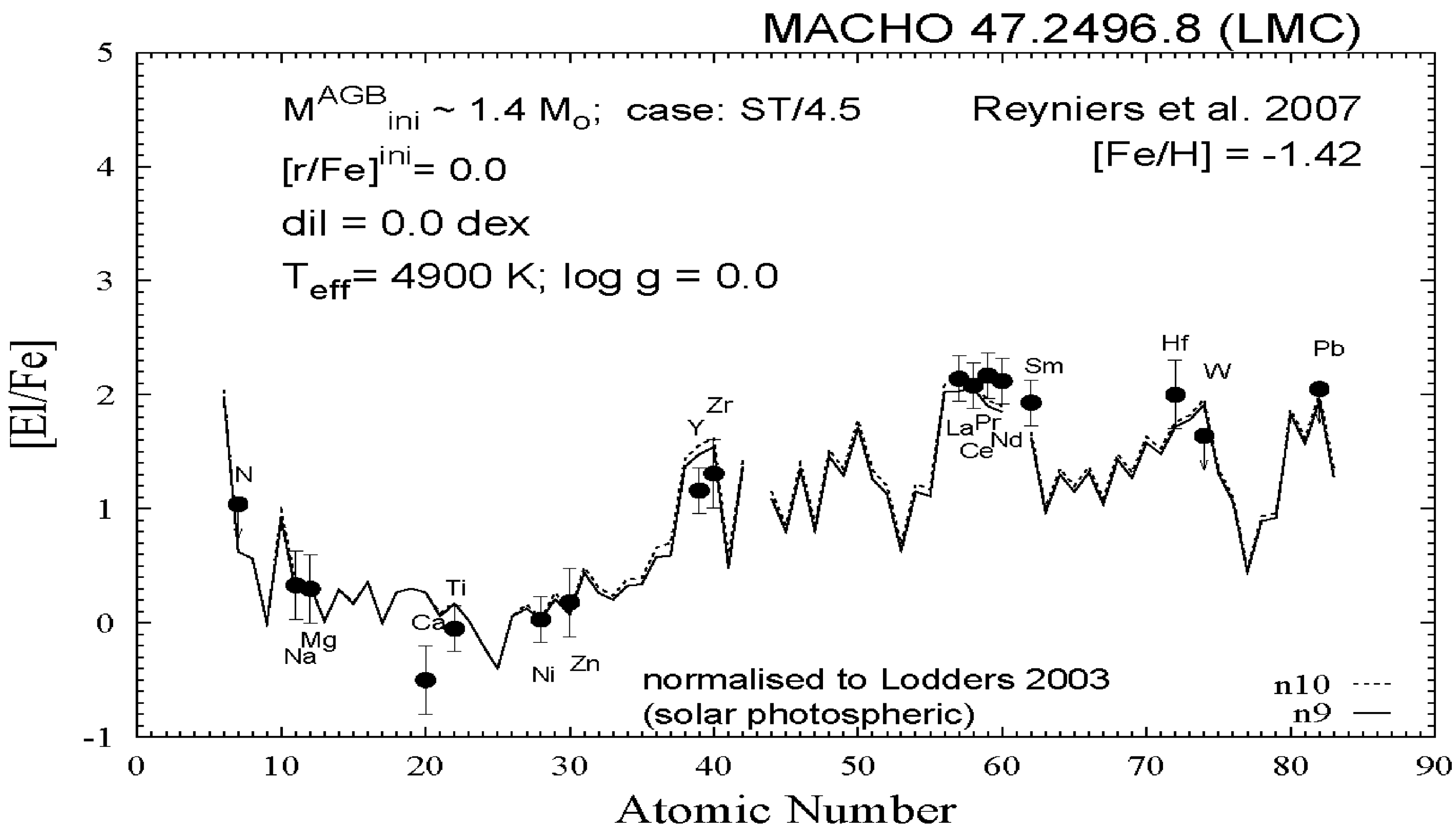

the full process of multi-D mixing is not fully understood yet (resolution and 3D), thus the mixing efficieny is introduced by a paramter (here ST*fac)

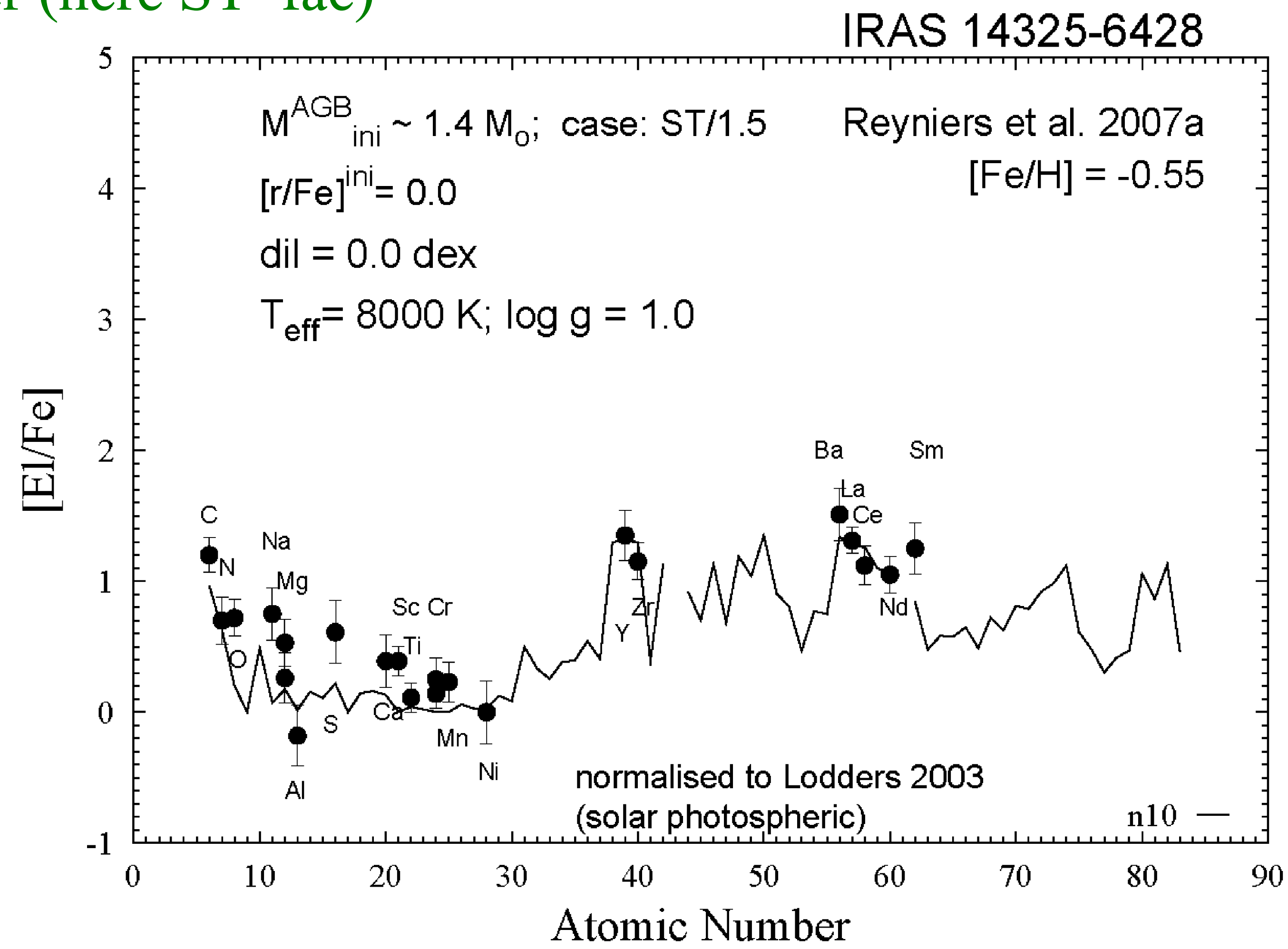

each star shows a specific stage of s-processing, i.e. we have no overall agreement with „solar“ s-process abundances in a single star. Solar s-abundances are only obtained via integrating over an IMF and over galactic evolution with increasing metallicity

Type Ia Supernovae from Accretion in Binary Stellar Systems

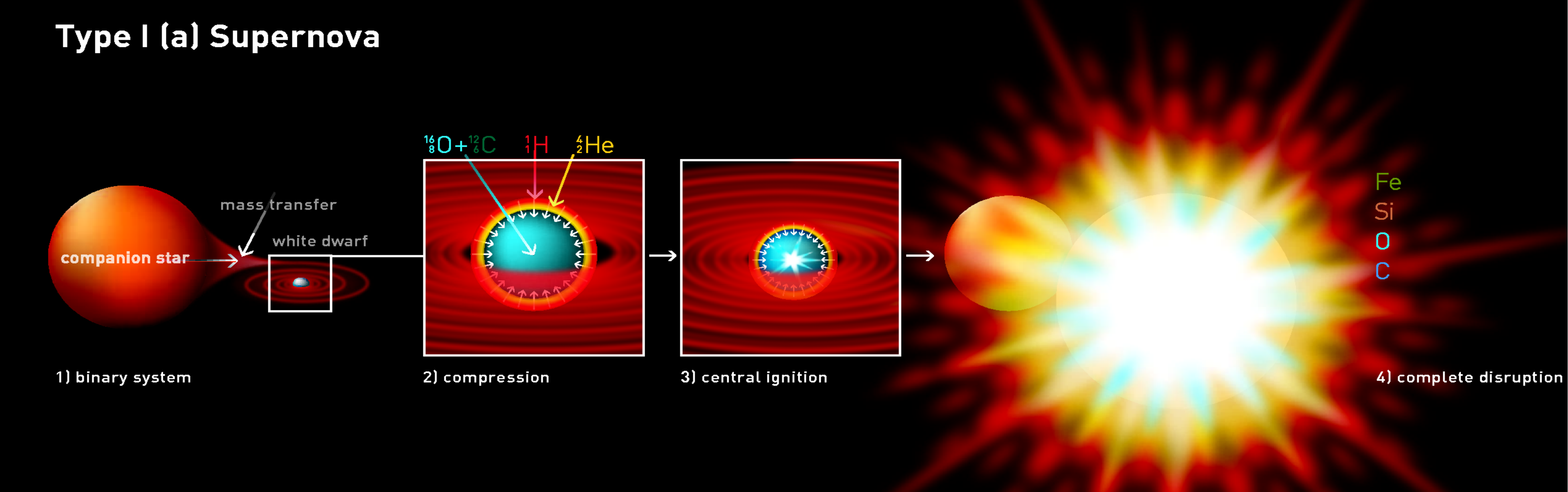

binary systems with accretion onto one compact object can lead (depending on accretion rate) to explosive events with thermonuclear runaway (under electron-degenerate conditions)

- white dwarfs (novae, type Ia supernovae)
- neutron stars (type I X-ray bursts, superbursts?)

Back of the Envelope SN Ia

e.g. W7 (Nomoto, Thielemann, Yokoi 1984); delayed detonations (Khokhlov, Höflich, Müller; Woosley et al.)

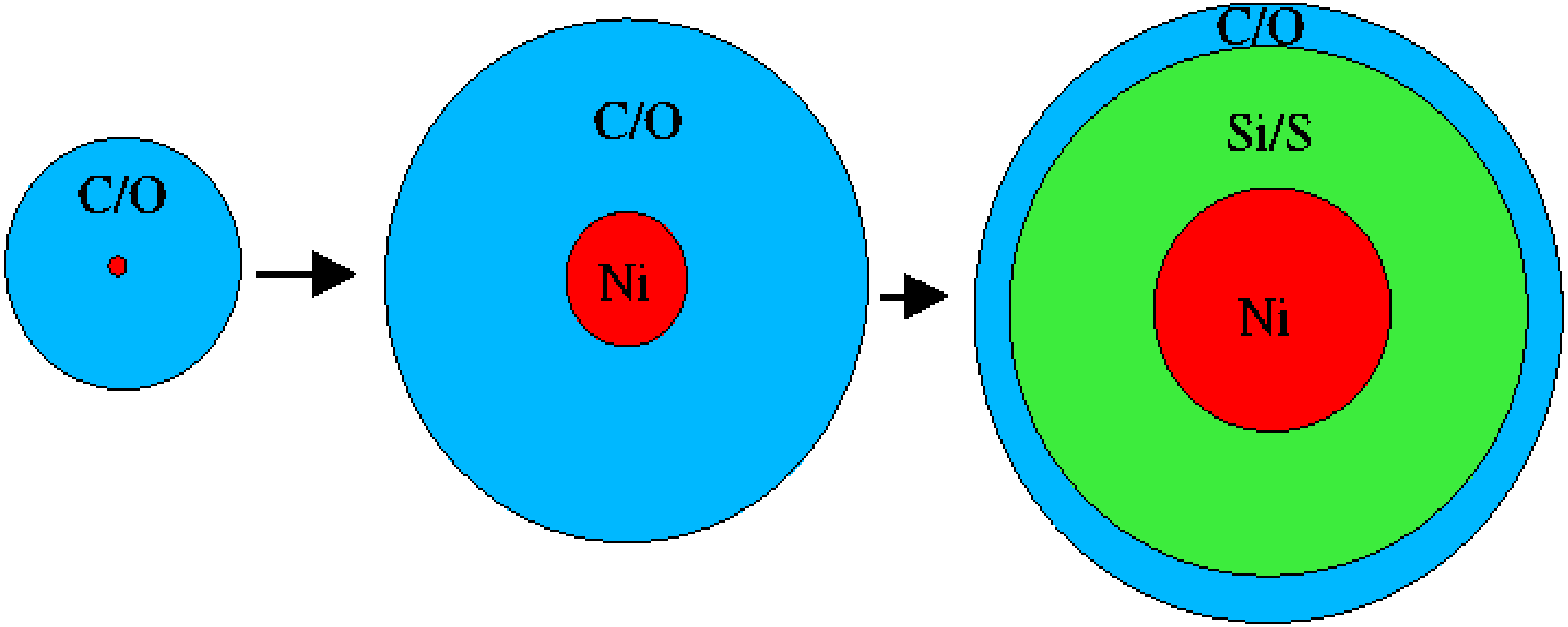

$M_{ch} \approx 1.4 M_\odot$ of $^{12}C/^{16}O$=1 WD $\rightarrow$ 1.398776 $M_\odot$ ^{56}Ni

$\rightarrow$ 2.19$\times 10^{51}$ erg - $E_{grav} \approx (5-6) \times 10^{50}$ erg

reduction due to intermediate elements like Mg, Si, S, Ca

$\rightarrow$ 1.3$\times 10^{51}$ erg

in spherically symmetric models description of the burning front propagation (with hydrodynamic instabilities) determines outcome!

W7 (Nomoto, Thielemann, Yokoi 1984)

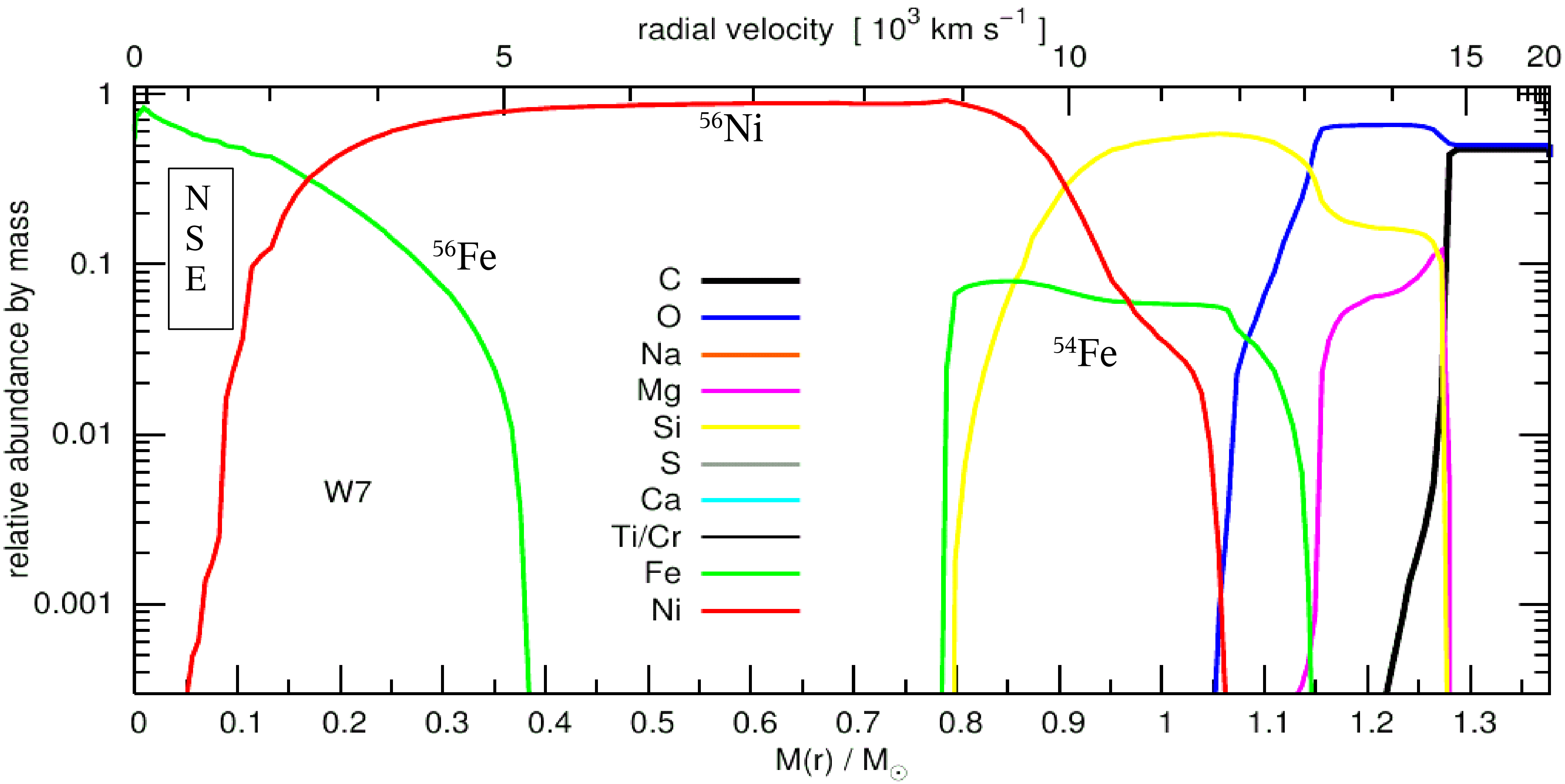

a deflagration (subsonic burning front) with a propagation speed related to a mixing length in time-dependent mixing length theory of 0.7 times the pressure scale height.

Neutronization via electron capture
(high Fermi energies at central densities)

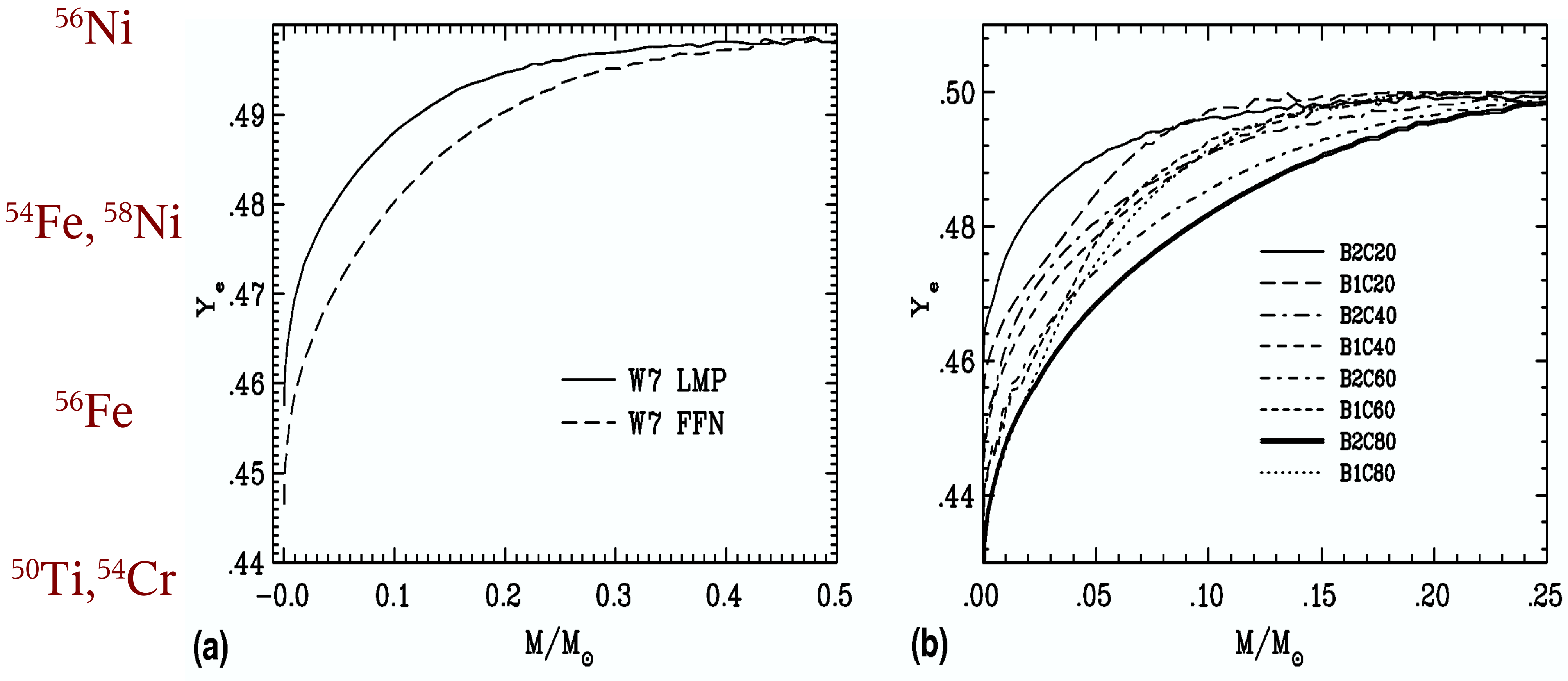

(a) Test for influence of new shell model electron capture rates (including pf-shell Langanke, Martinez-Pinedo 2003)

(b) Test for burning front propagation speed (Brachwitz et al. 2001)

direct influence on dominant Fe-group composition resulting from SNe Ia

Ignition density determines Ye and neutron-richness of (60-70% of) Fe-group

FKT et al. (2004)

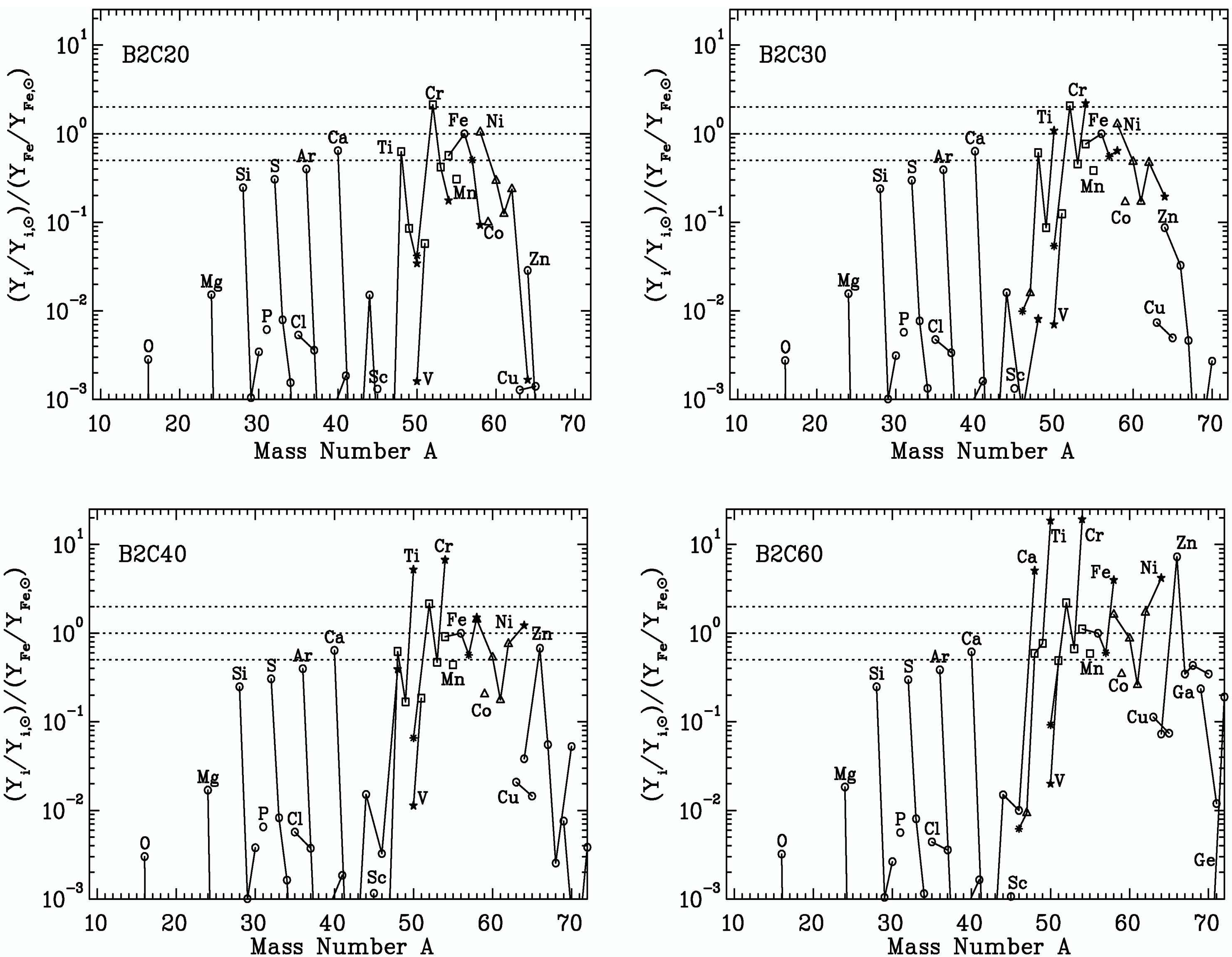

results of explosive C, Ne, O and Si-burning: Fe-group to alpha-elements 2/1-3/1

SNe Ia dominate Fe-group, over-abundances by more than factor 2 not permitted

→

maximum central density 3 10^9 gcm^{-3}

Future 3D Models

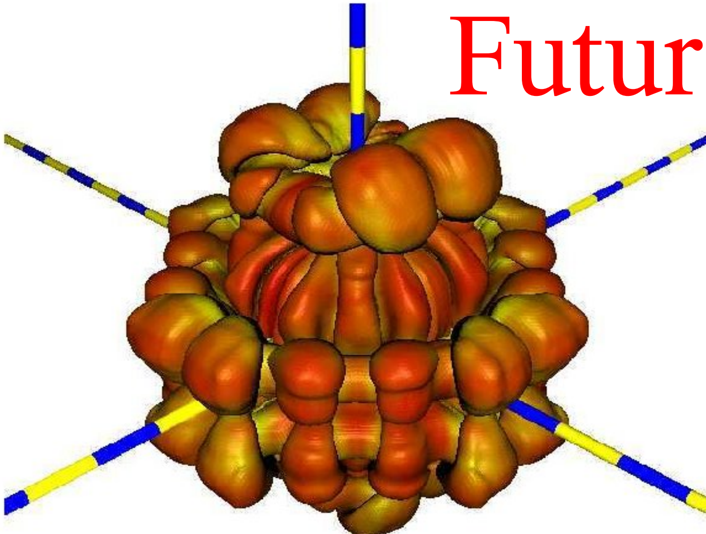

Travaglio, Reinecke, Hillebrandt, FKT (2004, 3D nucleosynthesis with tracer particles)

consistent treatment needed instead of parametrized spherical propagation, MPA Garching (Röpke et al. 2007), U. Chicago/SUNY Stony Brook (Calder et al. 2007)

- *distribution of ignition points uncertain*
- *hydrodynamic instabilities determine propagation of burning*
- *deflagration/detonation transition*

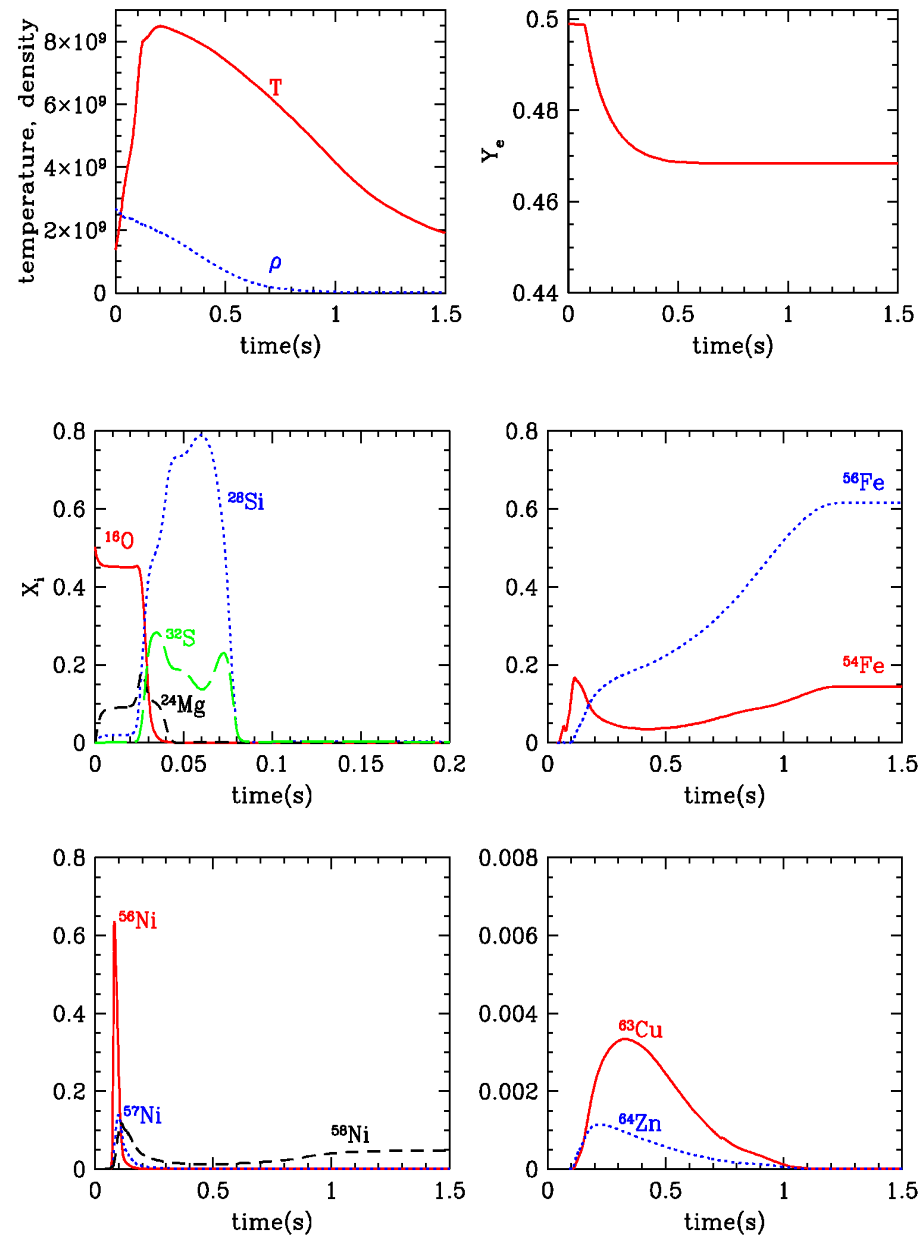

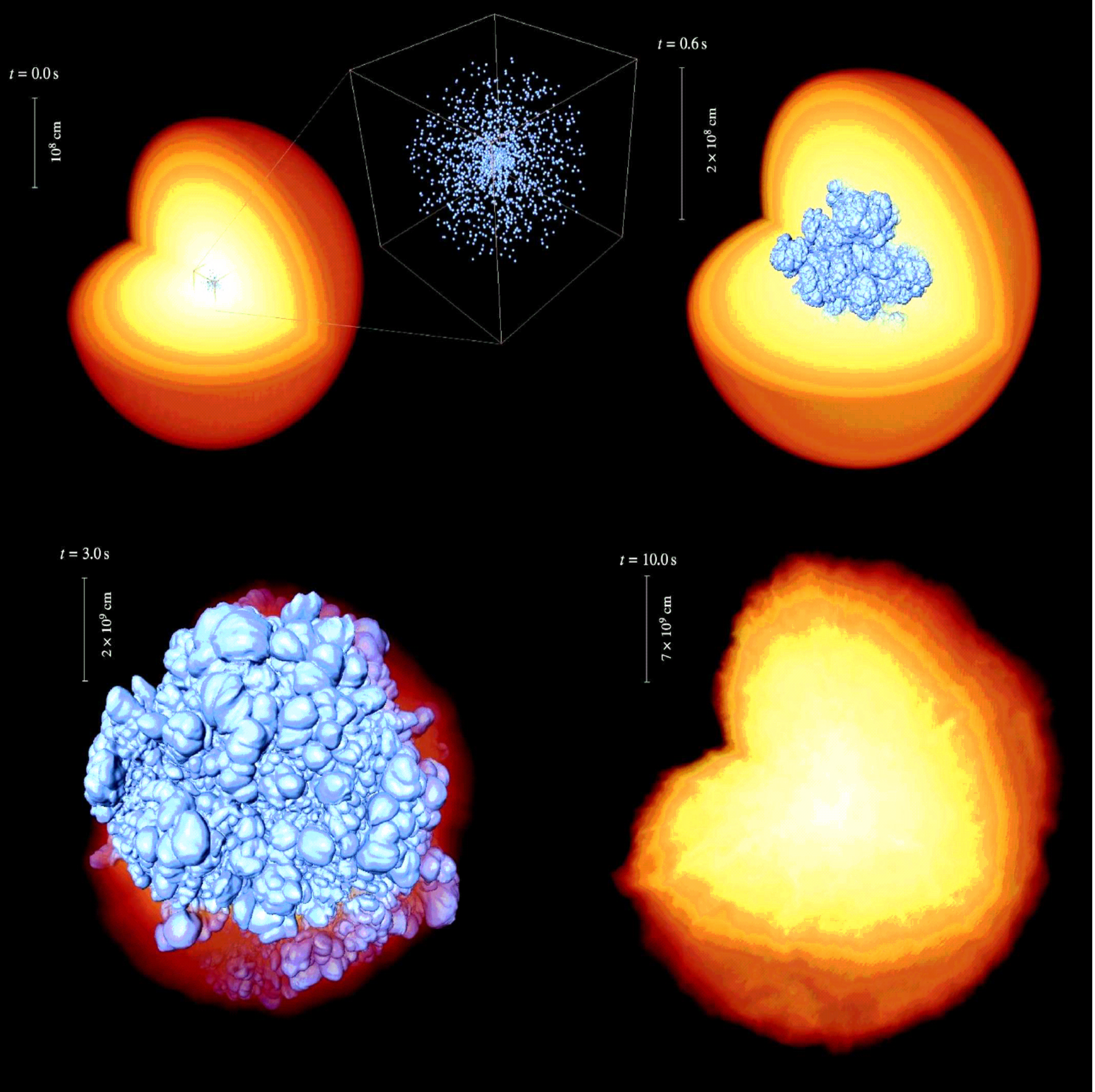

Multi-D Simulations

Snapshots of a full 3D multi-spot-ignited simulation of a SN-Ia deflagration (first three panels). Orange tones mark the WD itself, the blue surface is the flame front. Structures from Rayleigh-Taylor instabilities ('mushrooms') are evident. In the bottom-right panel the density structure of the ejecta is shown (from Röpke et al. 2007).

Alternatives: Gravitationally confined detonations (Plewa et al. 2004, 2007, Kasen & Plewa 2007)

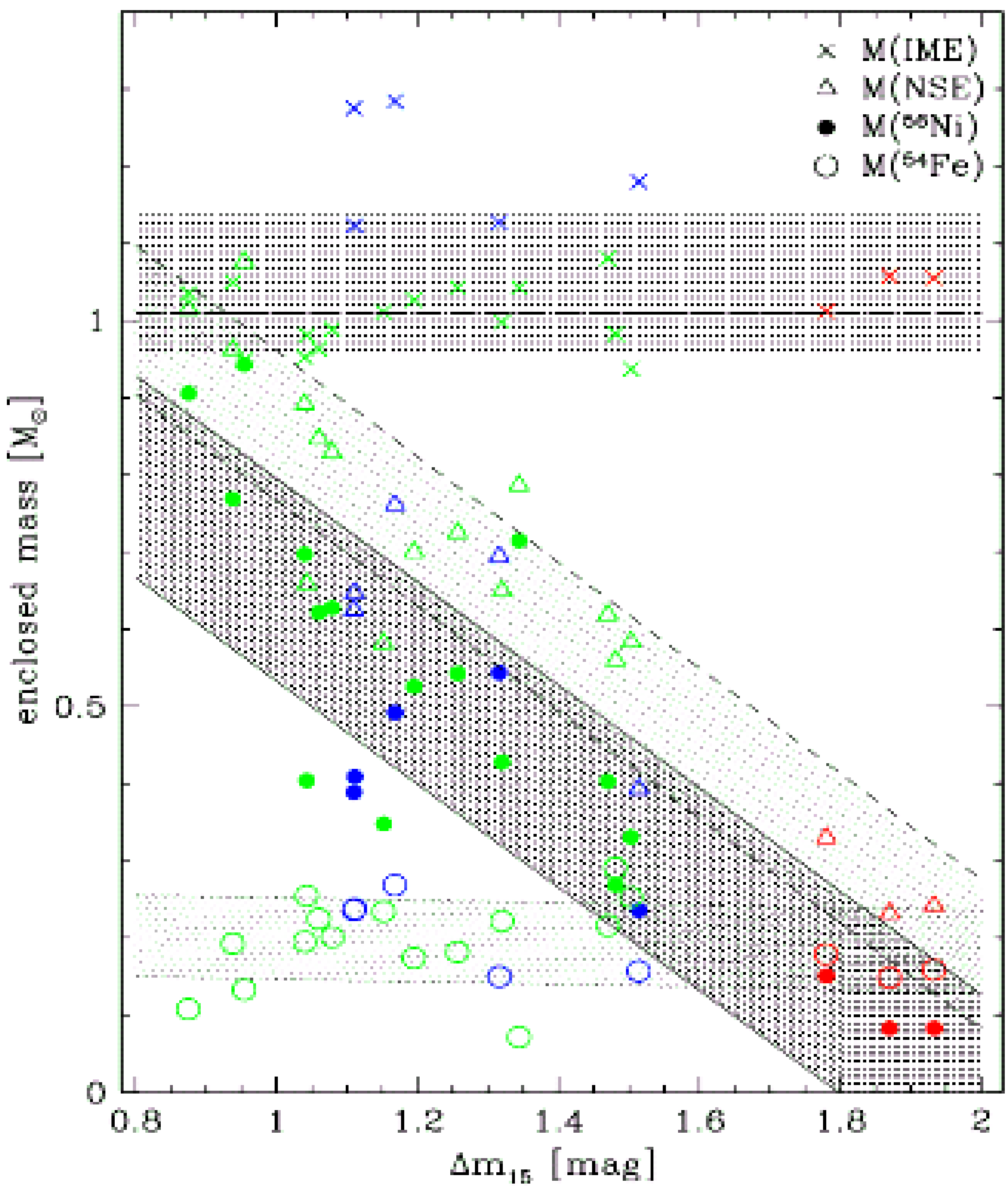

Zorro diagram

The distribution of the main abundance groups in a sample of SNe Ia. The enclosed mass of different burning products is plotted vs. Δm15 (B). Open circles refer to stable ^{54}Fe and ^{58}Ni; solid circles to ^{56}Ni, and open triangles to the sum of these. Crosses show the mass enclosed inside the layer of intermediate mass elements (IME), i.e., the total mass burned.
^{54}Fe and ^{58}Ni in the SN core are roughly constant over all luminosities,while ^{56}Ni determines the luminosity and correlates with Δm15 (B).
The mass enclosed by IME's is inferred to be similar for all SNe of the sample, and the explosion energy seems constant (from Mazzali et al. 2007).

Subluminous Type Ia Supernovae

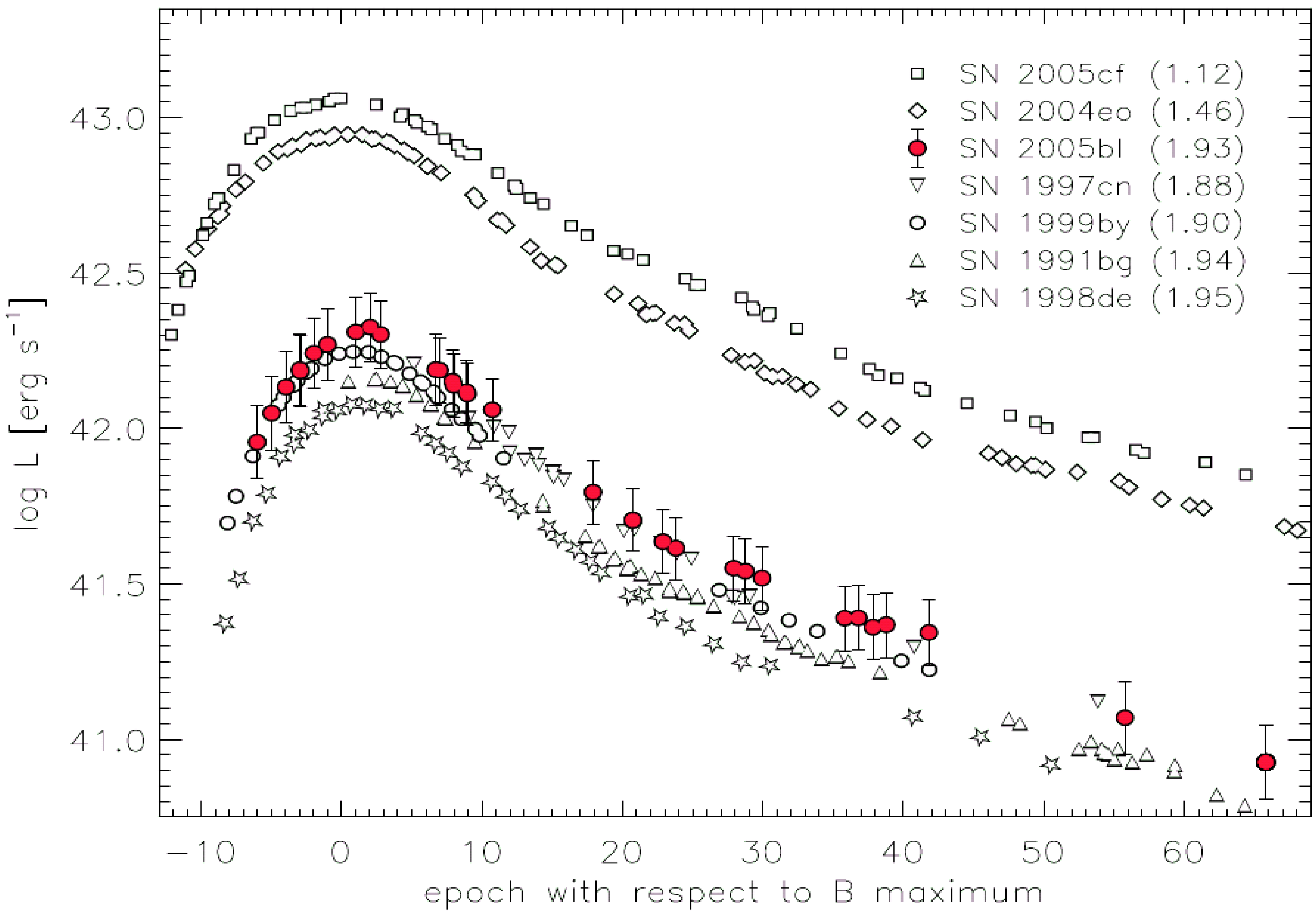

from Taubenberger (2008), Δm_{15} $(B)_{true}$ of these SNe is given in parenthesis

The underluminous Type Ia Supernova 2005bl (Taubenberger 2008)

	−6.0 d	−5.0 d	−3.0 d	+4.8 d	Solar
t [a]	11.0 d	12.0 d	14.0 d	21.8 d	
L_{bol} [b]	1.24×10^{42}	1.56×10^{42}	2.06×10^{42}	2.56×10^{42}	
v_{ph} [c]	7500	7350	7100	6000	
T_{bb} [d]	10 620	10 790	10 670	9230	
X(C)	0.045	0.030	0.010	0.000	2.16×10^{-3}
X(O)	0.905	0.878	0.847	0.788	5.36×10^{-3}
X(Mg)	0.015	0.040	0.060	0.080	6.04×10^{-4}
X(Si)	0.025	0.037	0.060	0.090	6.66×10^{-4}
X(S)	0.006	0.009	0.013	0.020	3.24×10^{-4}
X(Ti)	3.7×10^{-4}	7.3×10^{-4}	1.4×10^{-3}	4.5×10^{-3}	2.79×10^{-6}
X(Cr)	3.7×10^{-4}	7.3×10^{-4}	1.4×10^{-3}	4.5×10^{-3}	1.66×10^{-5}
X(stable Fe)	1.0×10^{-4}	1.2×10^{-4}	4.0×10^{-4}	1.4×10^{-3}	1.15×10^{-3}
X(^{56}Ni) [e]	–	–	2.0×10^{-4}	2.5×10^{-3}	

[a] Time from explosion.
[b] Bolometric luminosity [erg s^{-1}].
[c] Photospheric velocity [km s^{-1}].
[d] Photospheric blackbody temperature [K].
[e] Mass fraction of ^{56}Ni and its decay products.

^{56}Ni mass <0.1M_{sol} (but large Ti and Cr abundances), large amounts of IME's, at least 50% of ejecta unburned material, metallicity in unburned matter smaller than 1/10 solar. Due to spectroscopic similarities of SN 2005bl to SNe 1991bg, 1997cn, 1998de and 1999by and that most of the latter SNe also exploded in early-type, supposedly metal-rich galaxies, this could point towards a very long-lived progenitor population for all underluminous, 91bg-like SNe Ia.

Core Collapse Supernovae from Massive Stars

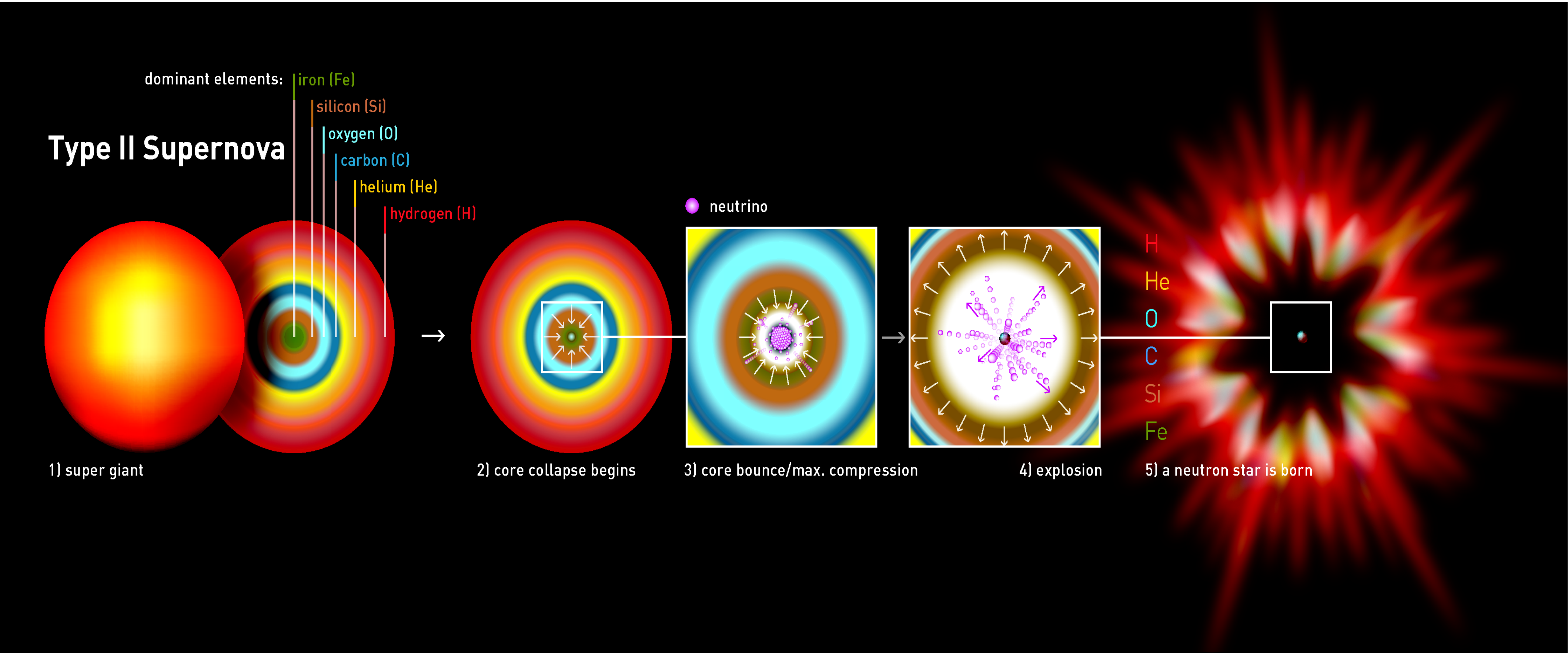

Neutrino-driven Core Collapse Supernovae

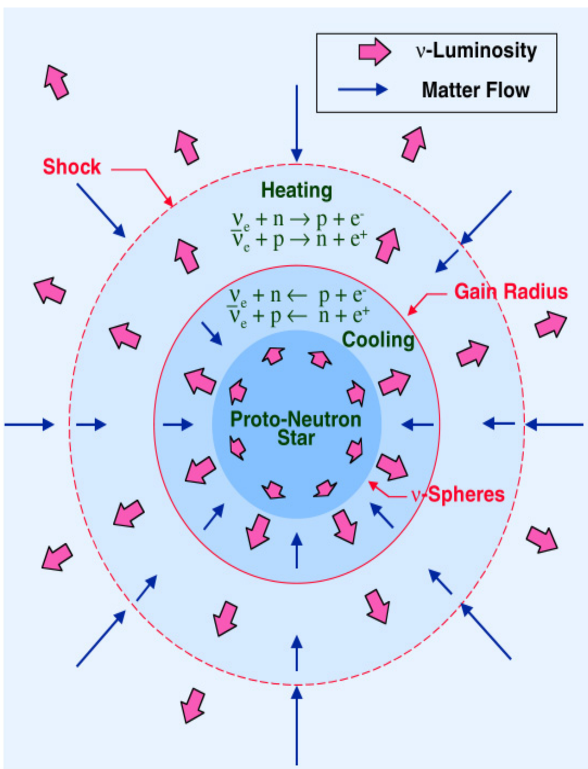

$\nu_e + n \leftrightarrow p + e^-$ heating
$\bar{\nu}_e + p \leftrightarrow n + e^+$

$\nu_e + A' \leftrightarrow A + e^-$ opacity
$\nu + N \leftrightarrow \nu + N$
$\nu + A \leftrightarrow \nu + A$

$\nu + e^- \leftrightarrow \nu + e^-$ thermalization
$e^+ + e^- \leftrightarrow \nu + \bar{\nu}$

$\nu = \nu_e, \nu_\mu, \nu_\tau$ source terms
$e^+ + e^- \leftrightarrow \nu + \bar{\nu}$
$\gamma + \gamma \leftrightarrow \nu + \bar{\nu}$

also
$e + \gamma \leftrightarrow e + \gamma + \nu + \bar{\nu}$
and
$\nu_e + \bar{\nu}_e \rightarrow \nu_{\mu,\tau} + \bar{\nu}_{\mu,\tau}$

Simulations with Rotation and Magnetic Fields

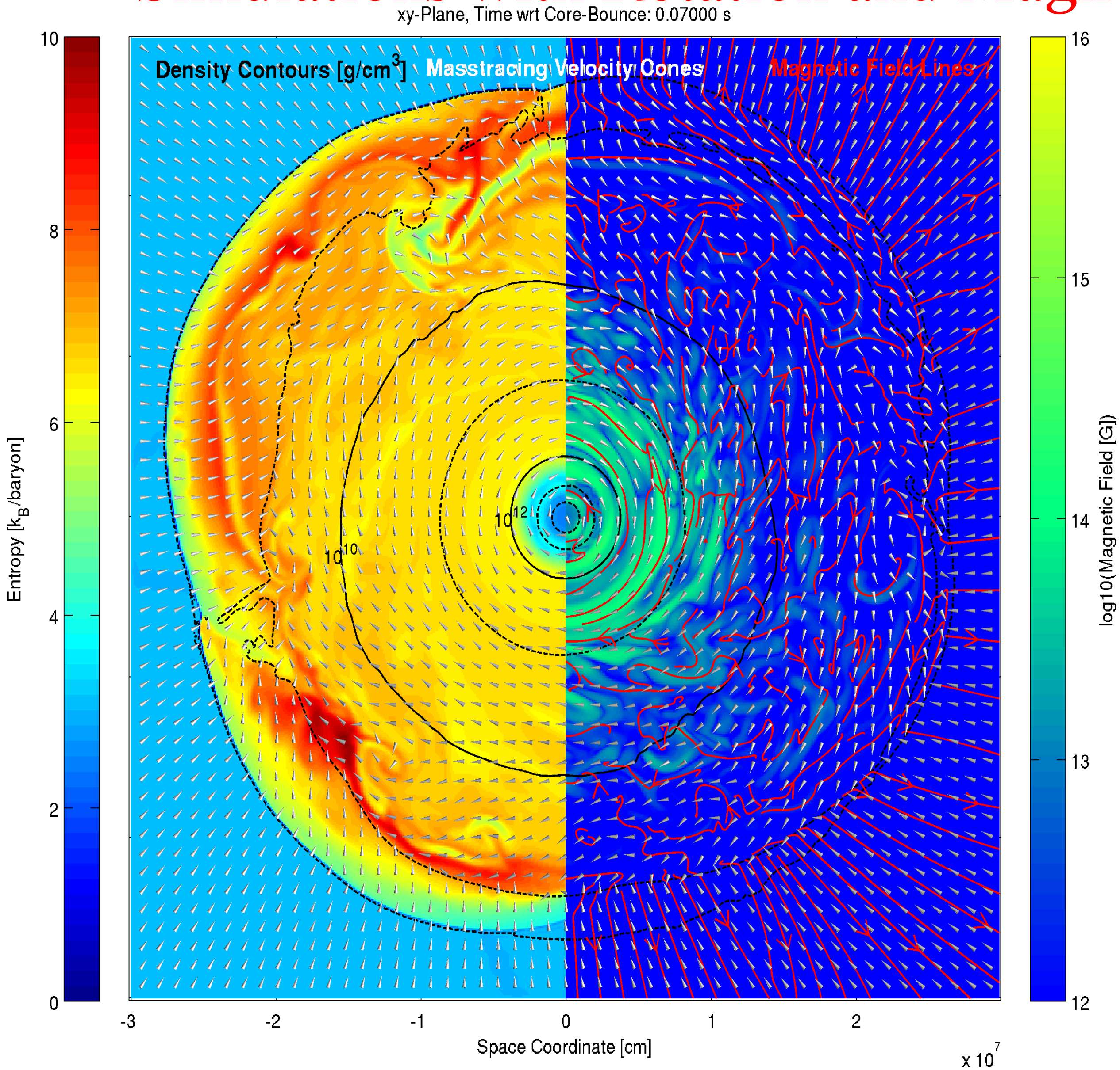

Liebendörfer et al (06) ,Whitehouse et al. (08)

entropy and magnetic field strength 0.07s after bounce

grav. wave signal should be seen with LIGO at 10kpc

full solution of the core collapse SN problem probably includes: 3D, SASI, accoustic modes, MHD, rotation, collective neutrino flav. oscillations? (Duan et al. 07, Dasgupta et al. 08)

“Faking” multi-D hydro with neutrinos

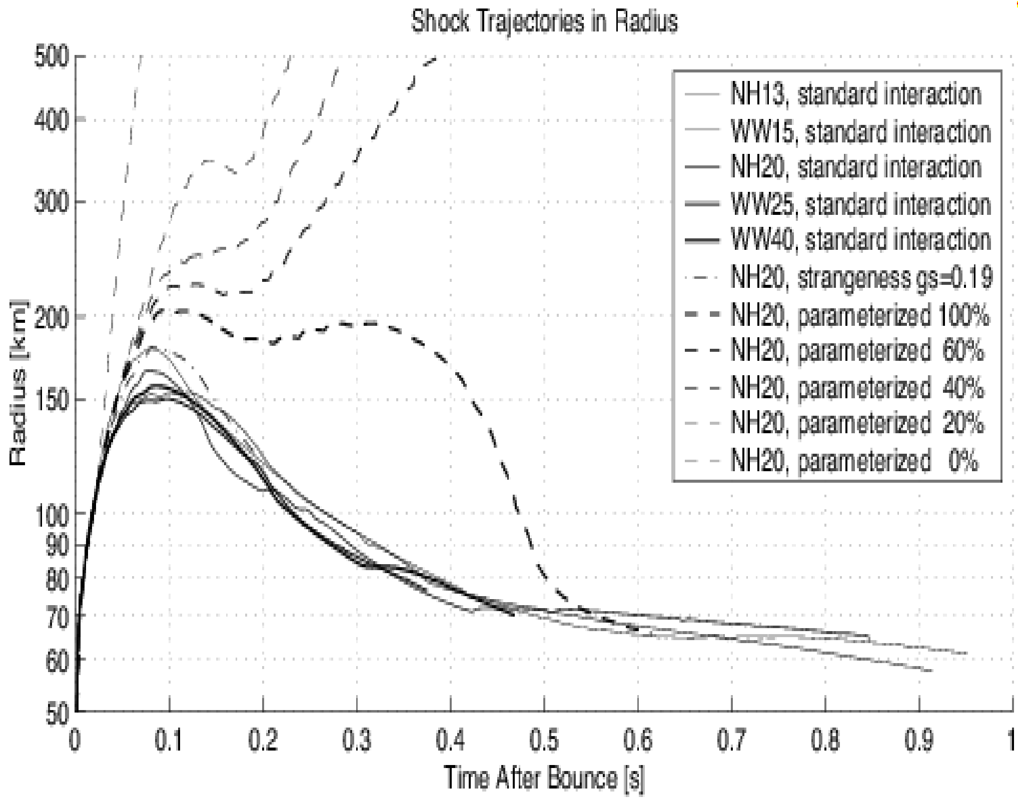

Supernovae do explode, but are changes in ν-scattering or absorption cross sections realistic (uncertainty ≈ 20-30%)?

- Multi-D models show convective instabilities
- proto-neutron star core convection leads to faster ν-transport → higher L_ν
- This acts similar to reduced scattering cross sections
- convection in deposition zone → more efficient energy deposition
- This acts similar to higher absorption cross sections
- → multi-D models are expected to explode!

Liebendörfer et al. (2004) code AGILE/BOLTZTRAN with full Boltzmann neutrino transport

We make use of 1D models and reduction factors on neutrino scattering or enlargement factors in neutrino absorption in order to obtain typical explosion energies

Black hole formation after 0.4 or 1.4s for $40M_{sol}$ star??

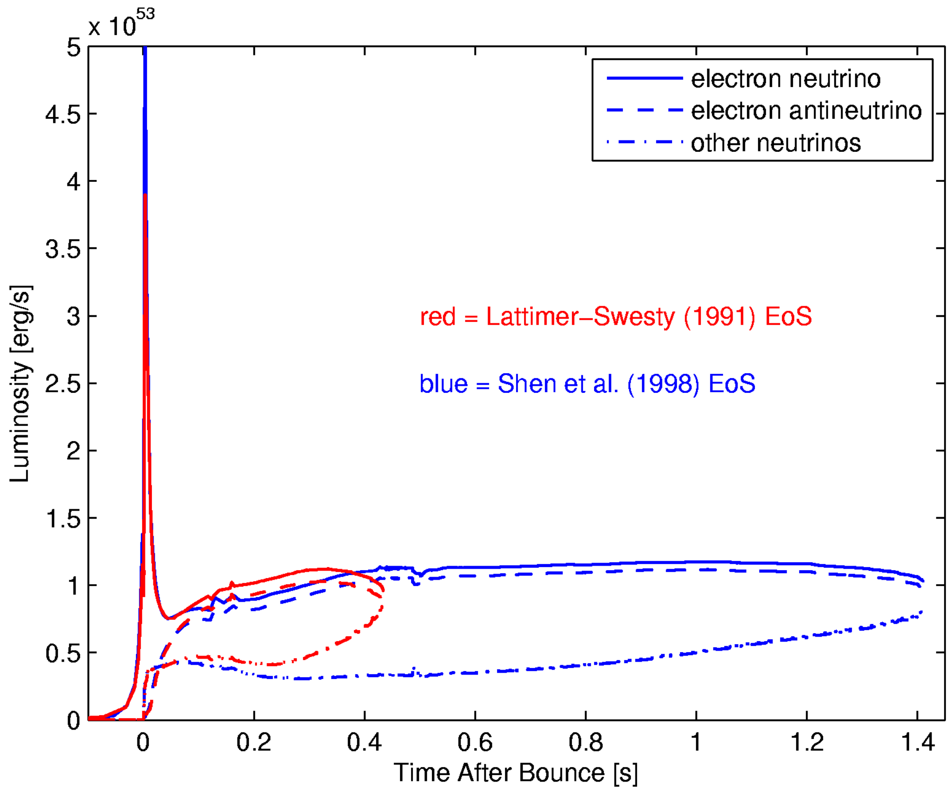

Fischer et al. (2008), effects purely due to nuclear matter treatment

Neutrino Emission

(luminosity and mean energy)
for a variety of stellar progenitors
(13, 15, 20, 25, 30, 35, 40 M_{sun})
by
Liebendörfer et al. (2004)

first peak in electron neutrinos due to electron captures on protons and nuclei when shock front reaches neutrino sphere

End Stages of Massive Stars (Nomoto et al. 2009)

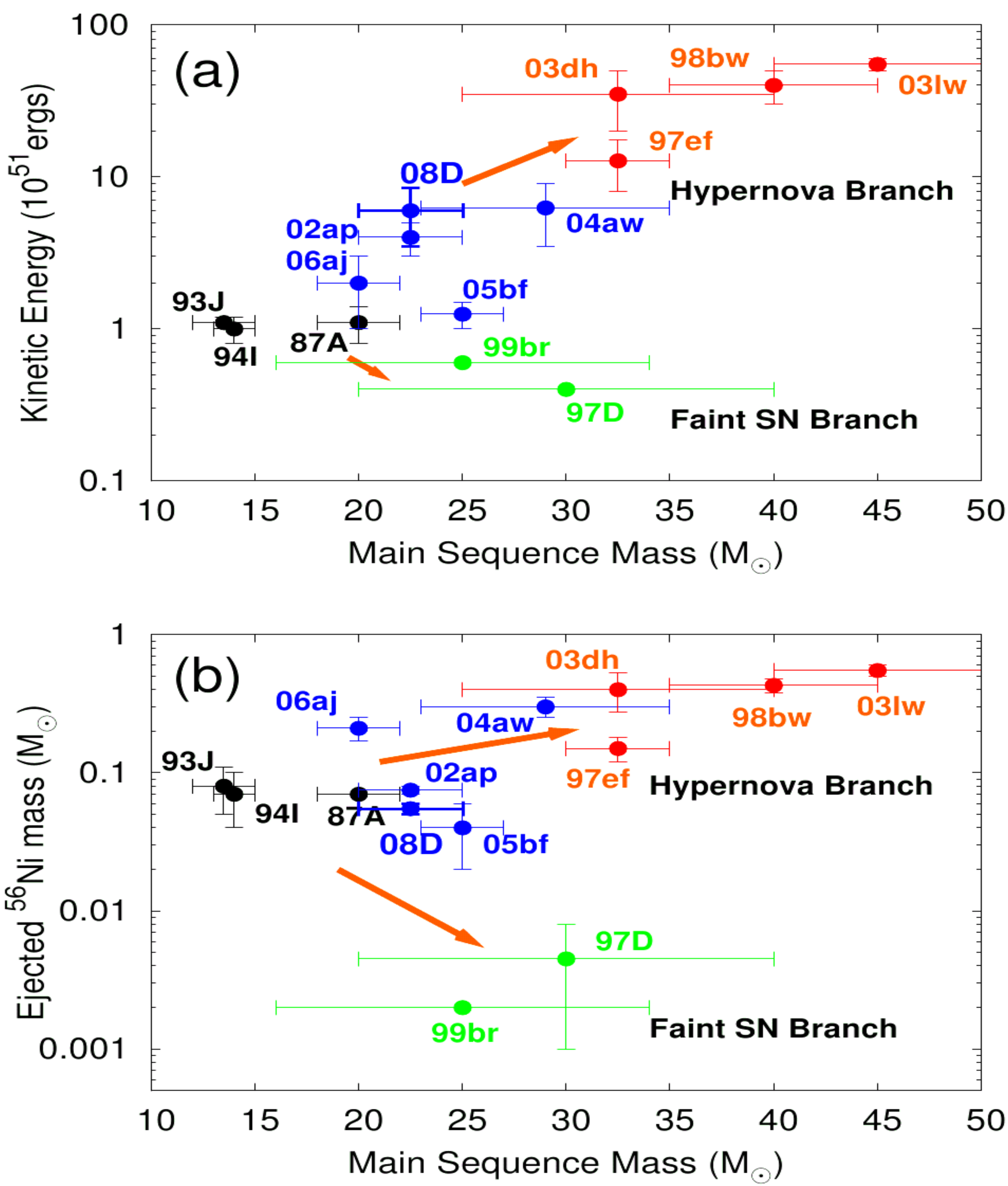

- *8 - 10 M⊙ super-AGB stars when O+Ne+Mg core collapses due to electron capture, produce little α-elements and Fe-peak elements*
- *10 - 90 M⊙ undergo Fe-core collapse. Nucleosynthesis in aspherical explosions might be important,*
- *90 - 140 M⊙ stars undergo pulsational nuclear instabilities at various nuclear burning stages, including O and Si-burning.*
- *140 - 300 M⊙ stars become pair-instability supernovae, if the mass loss is small enough.*
- *> 300M⊙ Very massive stars undergo core-collapse to form intermediate mass black holes.*

The GRB- Supernova Connection

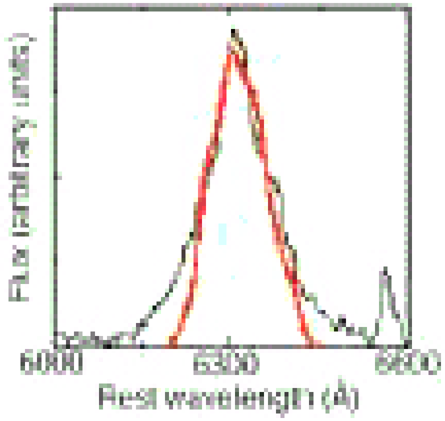

1998bw

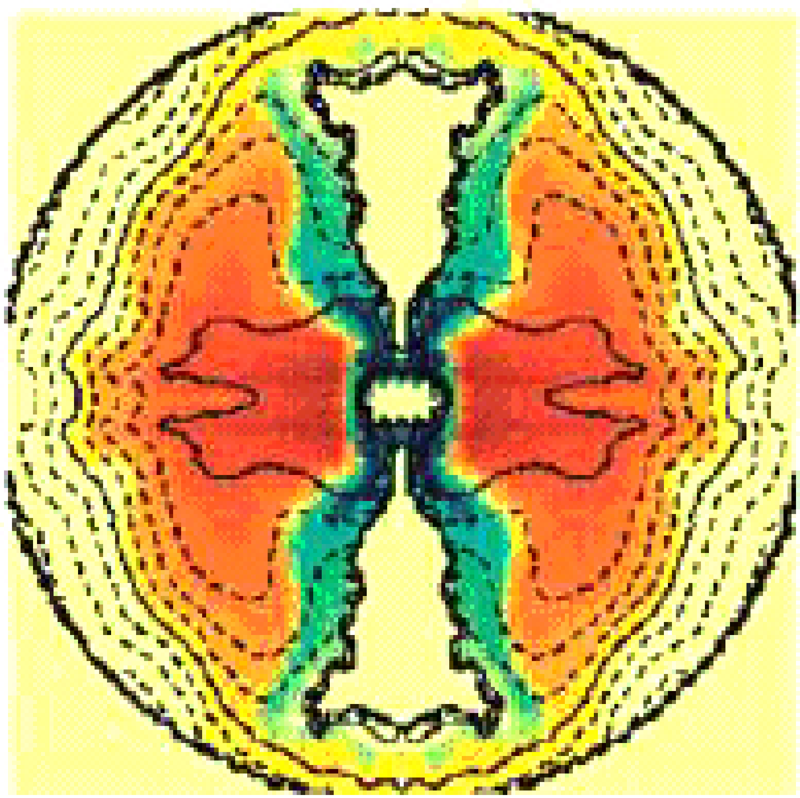

2003jd

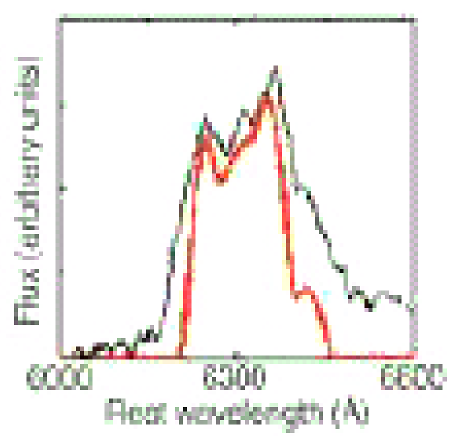

Ejecta distribution in a parametrized jet-model for GRB-SNe (Maeda et al. 2002). Blue and green colors stand for Fe-group material, red for oxygen. The resulting [O I] λλ6300, 6364 profiles for different viewing angles are also shown (from Mazzali et al. 2005).

Diversity in Type Ic Supernovae

Taubenberger (2008)

Comparison of absolute magnitudes, kinetic energy, ejecta mass and Ni mass of SNe Ic.[a]

SN	M_V (mag)	$E_{kin}/10^{51}$erg	$M_{ej}/M_{\odot}$	$M_{Ni}/M_{\odot}$	references
1994I	−17.62	1	0.9	0.07	N94,R96
2004aw	−18.02	3.5–9.0	3.5–8.0	0.25–0.35	this paper
2002ap	−17.35	4	3	0.08	M02,F03,T06
1997ef	−17.14	19	9.5	0.16	M00,M04
1998bw	−19.13	30	10	0.70	G98,N00

[a] For all SNe except SN 2004aw, the values for kinetic energy, ejecta mass, and nickel mass have been inferred from light curve and spectral models.

N94 = Nomoto et al. 1994;
R96 = Richmond et al. 1996;
M02 = Mazzali et al. 2002;
F03 = Foley et al. 2003;
T06 = Tomita et al. 2006;
M00 = Mazzali, Iwamoto & Nomoto 2000;
M04 = Mazzali et al. 2004;
G98 = Galama et al. 1998;
N00 = Nakamura et al. 2000

How to invoke induced explosions for nucleosynthesis purposes?

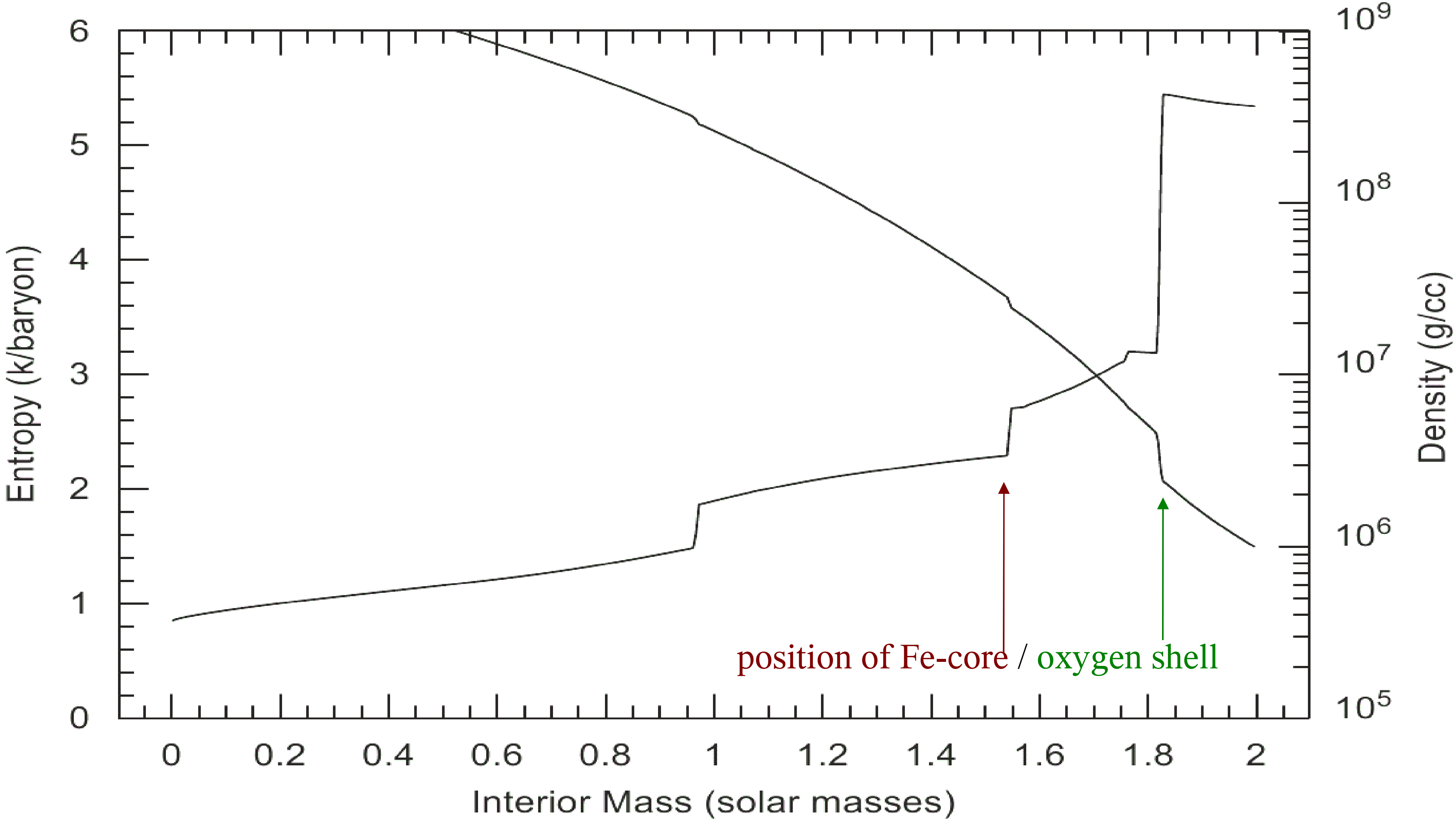

without a self-consistent mechanism nucleosynthesis can only be calculated with induced explosions. Woosley & Heger position a piston with 1.2B at S=4k_B/b, Nomoto/Thielemann applied thermal bomb and integrate from outside until expected ^{56}Ni-yield.

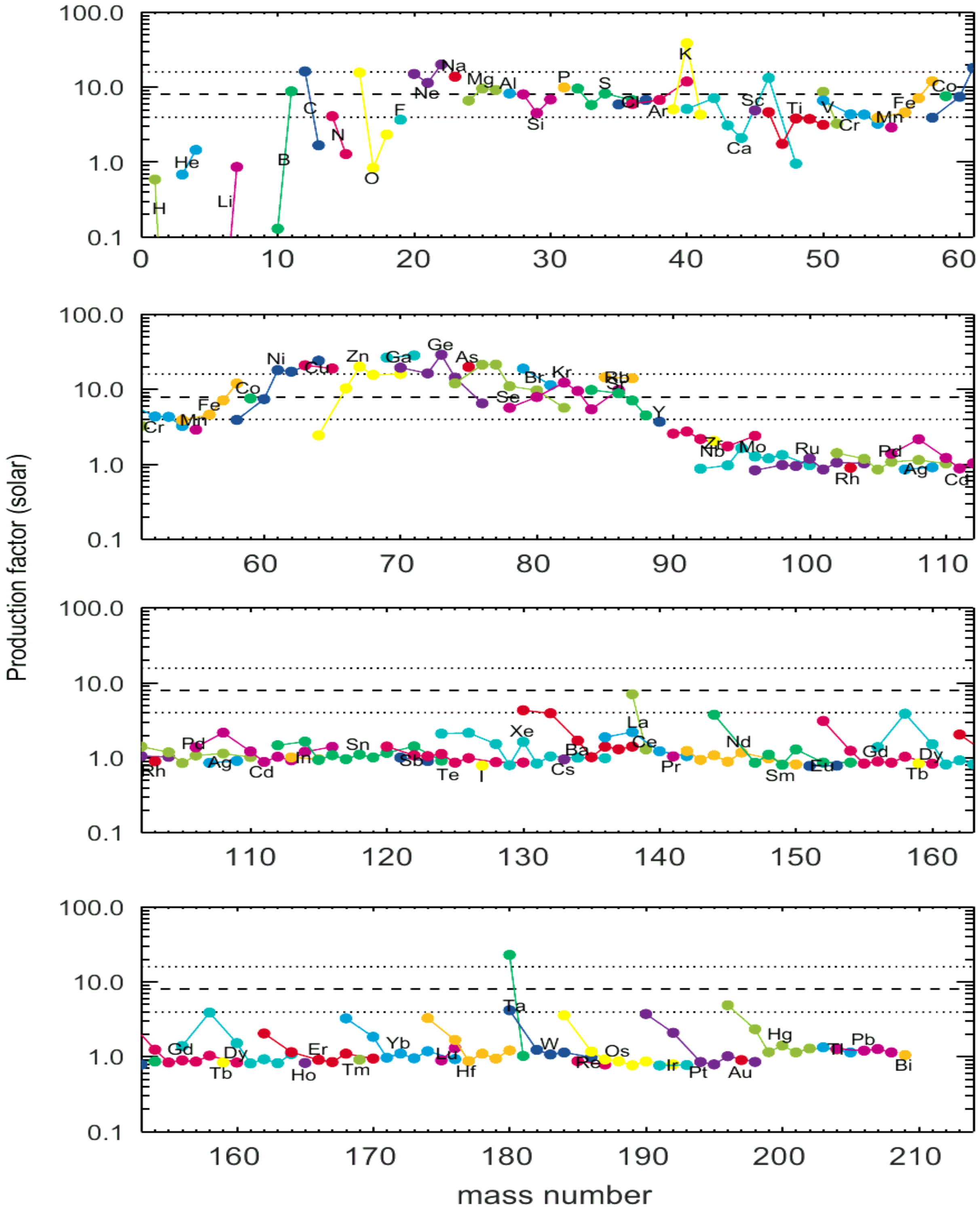

Wooley & Heger (2007):

Results for initial solar metallicity, integrated over a Salpeter initial mass function and divided by initial abundances -> overproduction factors.

Intermediate mass elements well reproduced, Fe/Ni-group depends on choice of mass cut/location of piston,

well pronounced weak s-process,

absence of r-process as not included in modeling,

p-process isotopes only well reproduced at high end.

Pop III yields (Heger & Woosley 2009)
Evolution of metal-free stars

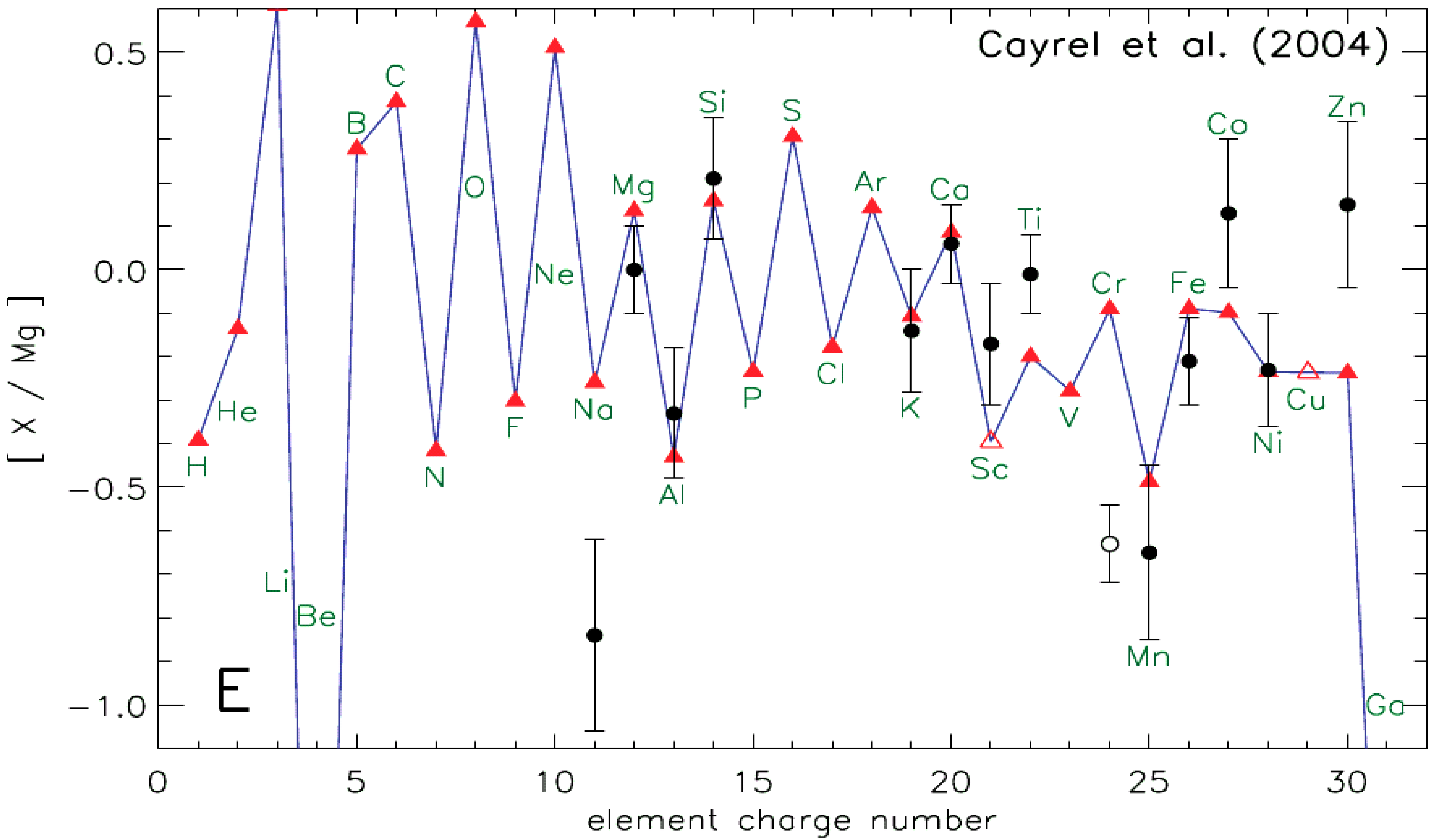

Cayrel et al. (2004). taken as representative sample for low metallicity stars (representing type II supernova yields). E: “Standard” IMF integration of yields from M = 10 − 100 M⊙, explosion energy E = 1.2 B.

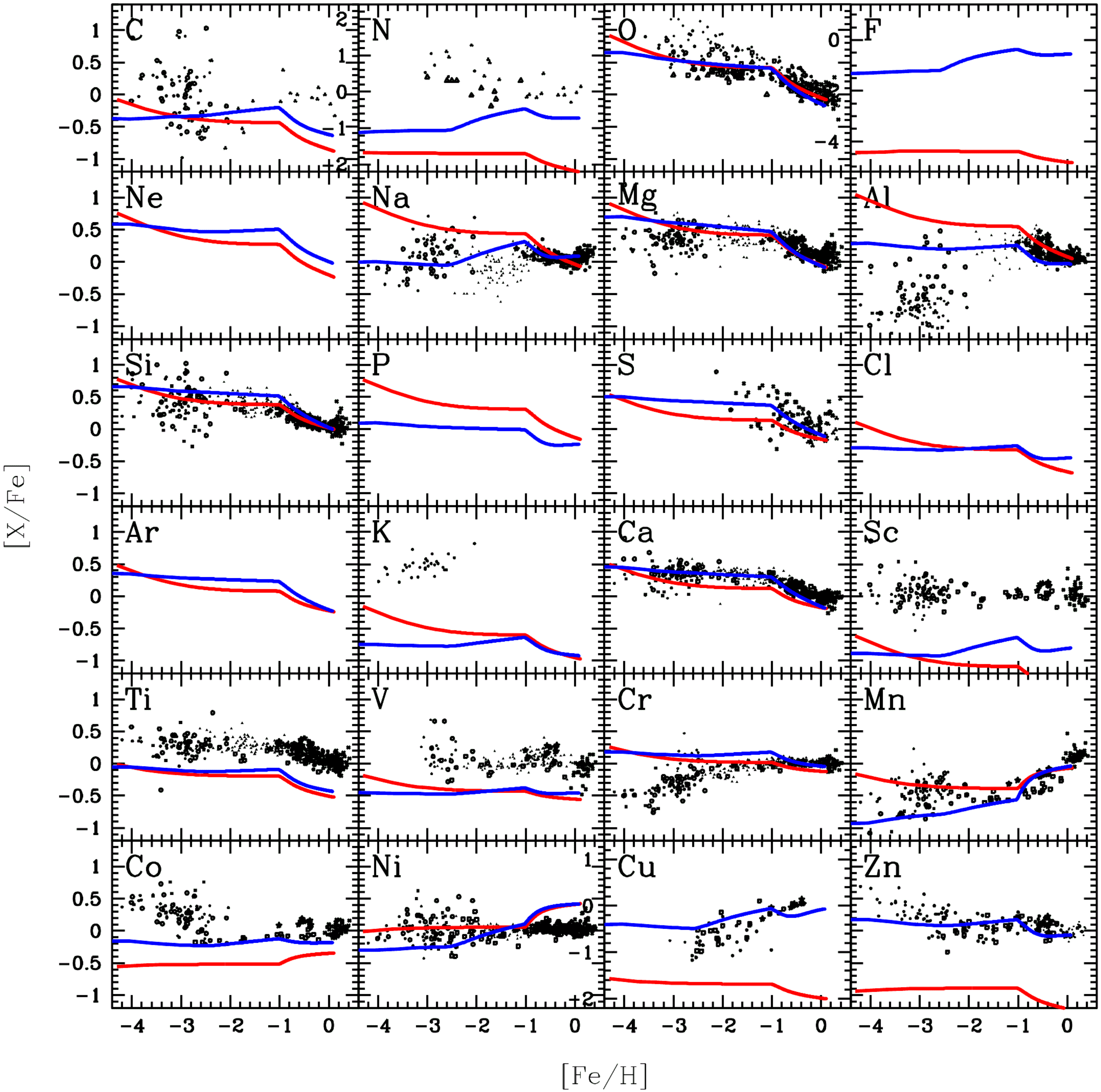

Nomoto et al. (2006)

chemical evolution with Salpeter IMF

red – regular supernova explosions with 1B

blue – 50% of stars >25M$_{sol}$ are assumed to become hypernovae with an explosion energy of 10B.

Nucleosynthesis problems in "induced" piston or thermal bomb models

utilized up to present to obtain explosive nucleosynthesis yields with induced explosion energies of 10^{51} erg

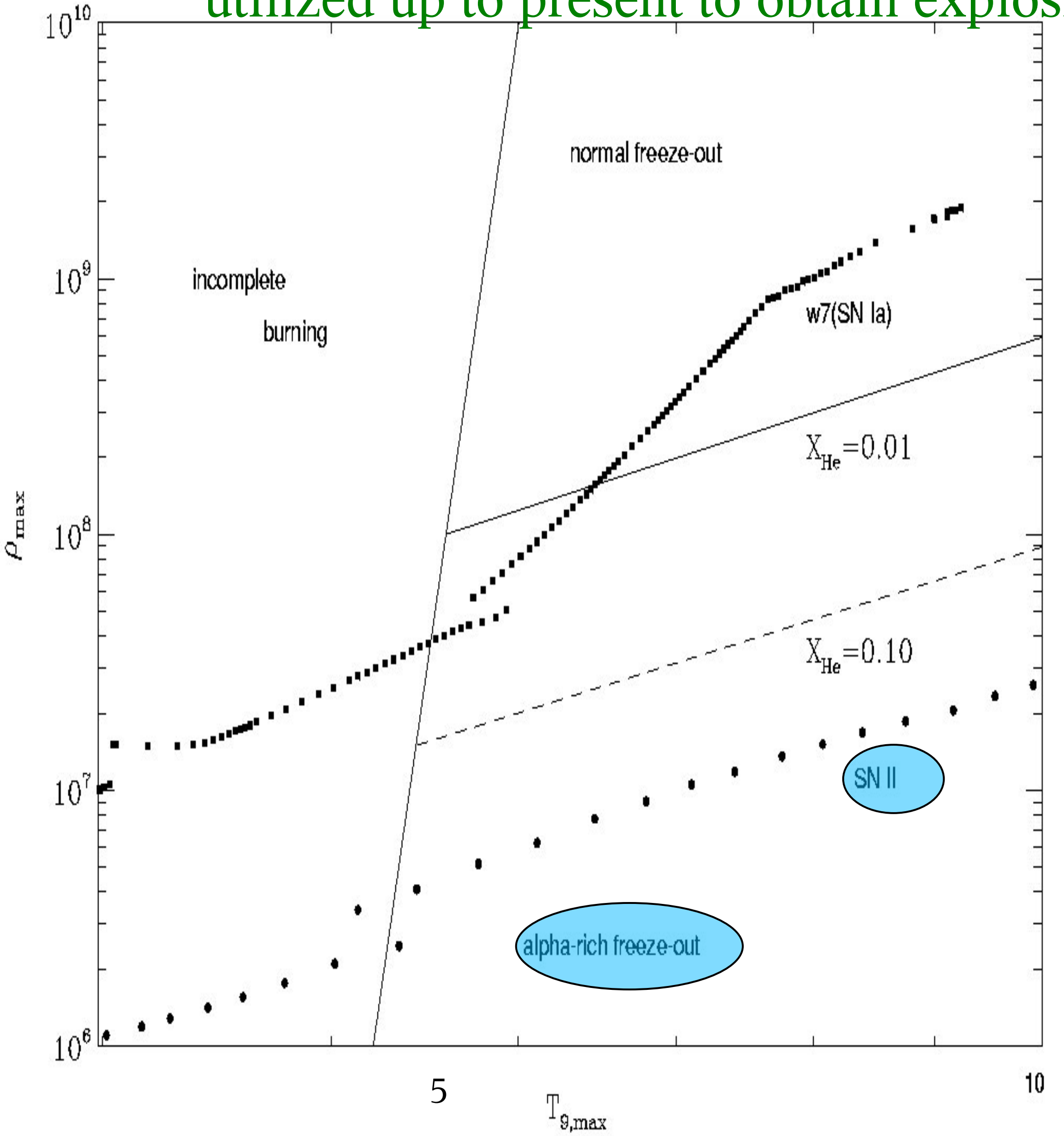

disconnected light element (n,p,He) and Si-Fe QSE-cluster, high alpha-abundance prefers alpha-rich nuclei (^{58}Ni over ^{54}Fe), Y_e determines dominant QSE-isotope.

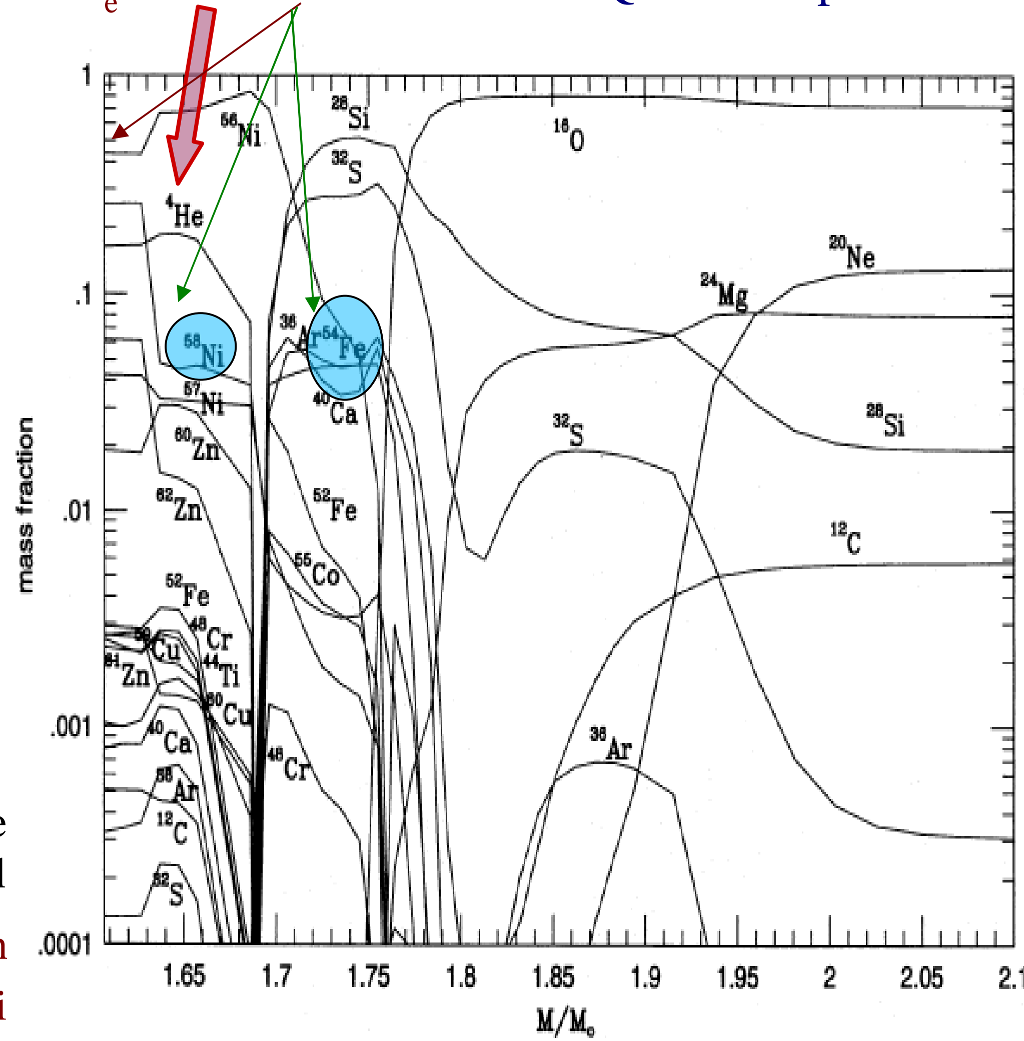

prior results of Thielemann, Nomoto, Woosley, Chieffi .. made use of initial stellar structure (and Y_e!) when inducing artificial explosion. This neglects the effect of the explosion mechanism on the innermost zones, causes strange overproductions of Ni

In exploding models matter in innermost ejected zones becomes proton-rich (Y_e>0.5)

if the neutrino flux is sufficiant (scales with $1/r^2$)! :

Y_e dominantly determined by $e^{\pm}$ and ν_e, $\bar{\nu}_e$ captures on neutrons and protons

$$\nu_e + n \leftrightarrow p + e^-$$

$$\bar{\nu}_e + p \leftrightarrow n + e^+$$

- high density / low temperature → high E_F for electrons → e-captures dominate → n-rich composition
- if el.-degeneracy lifted for high T → ν_e-capture dominates → due to n-p mass difference, p-rich composition
- in late phases when proto-neutron star neutron-rich, $\bar{\nu}_e$'s see smaller opacity → higher luminosity, dominate in neutrino wind → neutron-rich ejecta

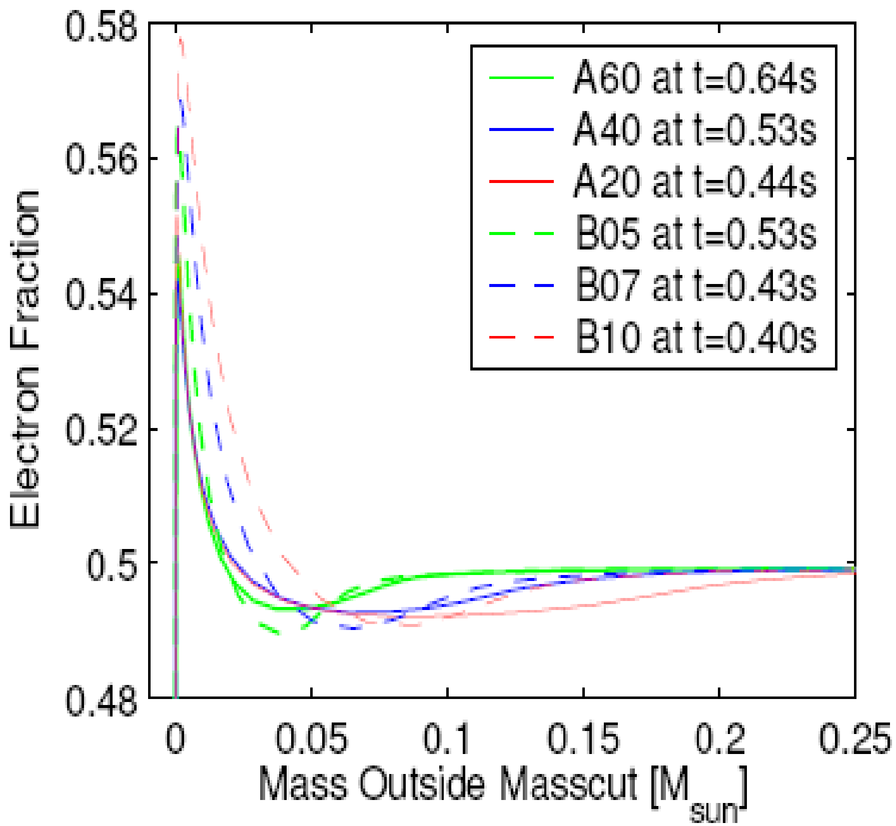

Fröhlich et al. (2006a)
A: neutrino scattering cross sections scaled (%)
B: neutrino absorption cross sections scaled (factor)

Improved Fe-group composition

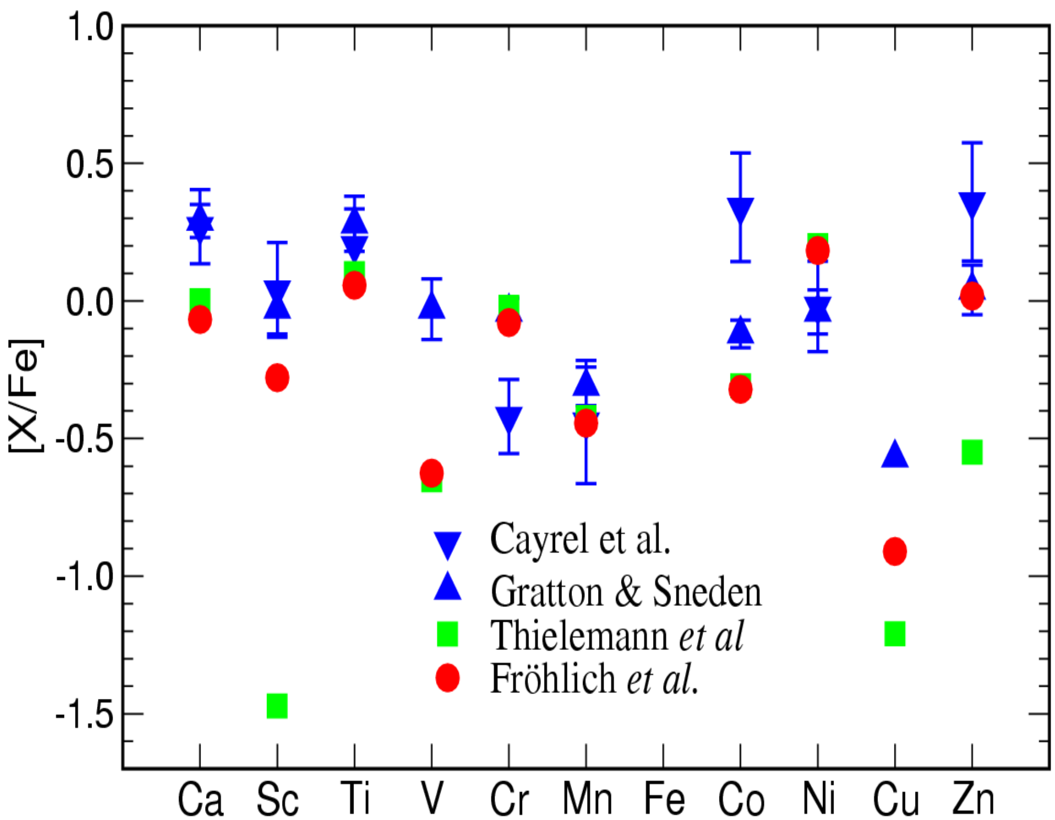

Fröhlich et al. (2004, 2006a), see also Pruet et al. (2005)

Models with Y_e>0.5 lead to an alpha-rich freeze-out with remaining protons which can be captured similar to an rp-process. This ends at ^{64}Ge, due to (low) densities and a long beta-decay half-life (decaying to ^{64}Zn).

This effect improves the Fe-group composition in general and extends it to Cu and Zn!

νp–process

$$\bar{\nu}_e + p \rightarrow e^+ + n; \quad n + {}^{64}\mathrm{Ge} \rightarrow {}^{64}\mathrm{Ga} + p; \quad {}^{64}\mathrm{Ga} + p \rightarrow {}^{65}\mathrm{Ge}; \ldots$$

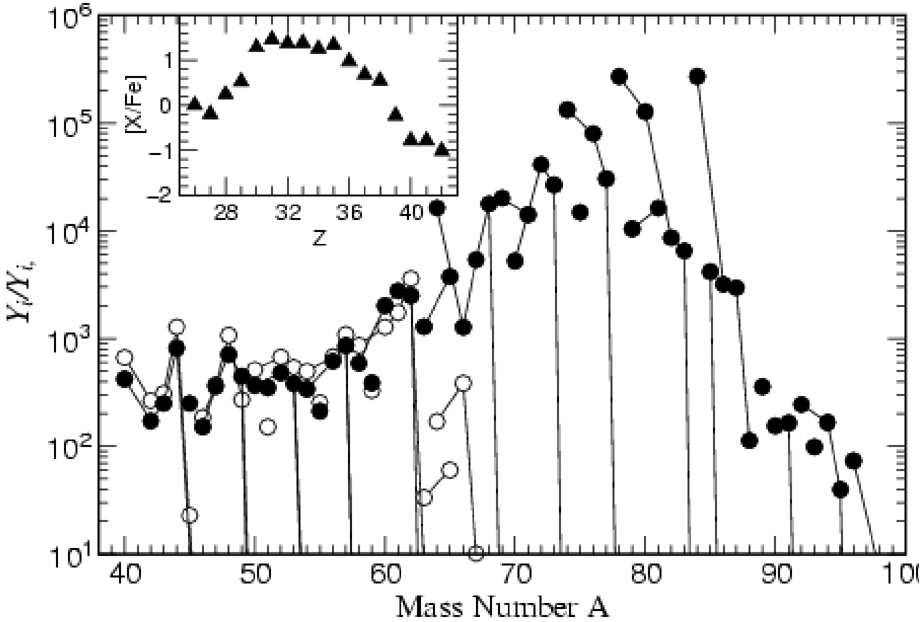

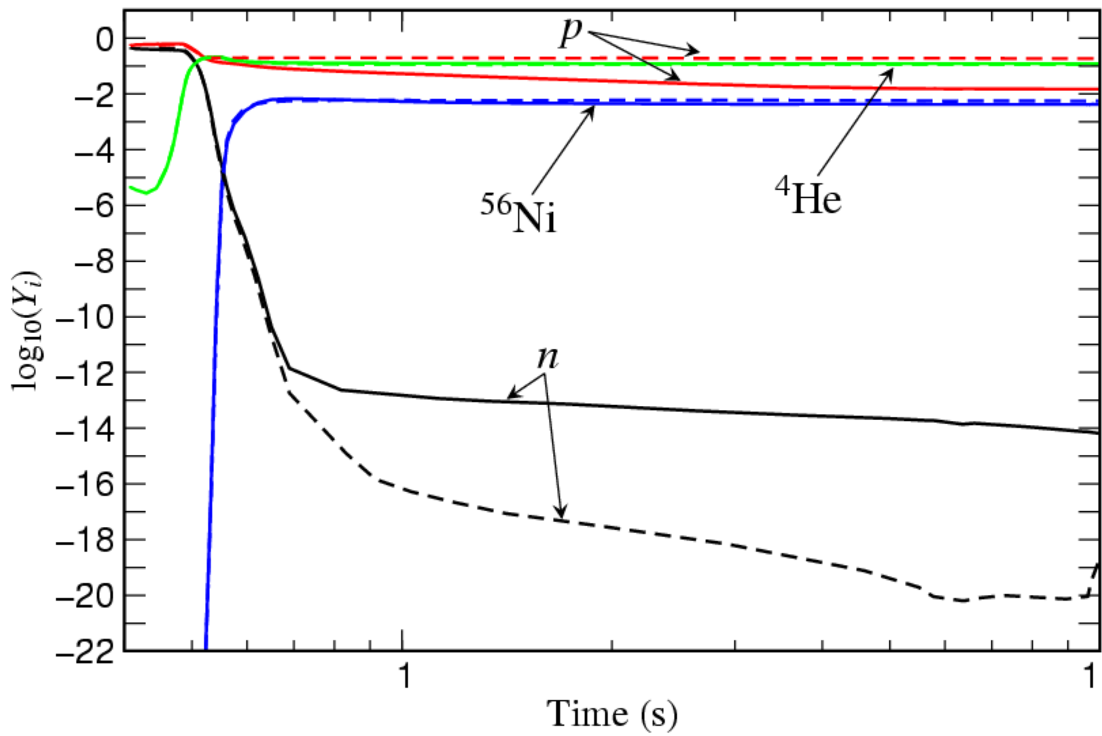

Fröhlich et al. (2006b);
also strong overabundances can be obtained up to Sr and beyond (light p-process nuclei)
see also Pruet et al. (2006), Wanajo (2006)

A new process, which could solve some observational problems of Sr, Y, Zr in early galactic evolution and the problem of light p-process nuclei.

Anti-neutrino capture on protons provides always a small background of neutrons which can mimic beta-decay via (n,p)-reactions.

Observational Constraints on r-Process Sites

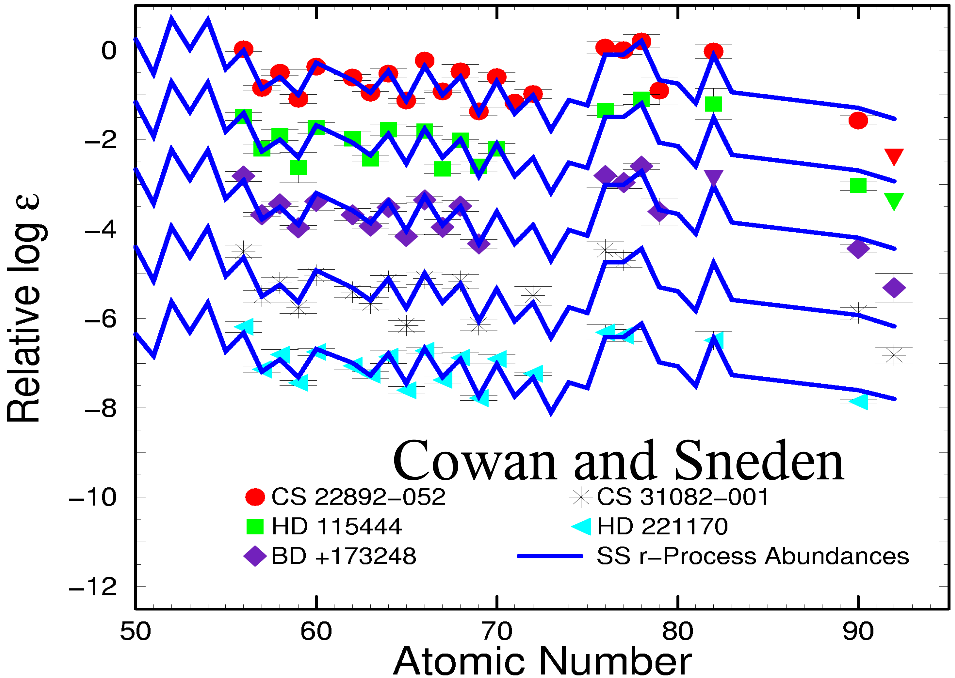

apparently uniform abundances above Z=56 (and up to Z=82?) -> "unique" astrophysical event which nevertheless consists of a superposition of ejected mass zones

"rare" event, which must be related to massive stars due to "early" appearance at low metallicities(behaves similar to SN II products like O, but with much larger scatter)

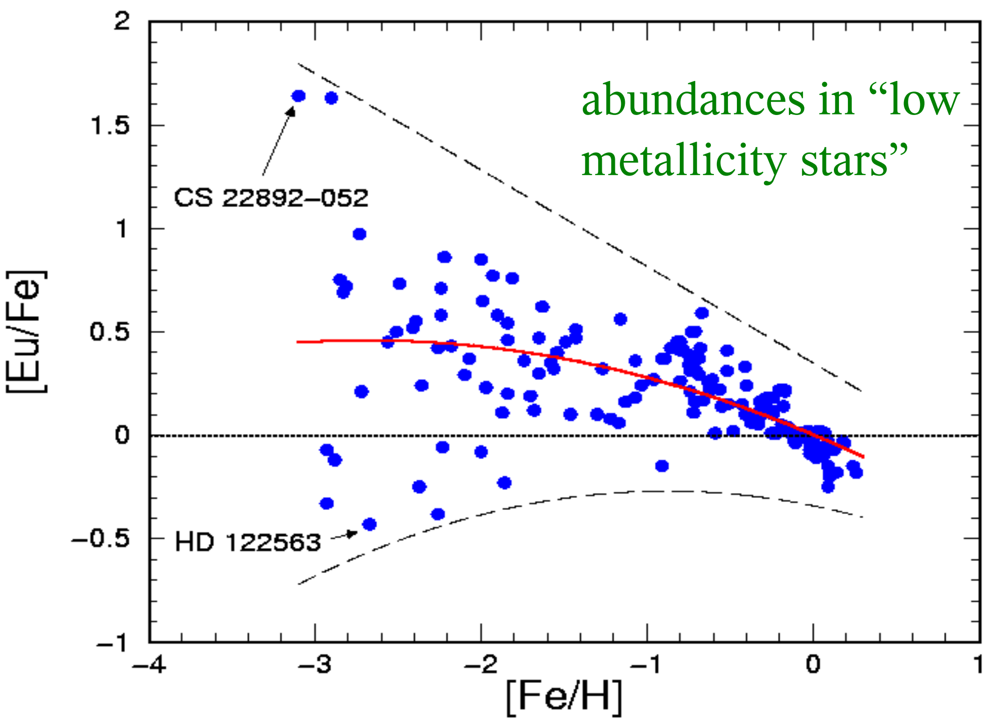

Observations of the weak r-process?

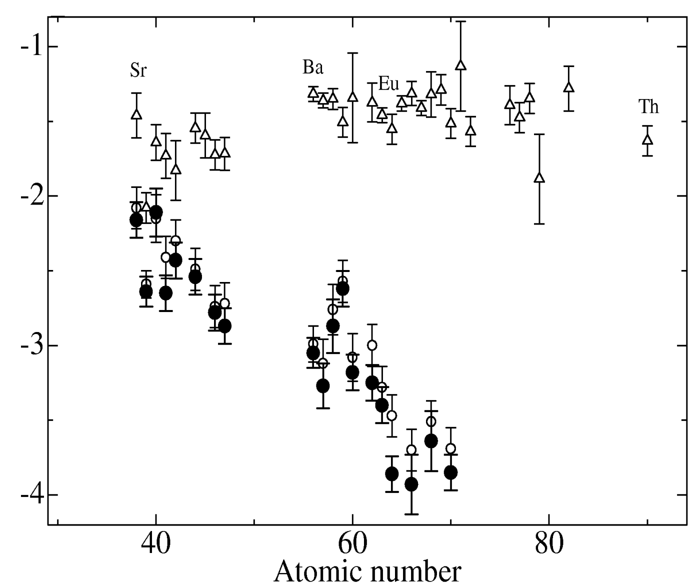

Honda et al. (2007)

(Realistic?) adiabatic expansions

n/seed ratios as function of S and Y_e

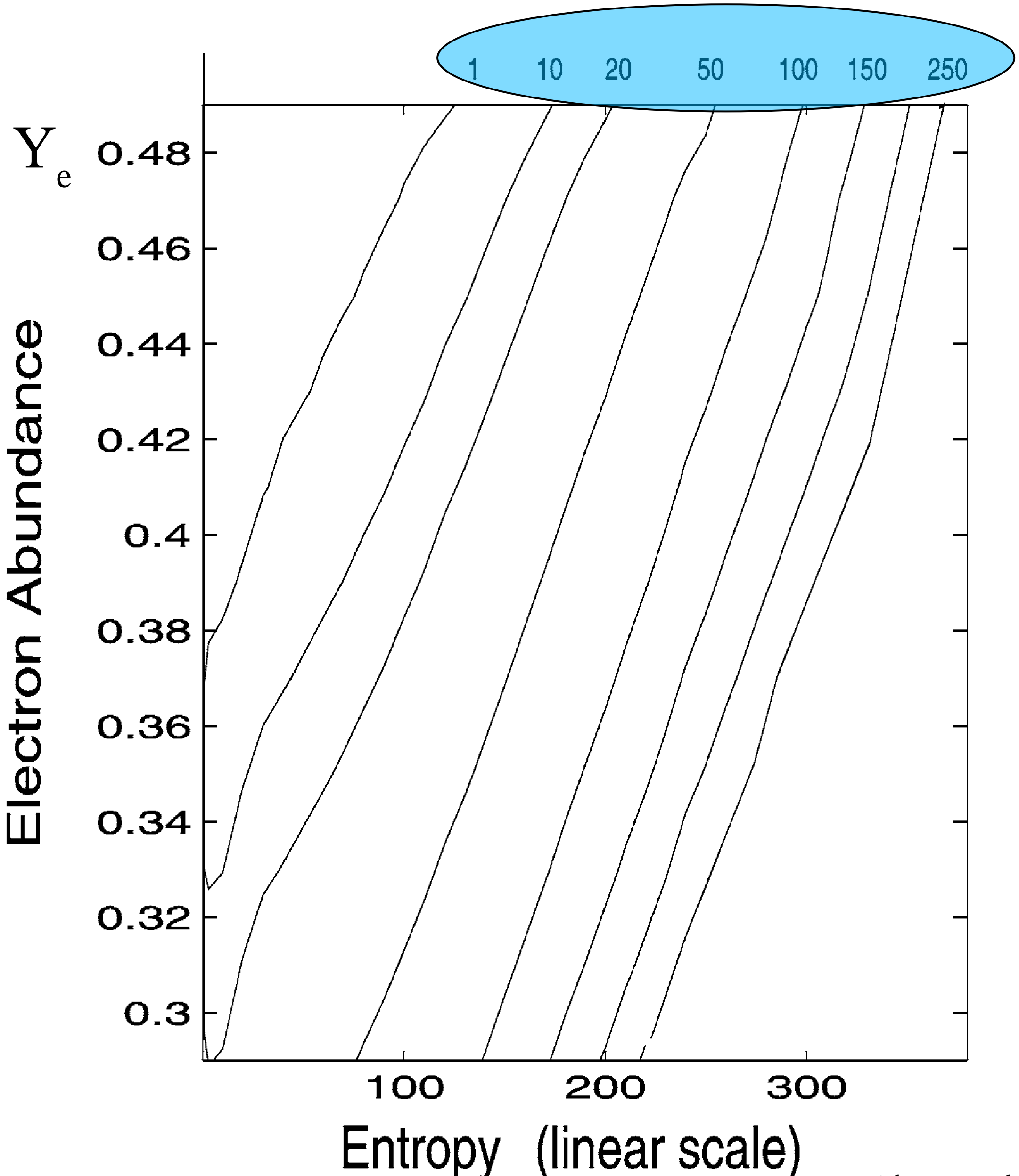

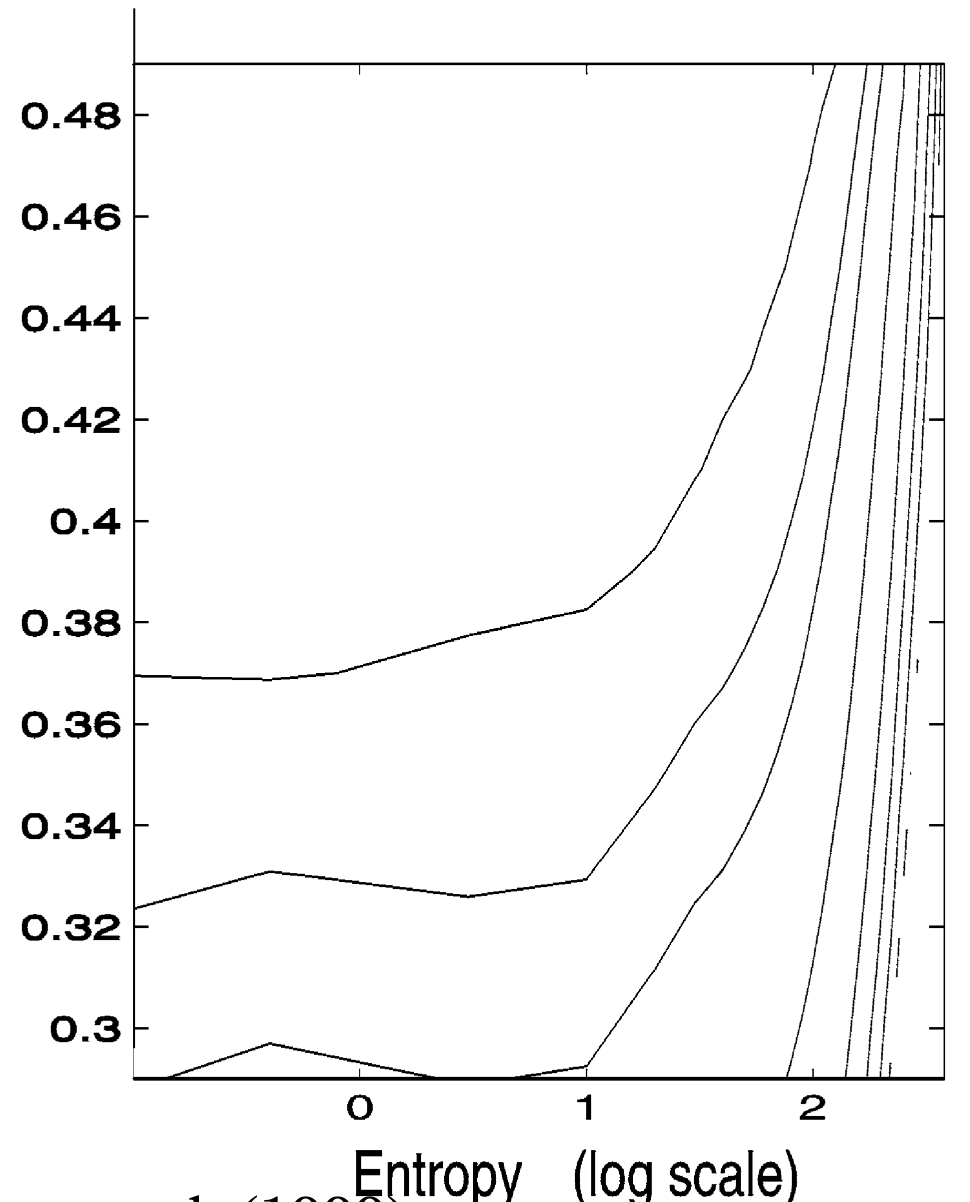

Freiburghaus et al. (1999)

n/seed ratios for high entropy conditions are are function of entropy

Farouqi et al. (2008)

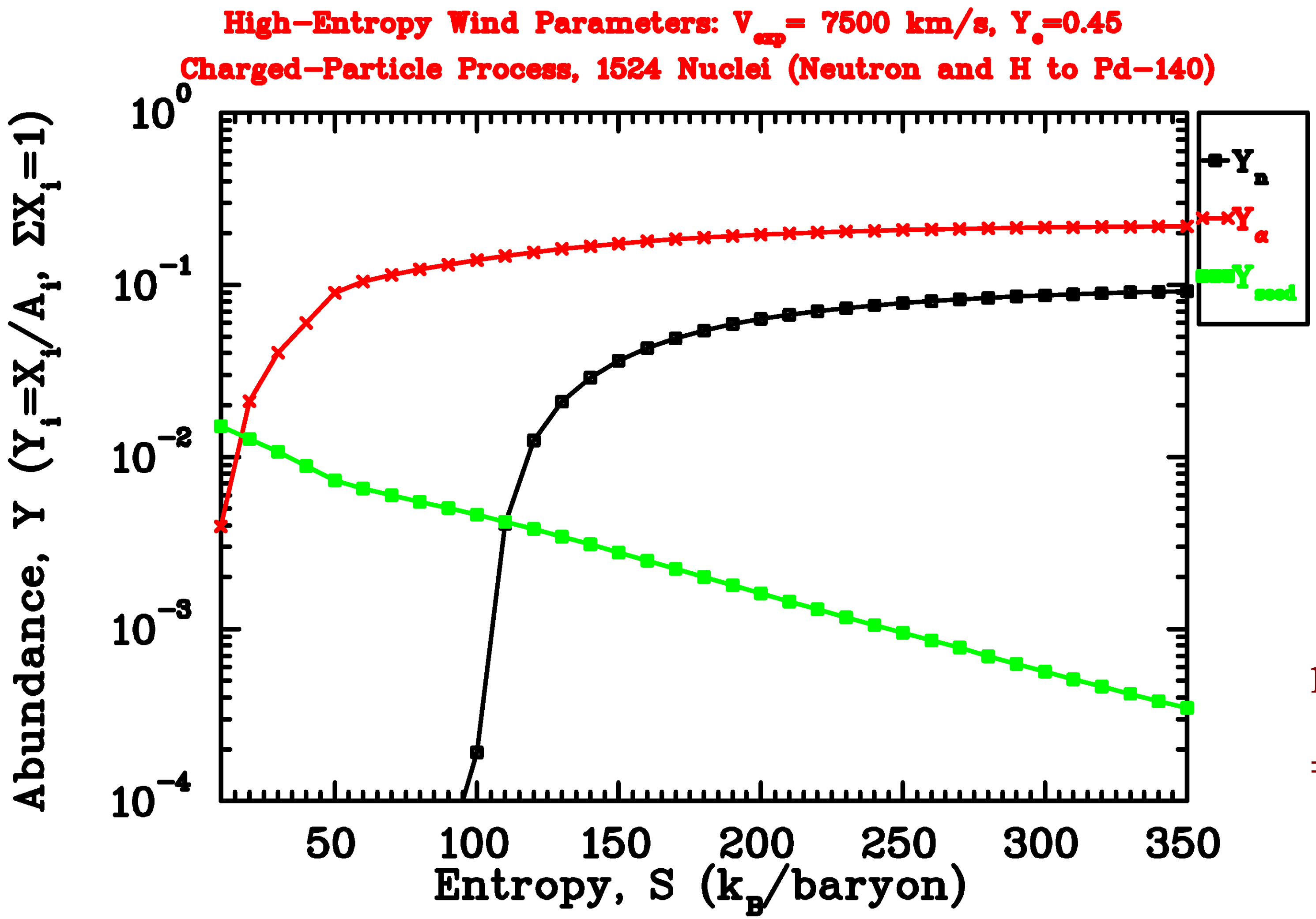

n/seed

$=Y_n/Y_{seed}$

Working of the r-Process

- (complete) Explosive Si-Burning

- 1. (very) high entropy alpha-rich (charged-particle) freeze-out with upper equilibrium extending up to A=80
  - quasi-equilibria in isotopic chains (chemical quilibrium for neutron captures and photodisintegrations) with maxima at specific neutron separation energies S_n
  - neutron/seed(A=80) ratio and S_n of r-process path dependent on entropy and Y_e

  (Meyer, Howard, Takahashi, Hoffman, Qian, Woosley, Freiburghaus, Thielemann, Mathews, Kajino, Wanajo, Otsuki, Terasawa, Farouqi, Goriely ...)

- 2. low entropies and normal freeze-out with very low Y_e, leading also to large n/seed ratios
  - S_n function of Y_e

  (Freiburghaus, Rosswog, Thielemann)

What is the site of the r-process?

from S. Rosswog

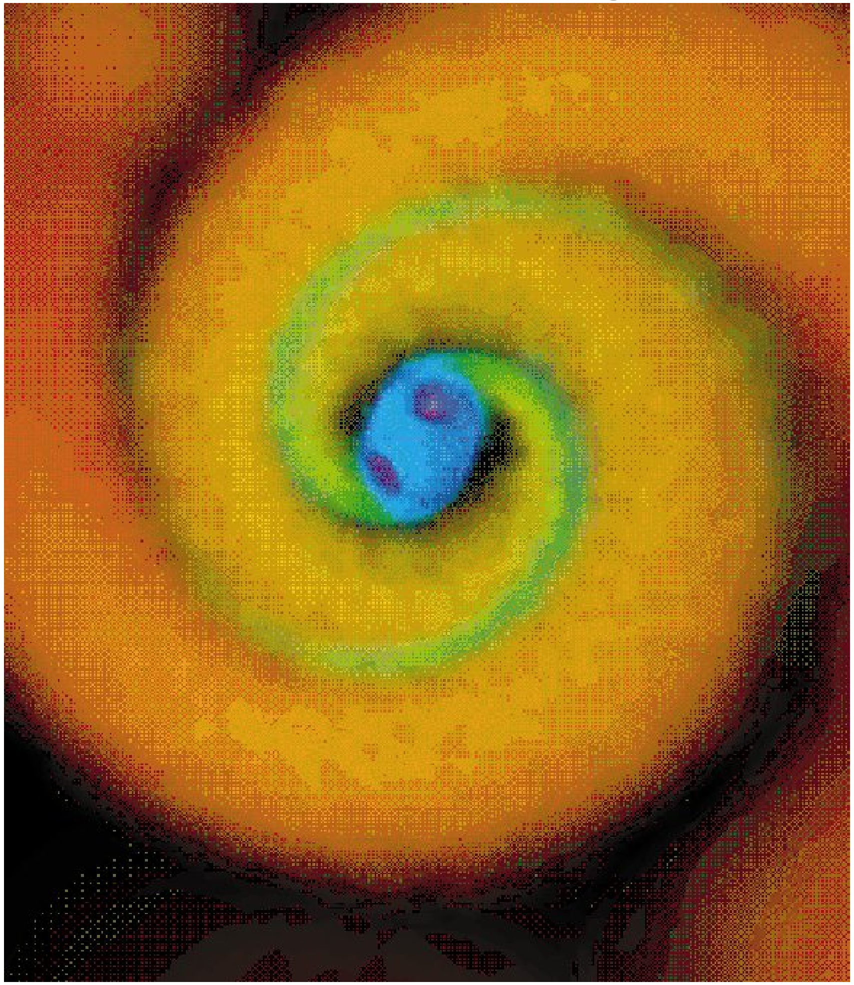

NS mergers, BH-NS mergers, problems: ejection too late in galactic evolution (or alternatively polar jets from supernovae, Cameron 2003)

from H.-T. Janka

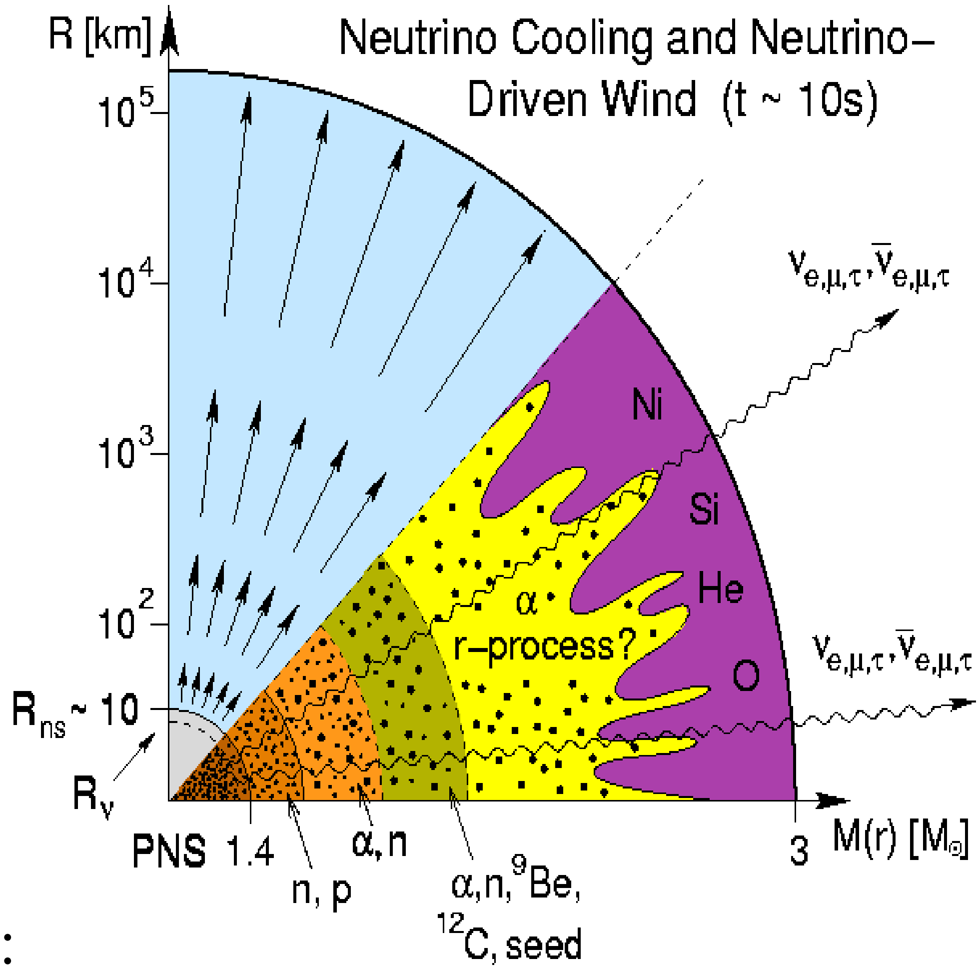

SN neutrino wind, problems: high enough entropies attained? neutrino properties???

Individual Superpositions of Entropy Components

Farouqi et al. (2008), above S=270-280 fission back-cycling sets in

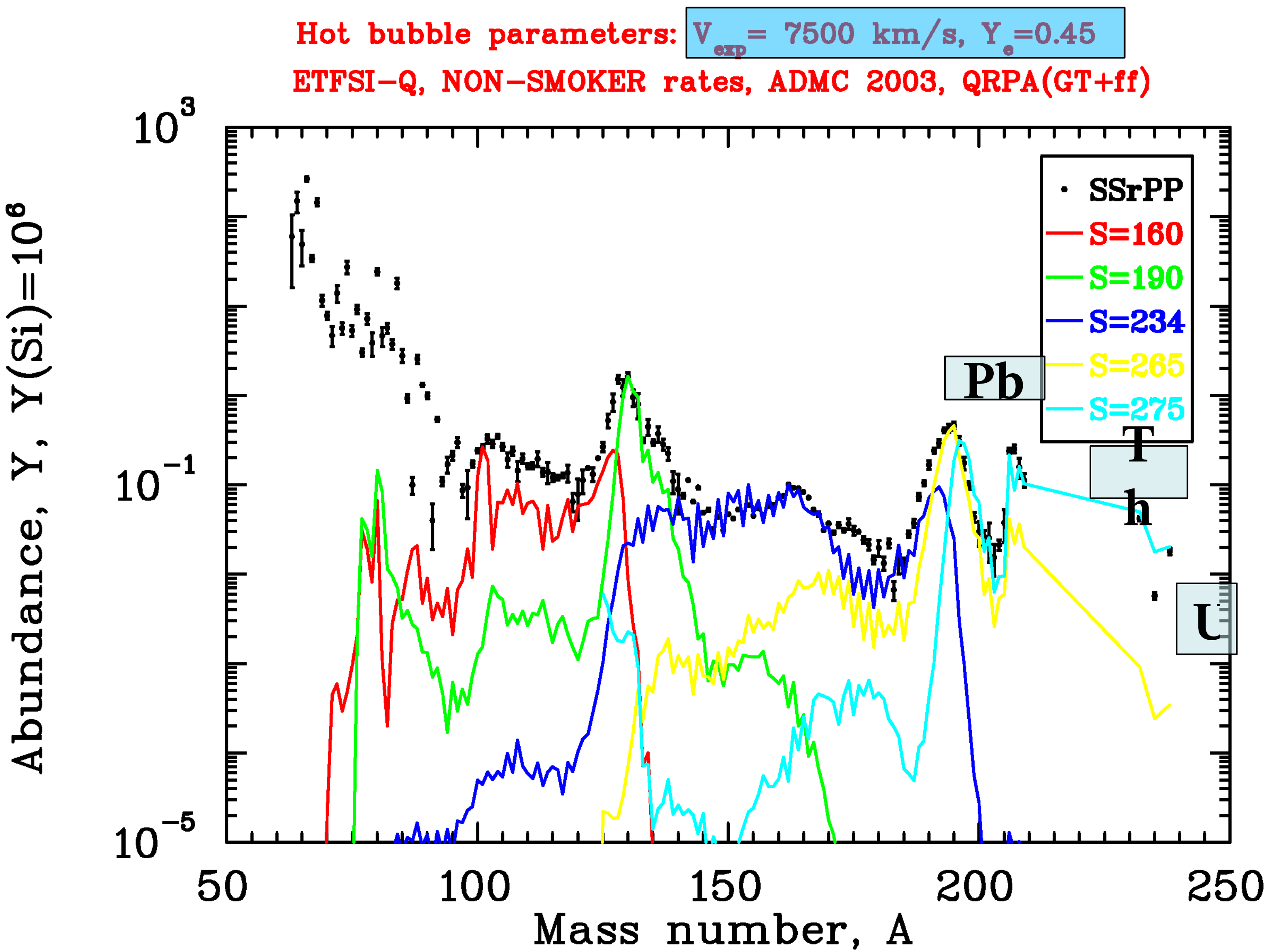

Superposition of entropies for different mass models

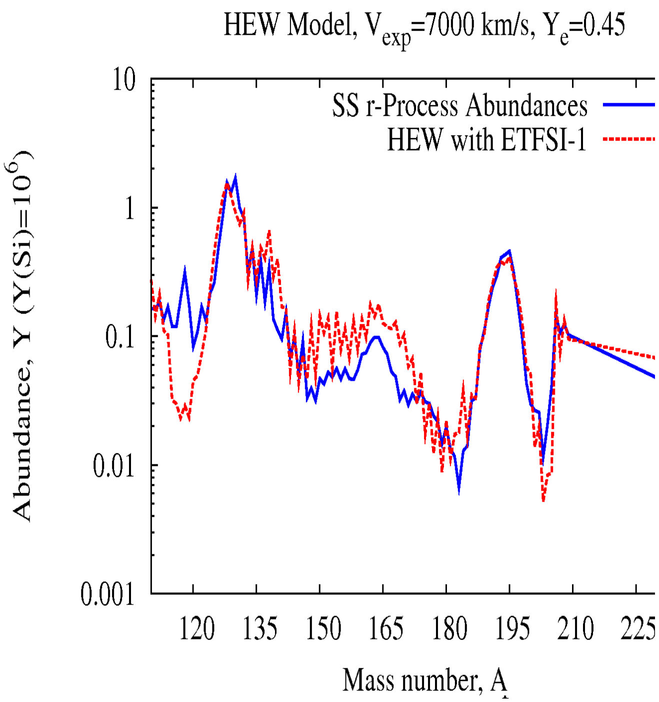

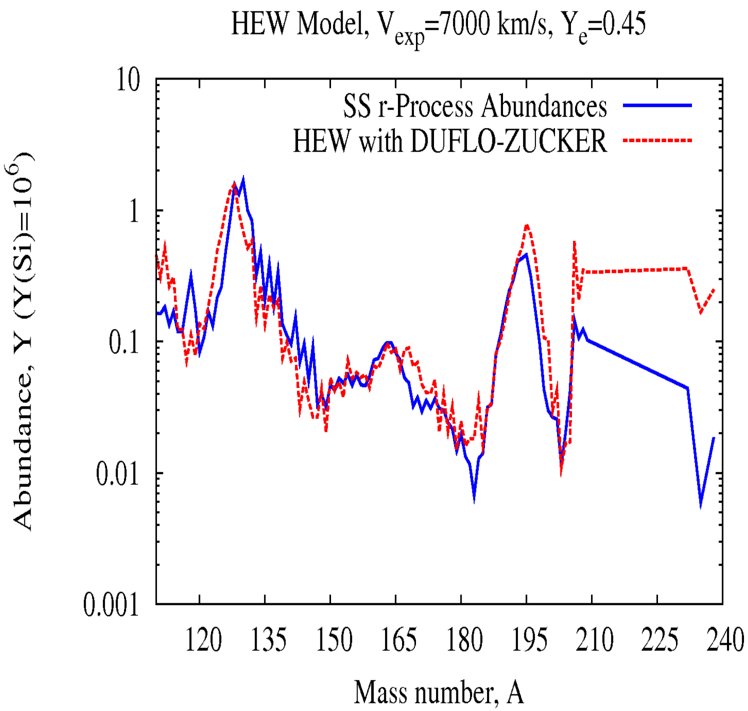

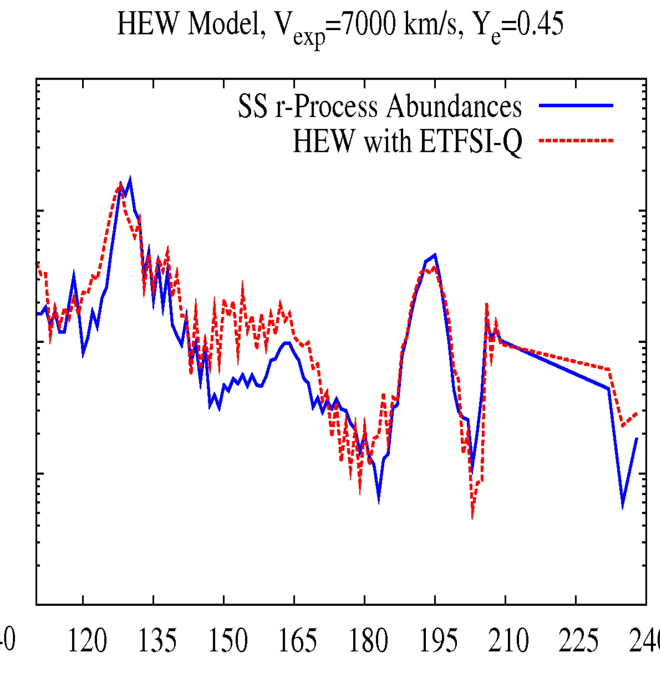

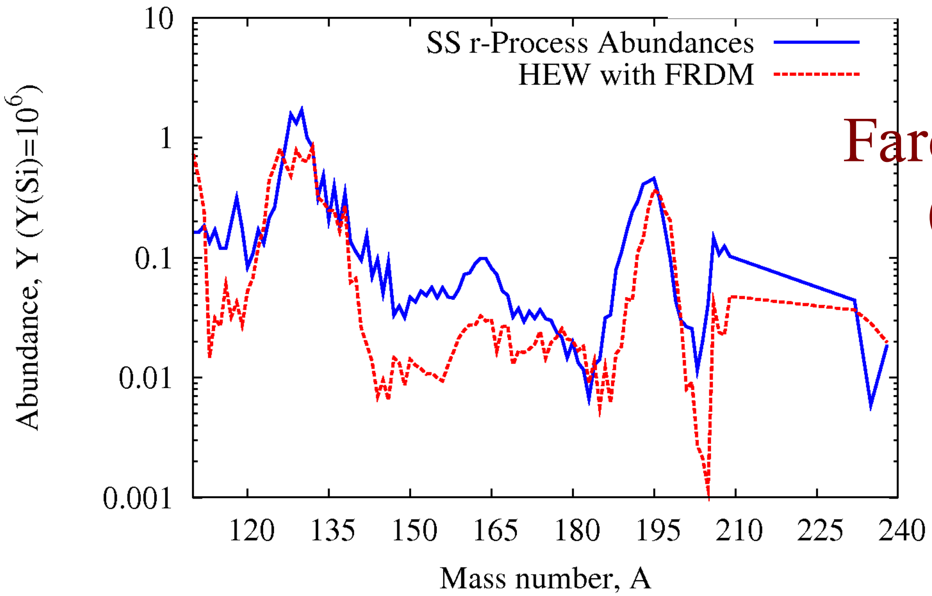

Farouqi et al.
(2008)

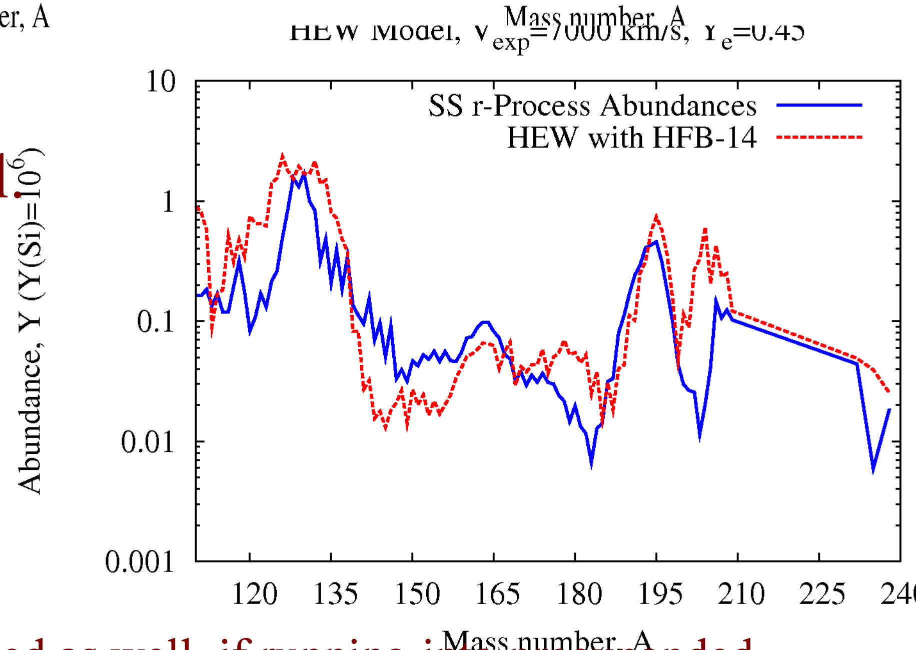

a superposition of expansion velocities might be needed as well, if running into preexpanded material, shocks etc. (Arcones et al. 2007, Panov & Janka 2008)

Can Sr/Y/Zr be co-produced with r-process elements in high entropy environments?

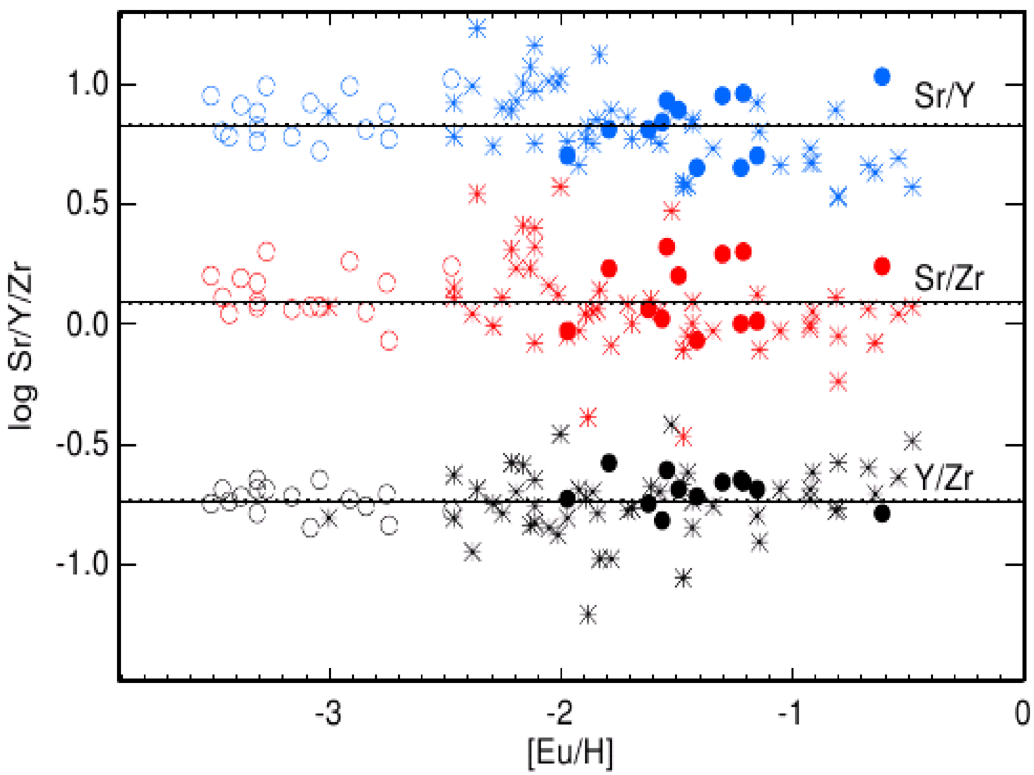

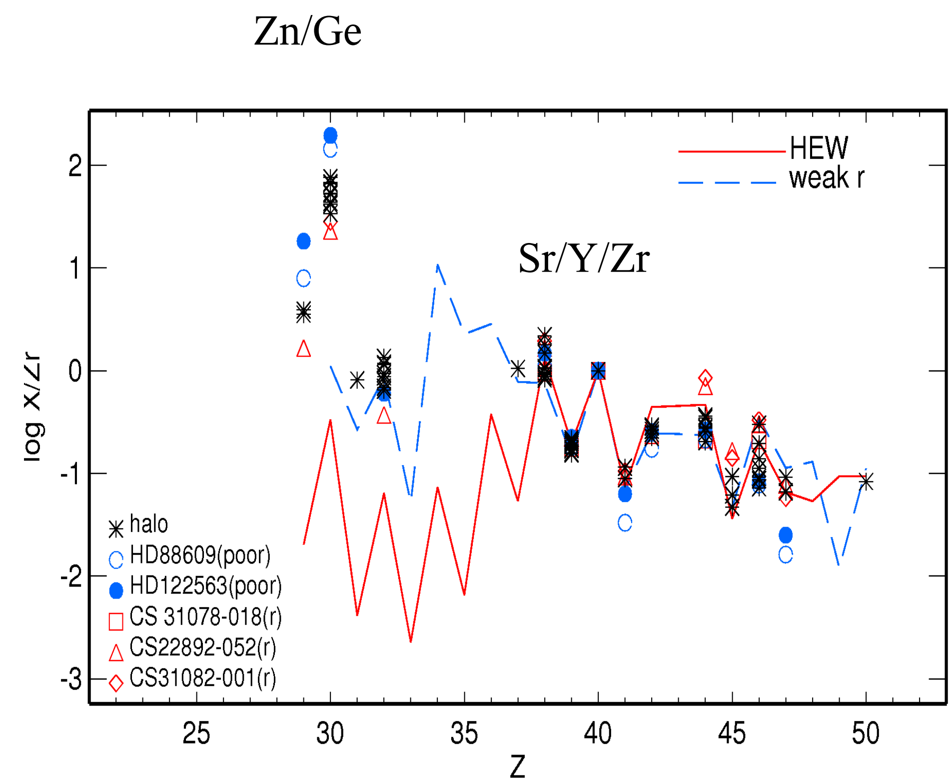

early work of Hoffman et al. (1996) seemed to indicate that such ratios are highly Ye-dependent (for low entropies S<50). It turns out that for reasonably high entropies the observed ratios are reproduced (Farouqi et al. 2008b)

Observational indications: heavy r-process and Fe-group uncorrelated, Ge member of Fe group, Zr intermediate behavior, weak correlations with Fe-group as well the heavy r-elements (Cowan et al. 2005)

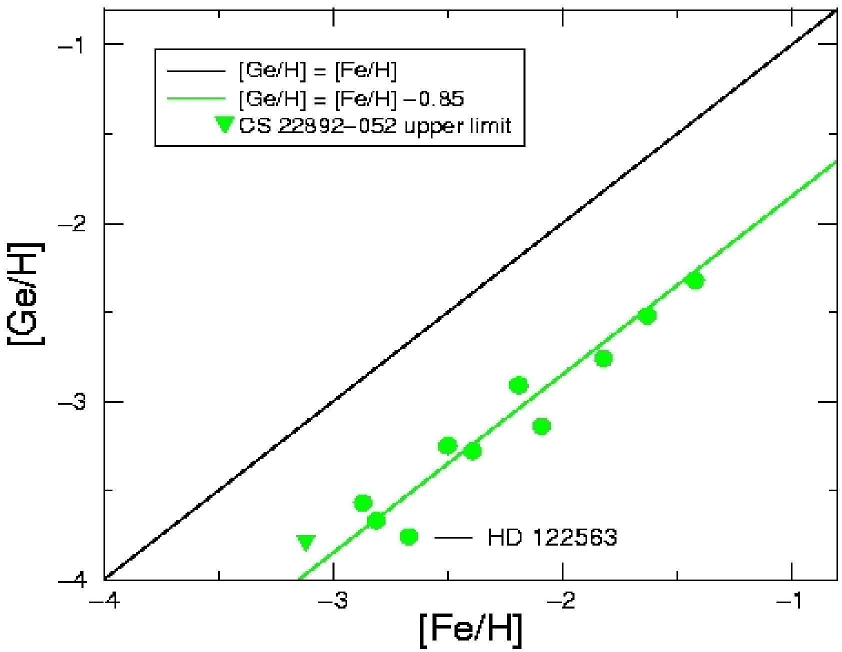

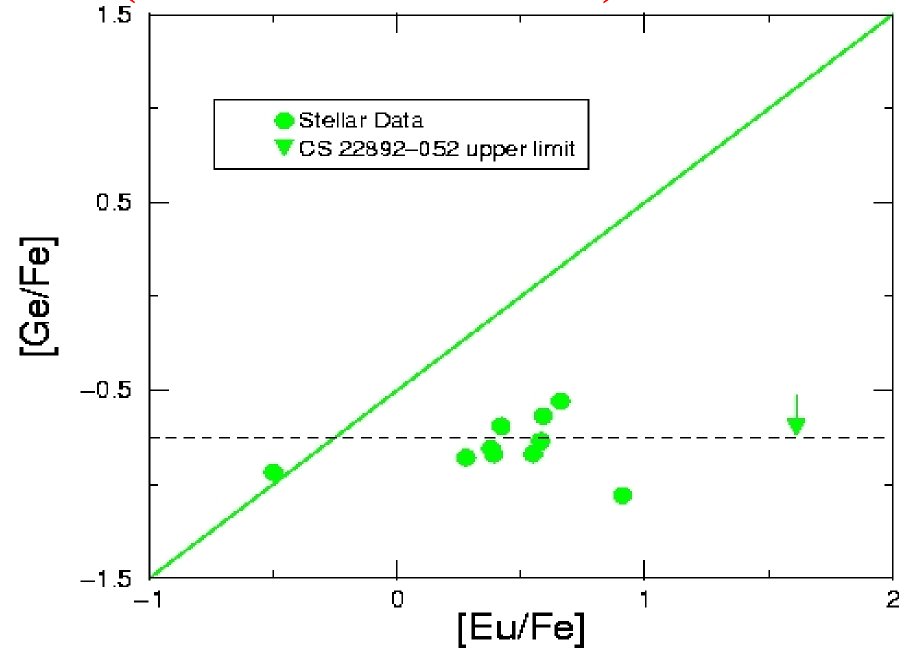

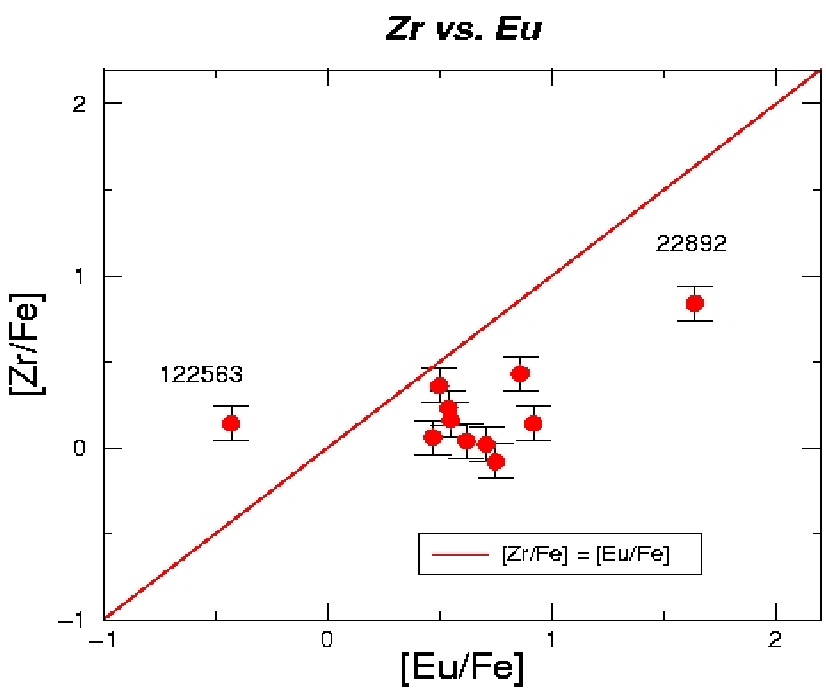

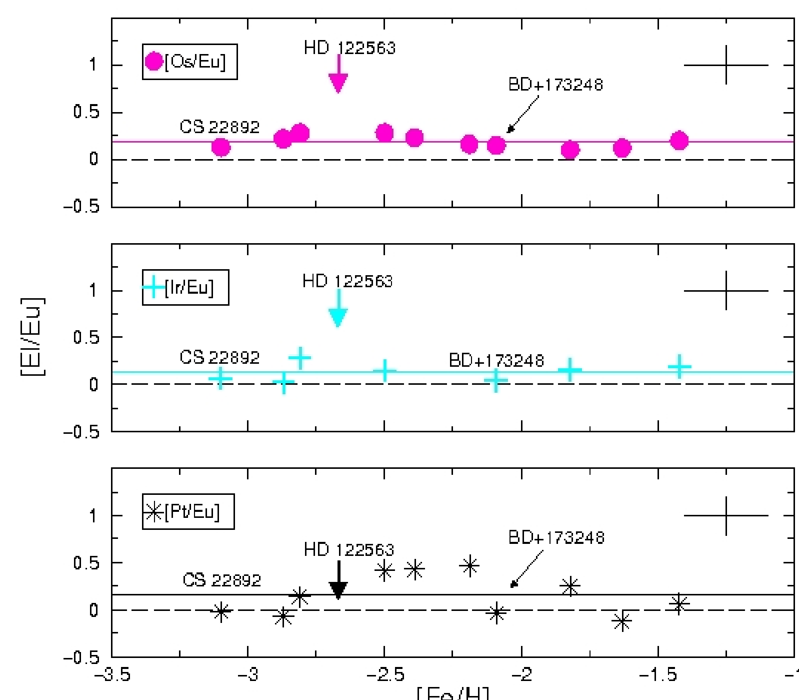

Almost identical behavior of heavy r-element abundances, variations in light r-elements, often underabundances in comparison to solar r-abundances

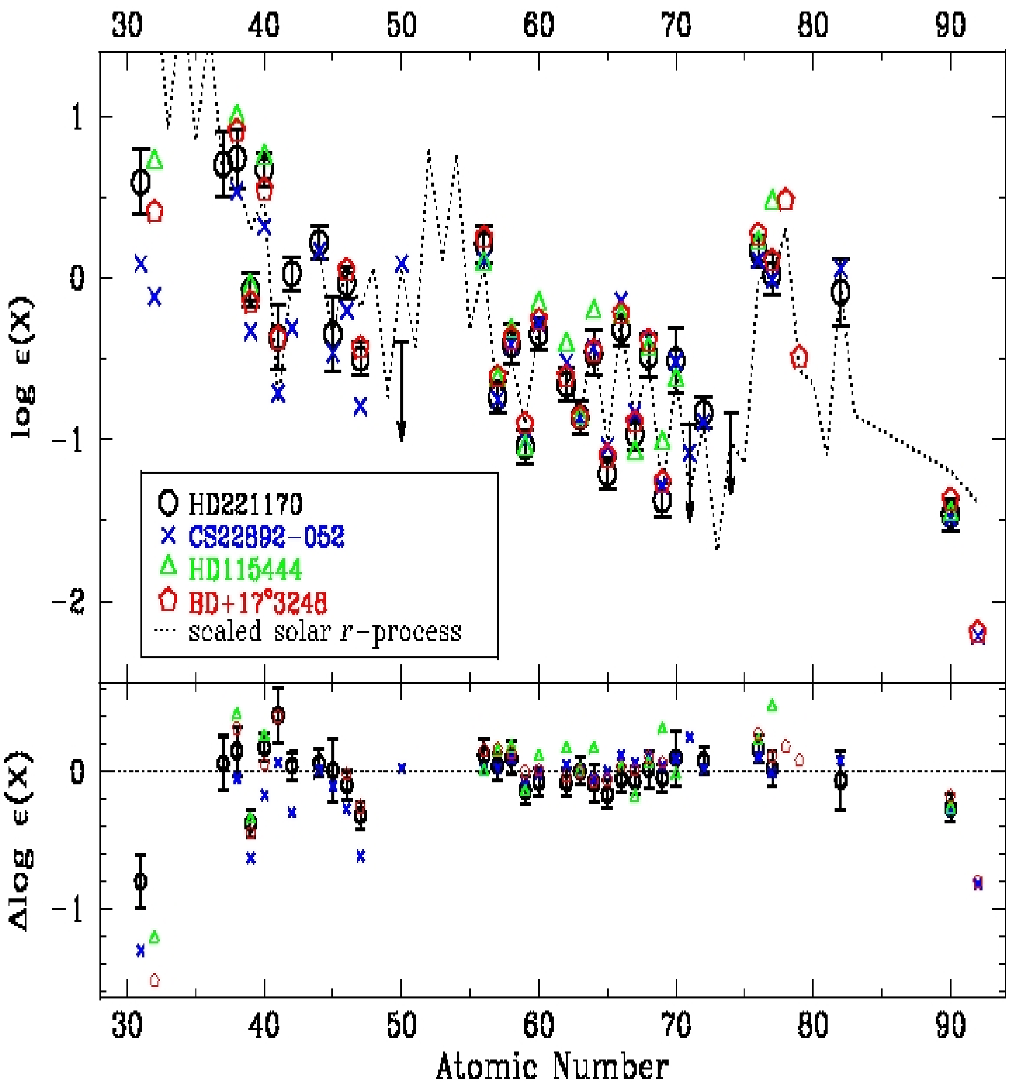

Ivans et al. (2006)

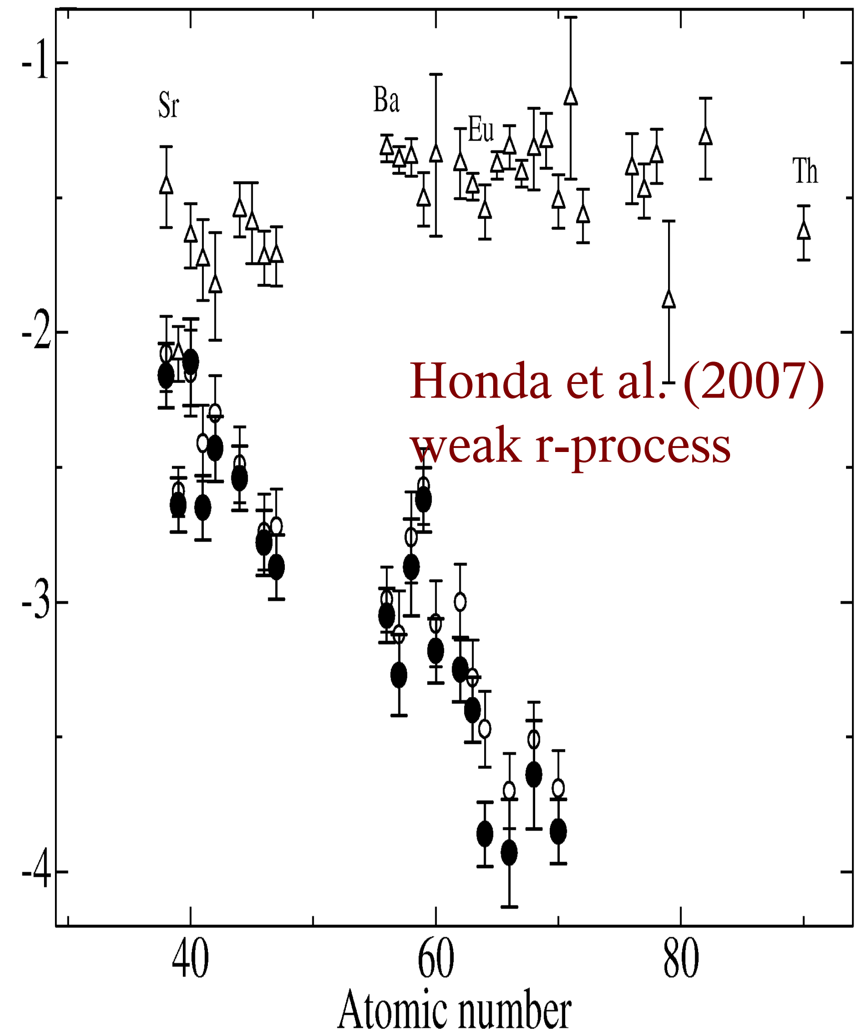

Fig. 5.— Logarithmic differences from the solar system r-process pattern ($\log\varepsilon_{\rm object} - \log\varepsilon_{\rm solar-r}$). The open triangles mean CS 22892-052, the open circles mean HD 122563, and the filled circles mean HD 88609.

Full fission "cycling" for different mass models

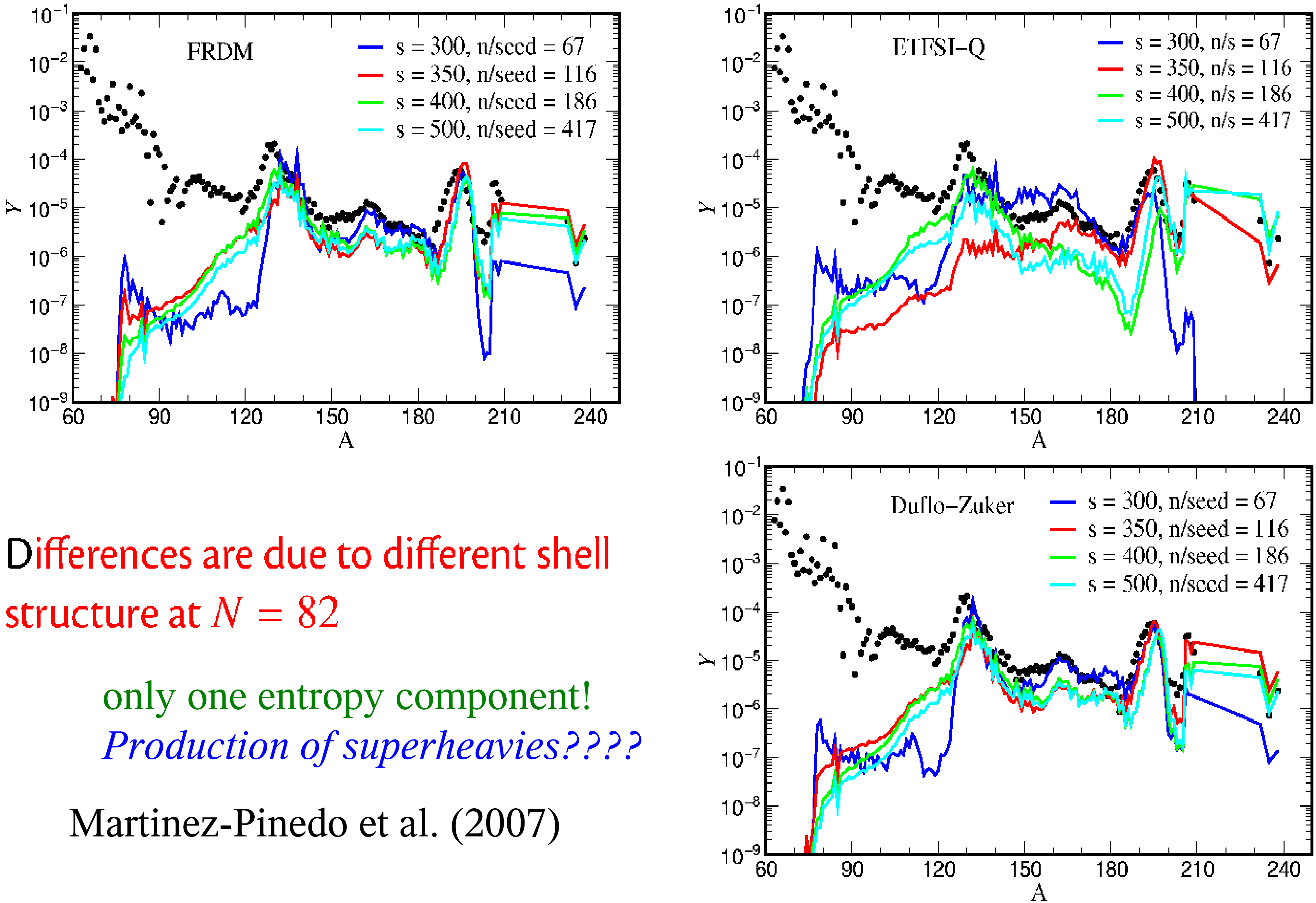

Differences are due to different shell structure at $N = 82$

only one entropy component!

Production of superheavies????

Martinez-Pinedo et al. (2007)

Fission Cycling in Neutron Star Mergers

Trajectory from Freiburghaus, Rosswog, and Thielemann 1999 ($Y_e = 0.1, n/Seed = 238$).

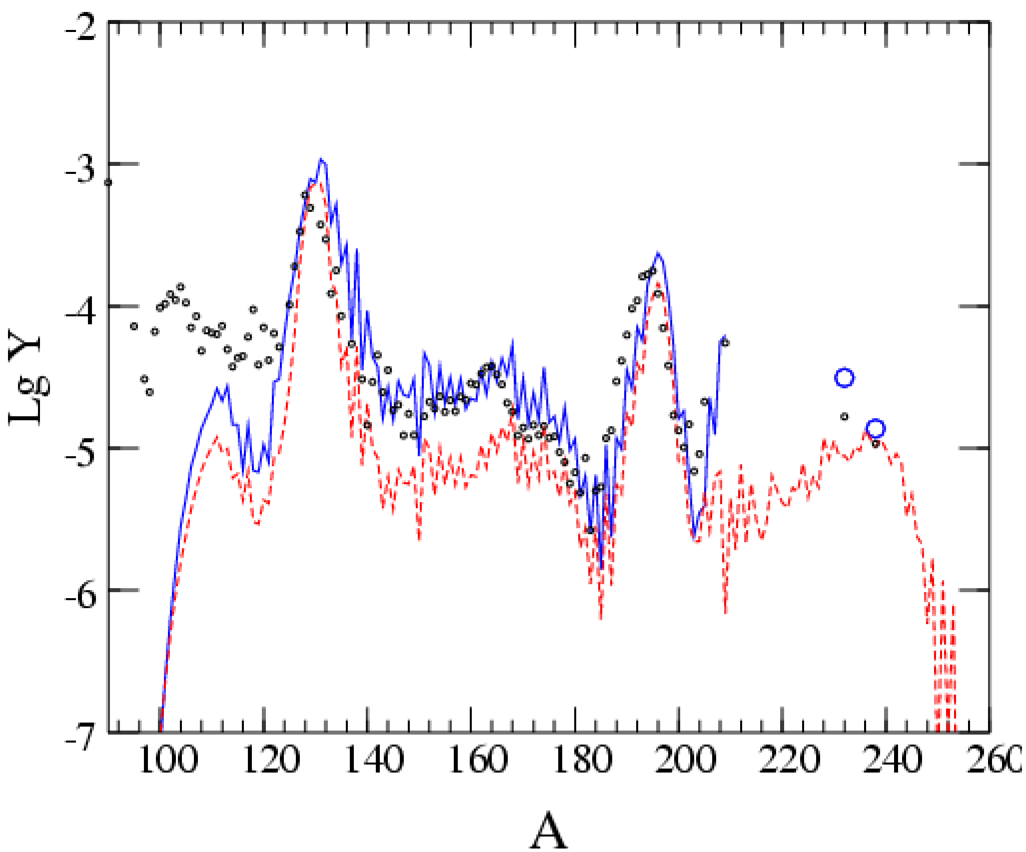

Panov and FKT (2007) with parametrized fission yield contribution

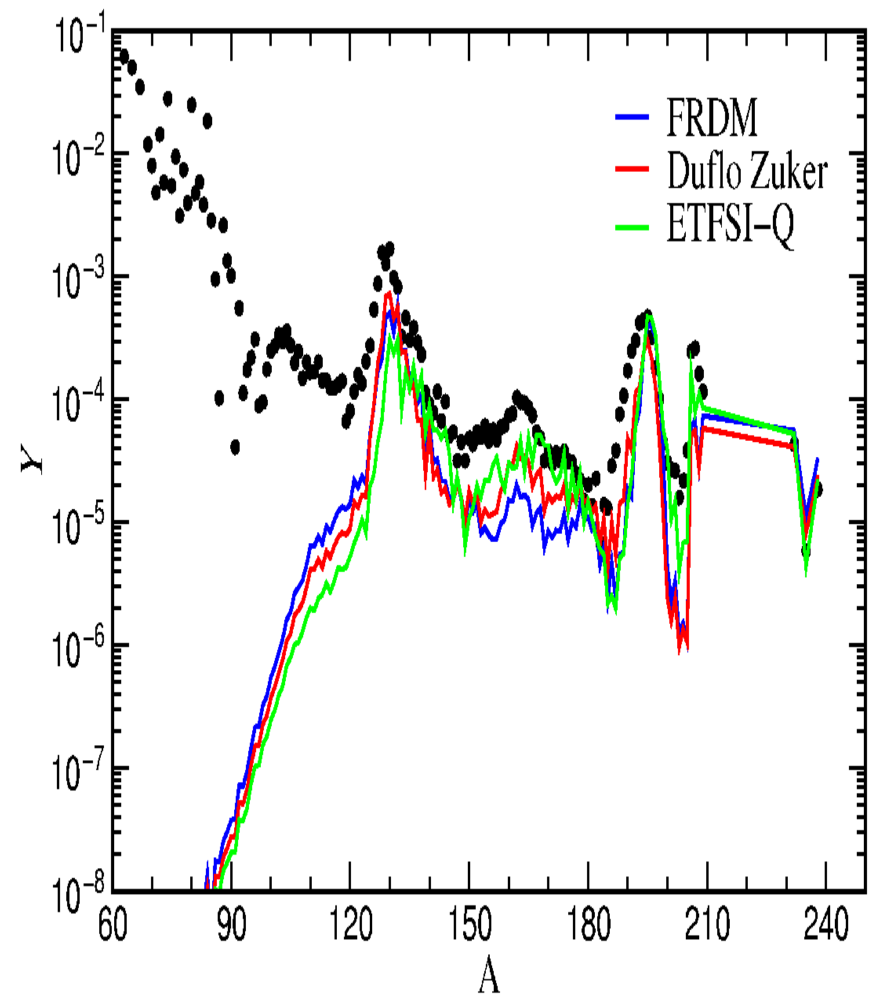

Martinez-Pinedo et al. (2006)

in principle contradicted from gal. evol. calc., but similar conditions in SN polar jets? (Cameron 2003)

Further alternative Scenarios

accretion disks around black holes after merger events (Surman et al. 2008)

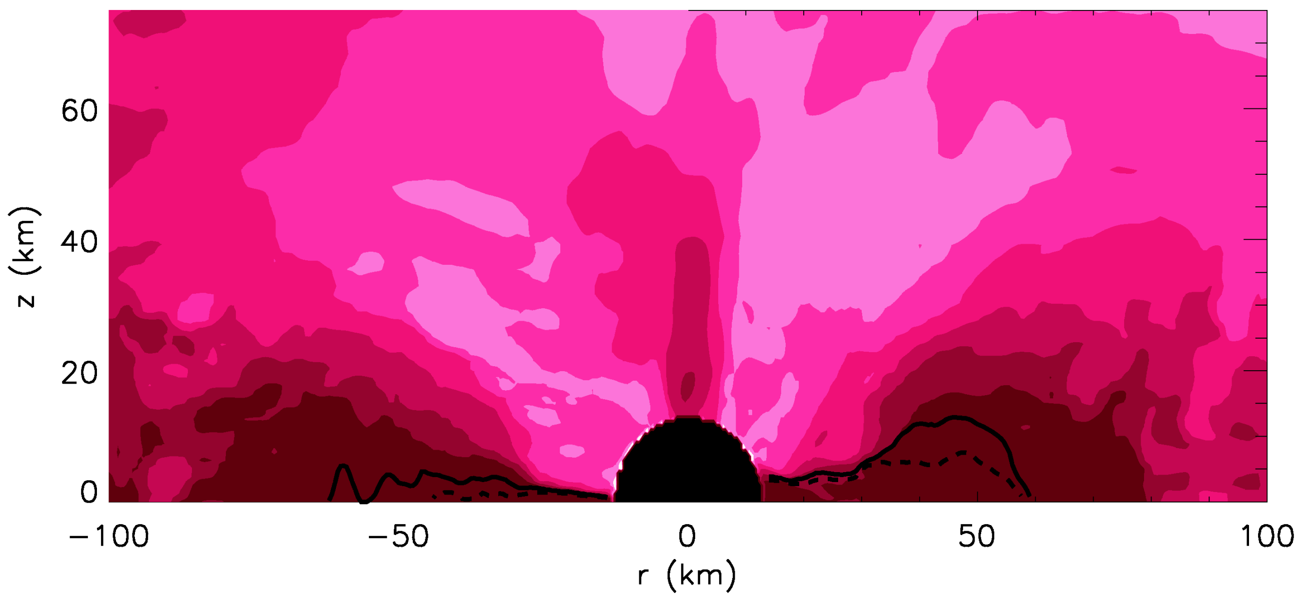

Fig. 2.— Shows density along a vertical slice of the disk. The shaded regions, from lightest to darkest, show densities of $10^{8.5}$, 10^{9}, $10^{9.5}$, 10^{10}, $10^{10.5}$, and 10^{11} g/cm^3. The solid line shows the electron neutrino surface while the dashed line shows the electron antineutrino surface. The dark center indicates the inner boundary of the numerical merger model.

r-process possible if choosing a fast ejection/expansion timescale